

1-29-2018

Investigation Of The Relative Effects Of Development And Impervious Surface On Two Watersheds In Connecticut Using PRMS

Scott Tardif
scott.tardif@uconn.edu

Recommended Citation

Tardif, Scott, "Investigation Of The Relative Effects Of Development And Impervious Surface On Two Watersheds In Connecticut Using PRMS" (2018). *Master's Theses*. 1177.
https://opencommons.uconn.edu/gs_theses/1177

This work is brought to you for free and open access by the University of Connecticut Graduate School at OpenCommons@UConn. It has been accepted for inclusion in Master's Theses by an authorized administrator of OpenCommons@UConn. For more information, please contact opencommons@uconn.edu.

Investigation of the Relative Effects of
Development and Impervious Surface on
Two Watersheds in Connecticut Using PRMS

Scott Tardif

B.S. Environmental Science, University of New Haven, 2014

B.S. Forensic Science, University of New Haven, 2014

B.S. Biology, University of New Haven, 2014

A Thesis

Submitted in Partial Fulfillment of the

Requirements for the Degree of

Master of Science

At the

University of Connecticut

2018

Approval Page

Master of Science Thesis

Investigation of the Relative Effects of
Development and Impervious Surface on
Two Watersheds in Connecticut Using PRMS

Presented by

Scott Daniel Tardif, B.S.

Major Advisor

Dr. Glenn S. Warner

Associate Advisor

Dr. Gary A. Robbins

Associate Advisor

Dr. David M. Bjerklie

University of Connecticut

2018

ACKNOWLEDGEMENTS

I would first like to thank my family for their constant love and support throughout this journey. My friends also played a most important role in motivating me to finish and keeping the graduate school experience fun. It was an absolute pleasure working with all of my colleagues and faculty in the Natural Resources and the Environment and Geosciences Departments. I would like to specially recognize my friend Timothy Bugden, who worked with me on multiple different aspects of this modeling project. Our constant discussions of PRMS and telling of jokes around made this an all-around more rewarding experience.

I would like to thank my primary academic advisor and committee member, Dr. Glenn Warner, for all of the guidance he has provided over the last two and a half years. Glenn has always encouraged me to pursue my dreams post academia and I will certainly miss our discussions in his office. I also need to thank my two committee members, Dr. Gary Robbins and Dr. David Bjerklie. Gary has been one of the most influential people in my life over the last few years. Dave's expertise in watershed modeling was absolutely crucial to this project.

This study could not have not taken place without the funding provided by the USDA Grant, Water Supply Capacity Credits within a Hydrologic Basin: Economics to Sustain Ecosystem Services and Revenues from Undeveloped Forests and Farms, courtesy of Dr. Stephen Swallow. I would also like to thank the Connecticut Water Company, the Town of Manchester, the Capitol Region Council of Governments, and the Pomperaug River Watershed Coalition for their consistent help with understanding the watersheds studied and providing invaluable data and resources. I would like to give an extra special thanks to the MOWS team at the U.S. Geological Survey, who provided significant troubleshooting support for PRMS.

TABLE OF CONTENTS

| | |
|--|------|
| ACKNOWLEDGEMENTS | iii |
| TABLE OF CONTENTS | iv |
| LIST OF TABLES | vii |
| LIST OF FIGURES | viii |
| INTRODUCTION | 1 |
| LITERATURE REVIEW | 3 |
| BACKGROUND ON HYDROLOGIC MODELING | 3 |
| OVERVIEW OF THE PRECIPITATION-RUNOFF MODELING SYSTEM | 5 |
| HYDROLOGIC RESPONSE UNITS (HRU'S)..... | 6 |
| REPRESENTATION OF WATER STORAGE AND FLOW IN PRMS | 7 |
| ORGANIZATION OF PRMS | 8 |
| SENSITIVITY, UNCERTAINTIES, LIMITATIONS TO PRMS MODELING | 9 |
| APPLICATIONS OF PRMS | 10 |
| COMPARISON OF PRMS TO OTHER HYDROLOGIC MODELS | 11 |
| DEVELOPMENTAL IMPACTS ON RIVERS | 13 |
| ESTIMATION OF EFFECTIVE IMPERVIOUS AREA | 14 |
| HYDROLOGICAL STATISTICS USED, SOFTWARE AND DATA SOURCES | 16 |
| STUDY OBJECTIVES | 16 |
| METHODS | 17 |
| STUDY AREA OVERVIEW | 17 |
| POMPERAUG RIVER WATERSHED..... | 17 |
| POMPERAUG RIVER WATERSHED CLIMATE | 19 |
| POMPERAUG RIVER WATERSHED GEOLOGY | 20 |
| POMPERAUG RIVER WATERSHED LAND USE | 20 |
| POMPERAUG RIVER WATERSHED WATER USE | 21 |
| PARAMETERIZATION OF THE POMPERAUG PRMS MODEL | 24 |

| | |
|--|----|
| HYDROLOGIC RESPONSE UNIT (HRU) DELINEATION..... | 24 |
| CLIMATIC MODULES..... | 25 |
| RUNOFF MODULES | 25 |
| IMPERVIOUS SURFACE..... | 26 |
| FULL BUILDOUT..... | 26 |
| STREAMFLOW ROUTING..... | 27 |
| HOCKANUM RIVER WATERSHED | 29 |
| HOCKANUM RIVER WATERSHED CLIMATE | 30 |
| HOCKANUM RIVER WATERSHED GEOLOGY | 31 |
| HOCKANUM RIVER WATERSHED LAND USE..... | 32 |
| HOCKANUM RIVER WATERSHED WATER USE..... | 35 |
| PARAMETERIZATION OF THE HOCKANUM RIVER WATERSHED MODEL..... | 38 |
| HYDROLOGIC RESPONSE UNIT (HRU) DELINEATION..... | 39 |
| CLIMATIC MODULES..... | 40 |
| RUNOFF | 42 |
| IMPERVIOUS SURFACE..... | 42 |
| FULL BUILDOUT ANALYSIS | 42 |
| DETERMINATION OF DEVELOPMENTAL EXTENT | 44 |
| STREAMFLOW ROUTING..... | 45 |
| DEVELOPMENT SCENARIOS | 45 |
| SPECIFIC POMPERAUG RIVER WATERSHED DEVELOPMENT SCENARIOS | 46 |
| SPECIFIC HOCKANUM RIVER WATERSHED DEVELOPMENT SCENARIOS..... | 48 |
| TEST OF EFFECTIVE IMPERVIOUS ESTIMATION METHODS..... | 49 |
| PRMS OUTPUT VARIABLES UTILIZED | 49 |
| MODEL PERFORMANCE EVALUATION: NASH-SUTCLIFFE EFFICIENCY | 50 |
| RESULTS AND DISCUSSION OF THE PRMS INVESTIGATIONS..... | 52 |
| RESULTS OF THE POMPERAUG RIVER CURRENT CONDITIONS MODEL | 52 |

| | |
|--|-----|
| LONG-TERM WATER BALANCE..... | 52 |
| DAILY DISCHARGE TIMING AND BASE-FLOW RECESSION | 56 |
| FLOW DURATION AND EXCEEDANCES..... | 58 |
| BUILDOUT OF THE POMPERAUG RIVER WATERSEHD | 60 |
| DEVELOPMENT SCENARIOS IN THE POMPERAUG RIVER WATERSHED | 60 |
| ESTIMATING EIA WITHIN THE POMPERAUG RIVER WATERSHED..... | 65 |
| CALIBRATION OF THE HOCKANUM PRMS MODEL..... | 72 |
| LONG-TERM WATER BALANCE..... | 72 |
| DAILY DISCHARGE TIMING AND BASE-FLOW RECESSION | 76 |
| FLOW DURATION AND EXCEEDANCES..... | 78 |
| BUILDOUT OF THE HOCKANUM RIVER WATERSEHD..... | 80 |
| DEVELOPMENT SCENARIOS IN THE HOCKANUM RIVER WATERSHED..... | 80 |
| ESTIMATING EIA WITHIN THE HOCKANUM RIVER WATERSHED | 85 |
| OVERALL CONCLUSIONS | 91 |
| WATERSHED COMPARISON | 92 |
| MODEL SENSITIVITY, ASSUMPTIONS, AND LIMITATIONS | 93 |
| CONSIDERATIONS FOR FUTURE STUDIES..... | 95 |
| LITERATURE CITED | 97 |
| APPENDIX A..... | 105 |
| APPENDIX B | 107 |
| APPENDIX C | 108 |
| APPENDIX D..... | 110 |
| APPENDIX E | 113 |
| APPENDIX F..... | 127 |
| APPENDIX G..... | 133 |

LIST OF TABLES

| | |
|--|----|
| Table 1. Examples of different hydrologic modeling software in addition to PRMS..... | 12 |
| Table 2. Lands considered undevelopable and were removed from the buildout analysis. | 43 |
| Table 3. Urban and rural impervious area coefficients that were multiplied by developable land to determine the additional extent of impervious surface coverage. | 43 |
| Table 4. List of the primary output variables from PRMS used in this study..... | 50 |
| Table 5. Change in storage by year for the Pomperaug River watershed as simulated by PRMS..... | 55 |
| Table 6. Estimated groundwater contribution to streamflow in the Pomperaug River..... | 55 |
| Table 7. Daily, monthly, annual, individual month, and individual year NSE and Log NSE values for the Pomperaug River current conditions PRMS model. | 57 |
| Table 8. Observed and simulated streamflow for the Nonnewaug and Weekepeemee Rivers, and calculated NSE and Log NSE based on streamgauge data from water years 2003 to 2015. | 58 |
| Table 9. Observed and simulated 7Q10 and Q ₉₉ for the Pomperaug River. | 58 |
| Table 10. Simulated components of the water balance and high and low flow values for different development scenarios in the Pomperaug River watershed..... | 61 |
| Table 11. Statistical significance of increase or decrease in the water balance due to buildout..... | 61 |
| Table 12. Relationships between changes in streamflow due to development and subbasin area within the Pomperaug River watershed. | 64 |
| Table 13. Change in storage by year for the Hockanum River watershed as simulated by PRMS. | 75 |
| Table 14. Estimated groundwater contribution to streamflow in the Hockanum River..... | 75 |
| Table 15. Daily, monthly, annual, individual month, and individual year NSE and Log NSE values for the Hockanum River current conditions PRMS model. | 77 |
| Table 16. Observed and simulated 7Q10 and Q ₉₉ for the Hockanum River | 78 |
| Table 17. Simulated components of the water balance and high and low flow values for different development scenarios in the Hockanum River watershed. | 81 |
| Table 18. Statistical significance of increase or decrease in the water balance due to buildout..... | 82 |
| Table 19. Relationships between changes in streamflow due to development and subbasin area within the Hockanum River watershed..... | 84 |
| Table 20. List of sensitive PRMS parameters specific to this study..... | 93 |

LIST OF FIGURES

| | |
|--|----|
| Figure 1. Different methods of hydrologic simulation..... | 3 |
| Figure 2. Hydrologic cycle as simulated by PRMS | 7 |
| Figure 3. Map of Connecticut delineating the two study areas..... | 17 |
| Figure 4. Pomperaug River watershed including ungaged area..... | 18 |
| Figure 5. Digital elevation model of the Pomperaug River watershed | 22 |
| Figure 6. Percent impervious surface area in the Pomperaug River watershed..... | 23 |
| Figure 7. Land cover for the Pomperaug River watershed.. | 23 |
| Figure 8. Pomperaug River study area with previously delineated HRUs..... | 24 |
| Figure 9. Hockanum River watershed including ungaged area | 29 |
| Figure 10. Digital elevation model of the Hockanum River watershed..... | 33 |
| Figure 11. Percent impervious surface area in the Hockanum River watershed..... | 34 |
| Figure 12. Land cover for the Hockanum River watershed | 34 |
| Figure 13. Depiction of water usage affecting the Hockanum River watershed..... | 36 |
| Figure 14. Hockanum River study area with delineated HRUs. | 41 |
| Figure 15. The three subbasins that make up the Pomperaug River watershed..... | 47 |
| Figure 16. The three study areas used in the Hockanum River watershed | 48 |
| Figure 17. Observed versus simulated water balance data in the Pomperaug River. a. Maximum daily temperature averaged by month from between four observed weather stations and PRMS's simulated output; b. Minimum daily temperature averaged by month between four observed weather stations and PRMS's simulated output; c. Monthly precipitation averaged between four observed weather stations and PRMS's simulated output; d. Daily streamflow averaged by month between the USGS streamgage and PRMS's simulated output. | 53 |
| Figure 18. Example of a baseflow recession curve for the Pomperaug River current conditions model. .. | 57 |
| Figure 19. Flow duration curve comparing observed and simulated streamflows for the current conditions Pomperaug River PRMS model..... | 59 |
| Figure 20. Flow duration curve comparing simulated streamflows among the current conditions, undeveloped, and buildout with minimum and maximum stormwater collection scenarios in the Pomperaug River watershed. | 63 |
| Figure 21. Flow duration curve for the Pomperaug River watershed comparing the three methods of estimating EIA based on 12.5% TIA. | 67 |
| Figure 22. Flow duration curve for the Pomperaug River watershed comparing the three methods of estimating EIA based on 25% TIA.. | 68 |

| | |
|--|----|
| Figure 23. Flow duration curve for the Pomperaug River watershed comparing the three methods of estimating EIA based on 50% TIA.. | 69 |
| Figure 24. Flow duration curve for the Pomperaug River watershed comparing the three methods of estimating EIA based on 75% TIA | 70 |
| Figure 25. Flow duration curve for the Pomperaug River watershed comparing the three methods of estimating EIA based on 100% TIA. | 71 |
| Figure 26. Observed versus simulated water balance data in the Hockanum River watershed. a. Maximum daily temperature averaged by month from between three observed weather stations and PRMS's simulated output; b. Minimum daily temperature averaged by month between three observed weather stations and PRMS's simulated output; c. Monthly precipitation averaged between three observed weather stations and PRMS's simulated output; d. Daily streamflow averaged by month between the USGS streamgage and PRMS's simulated output | 73 |
| Figure 27. Observed and simulated hydrographs for the Hockanum River current conditions model depicting poor model performance. | 77 |
| Figure 28. Example of a baseflow recession curve for the Hockanm River current conditions model. | 78 |
| Figure 29. Flow duration curve comparing observed and simulated streamflows for the current conditions Hockanum River PRMS model..... | 79 |
| Figure 30. Flow duration curve comparing simulated streamflows among the current conditions, undeveloped, and buildout with minimum and maximum stormwater collection scenarios in the Hockanum River watershed | 83 |
| Figure 31. Flow duration curve for the Hockanum River watershed comparing the three methods of estimating EIA based on 12.5% TIA | 86 |
| Figure 32. Flow duration curve for the Hockanum River watershed comparing the three methods of estimating EIA based on 25% TIA | 87 |
| Figure 33. Flow duration curve for the Hockanum River watershed comparing the three methods of estimating EIA based on 50% TIA | 88 |
| Figure 34. Flow duration curve for the Hockanum River watershed comparing the three methods of estimating EIA based on 75% TIA | 89 |
| Figure 35. Flow duration curve for the Hockanum River watershed comparing the three methods of estimating EIA based on 100% TIA | 90 |

INTRODUCTION

Access to fresh water resources is declining in a world of rapid population growth and climatic stressors. Therein lies the necessity to determine the anthropogenic impacts of development on sources of water. One approach to understanding development on water resources is through the use of hydrologic modeling. Hydrologic modeling provides the opportunity to understand watershed processes on multiple scales. In this thesis, development scenarios and subsequent impacts on the water balance for two watersheds, the Pomperaug and the Hockanum River watersheds located in Connecticut, United States, are analyzed utilizing the United States Geological Survey software Precipitation-Runoff Modeling System (PRMS). This thesis is only intended to explore the quantitative impacts of development and is not intended to imply impacts on water quality. Therefore, results from a water quality perspective are not discussed.

This thesis contains three chapters. The first chapter contains a literature review on hydrologic modeling, an overview of PRMS and its applications, issues that development and impervious surface have on watersheds, and a background estimation of effective impervious area. The second chapter discusses the methodology used in this thesis. It first reviews the Pomperaug River watershed study area and details its climatic, geological, land use, and water use history based on a previous study. The Hockanum River watershed is detailed in the same way as the Pomperaug. The next section of the methods chapter describes parameterization of the two PRMS models for each watershed. The Pomperaug mostly required updates of model parameters, whereas the Hockanum model was parameterized from the beginning. Along with parameterization of the Hockanum River model, a section describes full buildout analyses to project future development and impervious surface coverage within the watershed. The last

section in the second chapter details the scenarios of development used to analyze locational effects of increased impervious coverage on streamflow on both watershed and localized scales.

The final chapter includes the results and discussion from running the Pomperaug River and Hockanum River watershed models. There are specific emphases on the impacts of various scenarios of development on: 1) location, such as the amount of development or upstream versus downstream, 2) variation of groundwater and surface runoff, and 3) resultant changes in low flow frequencies. A comparison between the two watersheds is made to highlight differences of modeling these two rural and urban watersheds. The results are discussed from both a hydrologic modeling perspective and a developmental and resource management viewpoint. The limitations and assumptions made in the study are discussed to assist the interpretation of results. Lastly, recommendations are made for future research.

LITERATURE REVIEW

BACKGROUND ON HYDROLOGIC MODELING

Models are used to represent an actual system (Ford, 2010). Hydrologic models were originally developed to predict outcomes, e.g. peak discharges, from an expected input such as extreme rainfall. They vary from simplistic equations to more intricate models to simulate the complex processes and the spatially variable nature of the hydrologic cycle. This is useful because hydrogeophysical and climatic data are often limited. Dingman (2015) defines a hydrologic simulation model as, “a physical system or mathematical algorithm that is intended to reproduce actually or symbolically the essential aspects of the operation of a portion of the hydrologic cycle”. The goal of a hydrologic model is to provide the most realistic results while reducing the model complexity (Devi et al., 2015). Hydrological models have many purposes such as to improve our understanding of hydrological processes, recreate past hydrologic events, predict future hydrologic conditions, and evaluate the effects of anthropogenic changes on the landscape (Brun et al., 2001; Dingman, 2015; Ford, 2010; Freeze & Harlan, 1969).

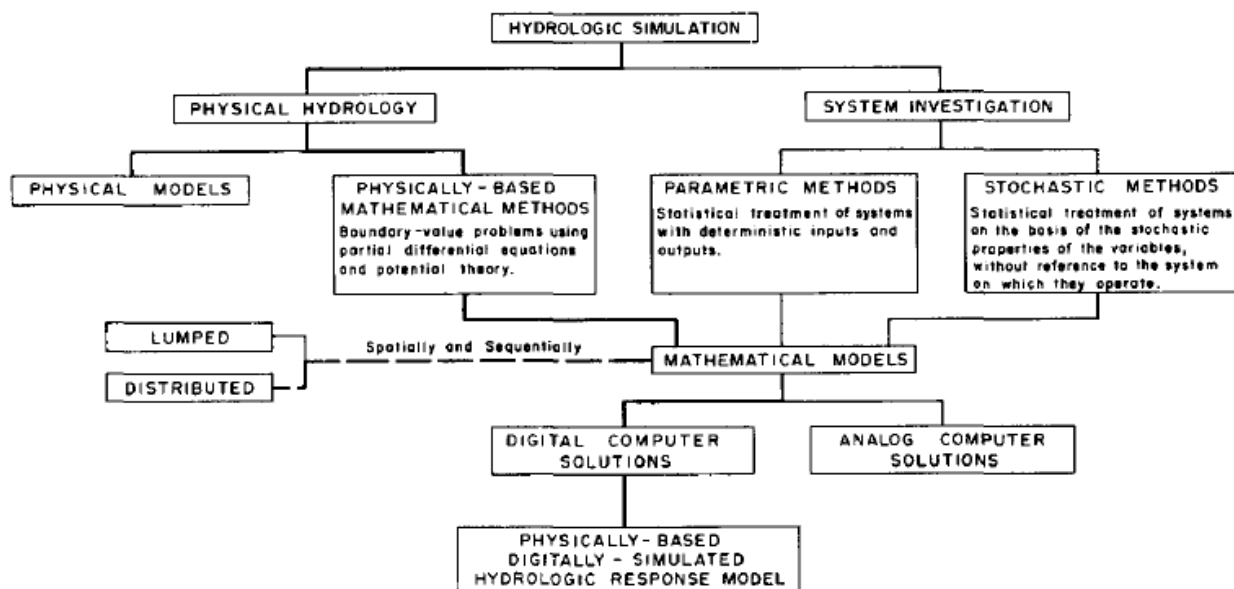


Figure 1. Different methods of hydrologic simulation (Freeze & Harlan, 1969).

The three main categories of simulation models used in hydrologic investigations are physical, analog, and mathematical models (Figure 1). A physical model is a representation of the natural world (Dingman, 2015) built to usually a miniature scale. In terms of hydrology, these types of models all help develop or understand physical laws or empirical relations for different hydrologic processes. An analog model is a simulation of one type of process based on an analogous process, or one in which a small scale laboratory experiment can represent a larger scale problem (Robinove, 1962). For example, electrical resistance in a wire can represent friction in a hydraulic system.

A mathematical model consists of equations in logical order that can calculate storage and fluxes of water at specified locations (Dingman, 2015). These mathematical models require various parameters and inputs to determine the model outputs. Parameters are often not certain but are meant to characterize a region, such as hydraulic conductivity over a given area. An input is a single or series of values of known data such as observed rainfall (Dingman, 2015). Whole watersheds can be modeled if these relationships portray the nature of hydrologic cycle in that given area (Freeze & Harlan, 1969).

Under the category of mathematical models are physics based simulation models, also commonly known as physically based models. Physics based hydrologic models are derived from conservation of mass, energy, and momentum, combined with empirical relationships to simulate flows and storages (Dingman, 2015; Ford, 2010). Some examples of physics based hydrologic relationships include Darcy's Law, the Laplace equation, or the Jensen-Haise equation for estimating evapotranspiration, although each of these require empirically determined coefficients for application. These physical laws and empirical relationships are

generally applied to parts of or whole watersheds after being scaled up, which is a potentially limiting assumption for hydrological modeling.

Hydrologic models represent spatial variability of the study area through different methods. Lumped models are simplistic in that the entire region is accounted for with a single set of parameters (Dingman, 2015). For example, one value for vegetative cover, slope, or soil type would represent the entire study area. A distributed model can account for the spatial variability of the study area by partitioning it into a more localized system (Dingman, 2015). At the finest scale, a distributed model is formed by a grid. This can potentially better represent a watershed, but scale and data availability issues may also arise. If the watershed is subdivided so much that it is too fine for available data, the results might not be as accurate as a simplified dataset.

Two types of investigations can be applied to hydrologic modeling. A deterministic model will output the same results with each run provided that the inputs and parameters are not altered. By contrast, a stochastic model will randomize the outputs with the same set of inputs and parameters (Devi et al., 2015). An advantage of deterministic modeling in hydrology is that the change in the results can be attributed to the specific alterations of input data.

OVERVIEW OF THE PRECIPITATION-RUNOFF MODELING SYSTEM

The Precipitation-Runoff Modeling System (PRMS) is a computer modeling software programmed by the United States Geological Survey (USGS). The PRMS was developed to simulate the response of a hydrologic system to changes in climatic or land use inputs. It was originally created in 1983 (Leavesley et al., 1983) and is currently at version PRMS-IV. The code for the PRMS software is FORTRAN 90 based and features a graphical user interface (GUI) (Markstrom et al., 2015).

PRMS is a deterministic modeling system (Markstrom et al., 2015); each output from the PRMS will be the same if input parameters have not been altered. The PRMS is a physical-process-based model; the algorithm's used are based on physical laws along with empirically determined values that related to specific characteristics of the watershed (Markstrom et al., 2015). The PRMS operates on a daily time-step and conserves the hydrologic mass-balance throughout the extent of the model runtime (Markstrom et al., 2015), which allows for outputs of the water balance such as simulated streamflow, interflow, groundwater flow, and evapotranspiration. The PRMS can produce more than 200 output variables to indicate a simulated hydrologic response of watershed over time (Markstrom, Hay, & Clark, 2016).

HYDROLOGIC RESPONSE UNITS (HRU'S)

The primary spatial discretizations of the model are hydrologic response units (HRU's). HRU's are smaller partitioned sections of the watershed which have boundaries as hydrologic drainage divides. Each HRU is based on physical and hydrological properties that include stream channels, surface elevation, slope, aspect, vegetative type, and land use. These parameters can be determined by GIS and are considered homogenous for a given HRU (Markstrom et al., 2015), but vary from HRU to HRU so it can better represent the watershed. PRMS does not calculate hydrologic processes for individual grid cells within HRU's. Therefore, PRMS is more considered to be a semi-distributed model as a opposed to fully distributed (Viger & Leavesley, 2007). Each HRU is given an arbitrary, unique, and consecutive number to identify it. The number of HRU's may vary by watershed and can also vary within the same basin depending on the coarseness of the input data. Although HRU's could be lake, swale, or inactive (Markstrom et al., 2015), for the purposes of simplification, all HRU's in this study are considered land.

REPRESENTATION OF WATER STORAGE AND FLOW IN PRMS

The conceptual model shown in Figure 2 depicts the hydrologic processes simulated within the PRMS. PRMS-IV uses conceptual reservoirs that should not be thought of as surface reservoir storage, but rather as the mechanism and process of water storage. Water that moves between these are considered fluxes. In PRMS-IV, there are three conceptual soil-zone storage reservoirs known as the preferential-flow, capillary, and gravity reservoirs (Figure 2). The preferential-flow reservoir accounts for fast lateral interflow through larger openings in the soil profile (Markstrom et al., 2015), but for simplification this study only used the latter two soil-zone reservoirs. Water in the capillary reservoir is the soil-water content between the wilting and field-capacity thresholds, and it is called the available water content of the soil profile (Markstrom et al., 2015). Water here is not available for interflow, but it can affect the gravity reservoir, surface runoff calculations, and the evapotranspiration process.

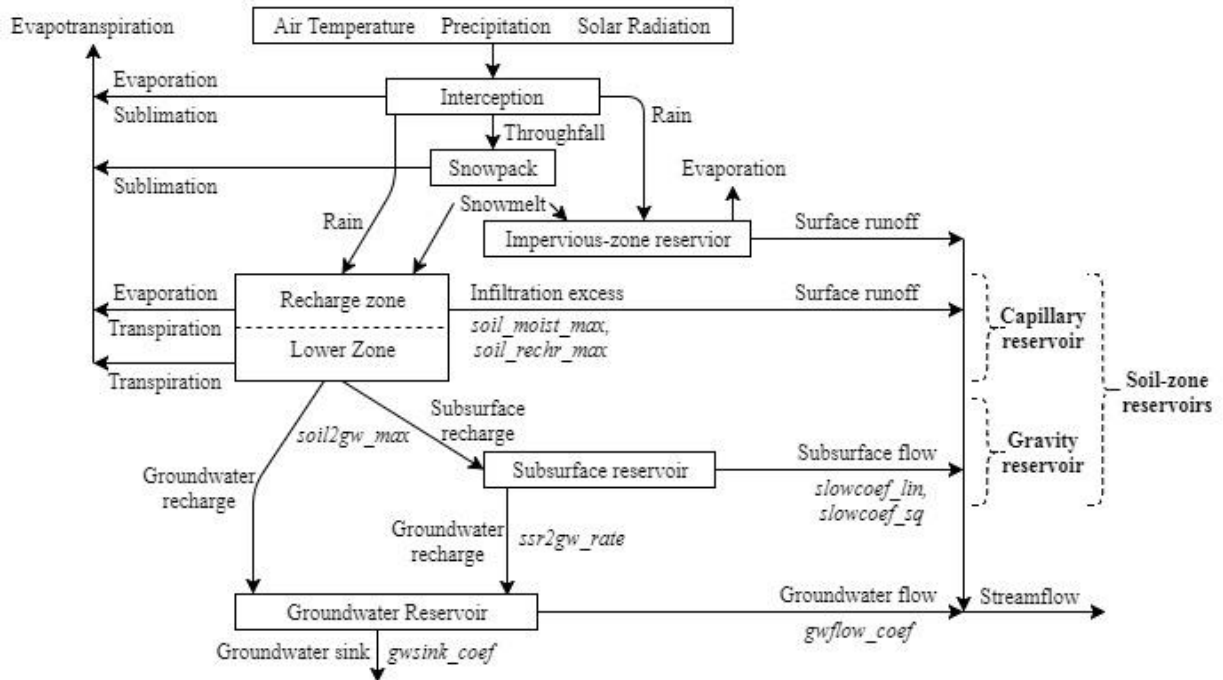


Figure 2. Hydrologic cycle as simulated by PRMS. Figure adapted from Markstrom et al. (2015) with the addition of the italicized parameters that influence soil zone water flux and discharge to streamflow.

The gravity reservoir accounts for slow lateral interflow (subsurface flow) and drains soil-water into the groundwater reservoir. The maximum amount of water in the gravity reservoir is calculated by the difference in total soil saturation and the field capacity (Markstrom et al., 2015). Recharge of the groundwater reservoir occurs as vertical flow from the conceptual soil-zone reservoirs. The groundwater reservoir accounts for the groundwater flow and baseflow component of streamflow. Water can also leave the model domain to the groundwater sink, which can be thought of as deep groundwater aquifers that do not contribute to the stream network.

ORGANIZATION OF PRMS

There are three types of input files used by the PRMS-IV. The Control File calls for processes, determines which modules are used, and names the parameters to be used in simulations. The Parameter File contains each input parameter, its defined dimensions, and either the monthly average (e.g. solar radiation) or HRU (e.g. average elevation) value for that parameter. Lastly, the Data File contains daily precipitation, maximum and minimum air temperatures, and observed streamgage data.

The PRMS-IV uses 17 processes to simulate the hydrologic cycle of a watershed; each process either is used for hydrological processes or administrative tasks, such as generating output reports (Markstrom et al., 2015). Modules in PRMS-IV are the source codes that simulate the hydrologic processes and operates in a twelve step sequence (Markstrom et al., 2015). Some hydrological processes have multiple modules, i.e. representing different methods for calculating that process, which are called for in the PRMS control file. If only one module exists for a process, it does not need to be specified in the Control File. The output used in this study was a Statistics Variables File; this text file allows the user to select variables to output as a time-series.

Further explanation of background information on the PRMS is available in Markstrom et al. (2015).

SENSITIVITY, UNCERTAINTIES, LIMITATIONS TO PRMS MODELING

PRMS is subject to parameter sensitivity when simulating streamflow volume and timing and determination of the long term water balance. Especially sensitive parameters include those that distribute temperature and precipitation to each HRU, those involved with estimation of PET, the soil water capacity, ground cover, and snow accumulation and melt processes (Bjerklie, Starn, & Tamayo, 2010). Markstrom, et al. (2016) identified processes and parameters to provide insight into PRMS model performance and allow the modeler to identify dominant processes based on which processes are associated with sensitive parameters. It concluded that model complexity may be reduced by focusing on processes that are associated with sensitive parameters and disregard those that are not (Markstrom et al., 2016), which was applied when studying model sensitivity in this thesis.

According to Bjerklie et al. (2010), sources of model uncertainty include misrepresentative or erroneous input data, incomplete representation of watershed processes or model domain boundaries, and unknown factors in a given study area such as unknown changes in land use, water diversions, or floodplain storage. Other model uncertainty arises from the potential use of different HRU scales (Bugden, 2018) or from random errors.

As is the case with hydrologic modeling in general, PRMS is limited by the amount of available data such as hydrogeologic properties that govern groundwater flow. In certain cases, hydrologic processes for PRMS were developed for specific region and therefore might not be representative of other regions. One other limitation to PRMS modeling is the HRU scale that is used. Although it can simulate watershed scale processes, an HRU that is 10 km² could not

capture localized impacts from changes such as a large scale housing development or specific hydraulic processes such as channelized flow (Dudley, 2008). PRMS modeling is also limited in that it is not a dynamic model. In other words, if the model is run with 2011 land use data for 1980 to 2015, those conditions remain static throughout the model's run. It cannot update mid-run to account for changes in development throughout the study period and therefore can only be run with one set of conditions. PRMS does not explicitly model water diversions or reservoir releases so the daily complexities of pumping or water supply cannot be captured.

APPLICATIONS OF PRMS

A few studies have analyzed the effects of land use change on a watershed with PRMS. Bjerklie, et al. (2010) studied land use change in the Pomperaug River watershed, Connecticut, which is the main model and basis for a majority of this thesis. The authors evaluated six land use scenarios, such as current conditions, pre-development, full build-out development (according to zoning regulations), and other arbitrary build-out levels (Bjerklie, et al., 2010). The results were discussed in terms of the Pomperaug and its two main tributaries, the Nonnewaug and the Weekepeemee Rivers. The study also considered different methods of estimating Effective Impervious Area (EIA) to simulate different stormwater management options for development.

Another PRMS land use study was conducted for the Flint River basin in Georgia (Viger et al., 2011). This study considered future development using the Forecasting Scenarios of Future-Land Cover (FORE-SCE) model created by the USGS. Development was forecast through 2050 over the entire watershed. This study did not assess spatial effects of development explicitly and focused more on the basin as a whole. The potential impact of various climate scenarios were also simulated.

Lastly, the North Fork Pheasant Branch basin, Wisconsin, had two developmental scenarios examined (Steuer & Hunt, 2001). The first case involved low-density residential developments in the watershed, and the second scenario involved medium or high commercial and medium-density development. The baseline model performed above average statistically, but had issues with snowmelt months (Stuer & Hunt, 2001). When the snowmelt months were removed, the model's statistical efficiency improved. This study examined the effects of urbanization in greater detail than any other PRMS study and had success with its calibration of storm events and baseflow recession.

All three of these studies found increases in overall streamflow and surface runoff, and decreases in groundwater flow and subsurface flow with increasing impervious coverage (Bjerklie et al., 2010; Steuer & Hunt, 2001; Viger et al., 2011). This is consistent with literature discussed later. Numerous other PRMS studies have been conducted, but are either a precursor for a land use change assessment or were used for other applications, such as climate change. Some examples include, but are not limited to, the Dennys River, Maine (Dudley, 2008), Delaware River in Pennsylvania, New Jersey, and New York (Goode et al., 2010), and the East River and Yampa River, Colorado (Battaglin et al., 2011). A comprehensive climate change study using PRMS models was conducted in 2012 and has become a major application for the USGS software (Markstrom et al., 2012).

COMPARISON OF PRMS TO OTHER HYDROLOGIC MODELS

There are many other hydrological models available for users to study a watershed and simulate river discharge. Some examples of other hydrological models and their uses are provided in Table 1. PRMS was chosen for this study above these other popular models for a number of reasons.

The Storm Water Management Model (SWMM) and the Hydrologic Engineering Center's River Analysis System (HEC-RAS) models have more specialized applications than what was desired for this study. SWMM was designed for single, urban precipitation events, while HEC-RAS was designed for 1D hydraulic flow in localized river or culvert channels; it should be noted that after this study began, HEC-RAS updated to include 2D flow. USGS's Modular groundwater flow process model (MODFLOW) can simulate groundwater flow in aquifers, stress from pumping wells, and flow through river beds. However, it does not simulate surface water processes. MODFLOW requires extensive hydrogeological and induced stress data for accurate groundwater flow estimations.

The Surface Water Assessment Tool (SWAT) and MIKE-Système Hydrologique Européen (SHE) both are well documented but require extensive parameterization and computer processing capabilities. SWAT has other water quality aspects to the modeling software that were not required for this study. The Hydrologiska Byråns Vattenbalansavdelning (HBV) model is generally used as a lumped model, but could be set up to as semi-distributed. HSPF is a popular hydrologic model used worldwide but data were not available for the watersheds analyzed in this study.

Table 1. Examples of different hydrologic modeling software in addition to PRMS.

| Model Name | Developer | Purpose |
|---|-------------------------|------------------------|
| MODFLOW (Harbaugh, 2005) | USGS | Groundwater Flow |
| HEC-RAS (Institute for Water Resources, 2016) | Army Corps of Engineers | River and Channel Flow |
| SWMM (Rossman, 2015) | US EPA | Stormwater Runoff |
| GSFLOW (Markstrom et al., 2008) | USGS | Watershed-scale |
| HSPF (Bicknell et al., 1997) | US EPA | Watershed-scale |
| SWAT (Neitsch et al., 2011) | Texas A&M, USDA | Watershed-scale |
| MIKE-SHE (DHI, 2017) | DHI | Watershed-scale |
| HBV (Bergström, 1992) | SMHI | Watershed-scale |

The Groundwater – Surface water FLOW (GSFLOW) modeling system is a USGS developed software that integrates its PRMS surface water and MODFLOW groundwater modeling. This software was a potential candidate to use for the Pomperaug River Watershed because prior PRMS and MODFLOW models had been parameterized and calibrated. However, in order to develop a new model for a different watershed, both models would have to be parameterized and calibrated to incorporate into a GSFLOW model. This would have required extensive work, especially with unknown field data, such as aquifer depths and thicknesses, for a MODFLOW model. Therefore, PRMS was chosen because of its overall complete documentation, troubleshooting support availability, and access to new and old data.

DEVELOPMENTAL IMPACTS ON RIVERS

A major component of surface runoff is generated by impervious surface. Impervious surfaces are those materials that prevent infiltration of water into soil, such as roads, rooftops, and compacted soils (Arnold Jr. & Gibbons, 1996). Impervious land cover has emerged as an ecological indicator and can predict environmental health (Arnold Jr. & Gibbons, 1996). The effects impervious surfaces have on water resources quantity and quality are both multifaceted and innumerable. These impacts of urbanization have been researched throughout a variety of environments and climatic regions. Urbanization and imperviousness have negatively affected biological and chemical characteristics of rivers (Beaulieu et al., 2012; Bellucci, 2007; Coles et al., 2004; Giddings et al., 2009; Rose & Peters, 2001; Sun & Caldwell, 2015), increased non-point source pollution (Arnold Jr. & Gibbons, 1996; Sleavin et al., 2000; Sun & Caldwell, 2015) and increased erosion and sedimentation of waterbodies (Arnold Jr. & Gibbons, 1999; Smucygz et al., 2010). Increased impervious coverage also creates negative alterations to stream channel morphology (Arnold Jr. & Gibbons, 1999; Taniguchi & Biggs, 2015), reduction of baseflow and

groundwater recharge (Arnold Jr. & Gibbons, 1999; Furtsch, 2015; Rose & Peters, 2001), and increased volume and velocity of surface runoff and flooding severity (Arnold Jr. & Gibbons, 1999; Rose & Peters, 2001; Sauer et al., 1983). These impacts present challenges for storm water management and wastewater treatment systems in urban cities with aging infrastructure.

Development management plans can minimize the impacts created by urbanization on stormwater runoff. One of the initial stages of a development management plan is watershed characterization (U.S. Environmental Protection Agency, 1998). The purposes of this study fit into this step of planning; it is an initial assessment of how increasing imperviousness in urban or rural watersheds affect rivers. Understanding the mechanisms that altering landscapes have on a watershed can predict how development may affect components of streamflow, induced seasonal changes, or water quality related issues.

ESTIMATION OF EFFECTIVE IMPERVIOUS AREA

The total impervious area (TIA) does not necessarily reflect how the impervious surface contributes stormwater runoff to the stream network. This is because not all impervious surfaces route water to a stormwater drainage system. For example, precipitation that falls on a rural house could infiltrate into the surrounding soil, whereas precipitation falling on an urban apartment will drain through the stormwater management system that rapidly contributes to streamflow. Therefore, the effective impervious area (EIA), or directly connected impervious area, is a more important parameter than TIA for hydrologic modeling (Bjerklie et al., 2010; Lee & Heaney, 2003; Zimmerman, 2011). Estimation of EIA is complex due to specific localized spatial effects of where storm drains are located (Zimmerman, 2011). Highly compacted soils in developed sites where heavy-equipment had been used may act the same as these impervious surfaces, but might not necessarily show in impervious surface data.

In PRMS specifically, the impervious surface parameter is very sensitive (Bjerklie et al., 2010; LaFontaine et al., 2013). PRMS assumes that runoff from impervious surfaces is routed directly to streamflow (Bjerklie et al., 2010). The following equation is a common method of estimating EIA as a function of the TIA computed by Equation 1:

$$\mathbf{EIA} = \mathbf{k_1} \times (\mathbf{TIA})^{\mathbf{N}} \quad (1)$$

where k_1 is the intercept of the log regression, N is the slope of the log regression, and TIA is expressed as a percent. The k_1 and N values are typically assumed to be 0.15 and 1.41, respectively, for an area with storm sewers (Alley & Veenhuis, 1983). This equation is called the “Urban method of estimating EIA” for the remainder of this study.

Equation 1 was modified for Connecticut through a storm-runoff analysis described by Bjerklie et al. (2010). The modified EIA estimation model for Connecticut is Equation 2:

$$\mathbf{EIA} = \mathbf{0.008} \times (\mathbf{TIA})^2 + \mathbf{0.191} \times (\mathbf{TIA}) \quad (2)$$

where TIA is expressed as a percent. This equation was formed as a composite of Alley & Veenhuis and Connecticut runoff data. Bjerklie et al. suggest to use this estimation for areas in Connecticut that are transitioning from rural to urban (2010), which is appropriate for the majority of the Hockanum River watershed. This equation is called the “Transitional method of estimating EIA” for the remainder of this study.

With just Connecticut runoff data, Equation 3 was developed and tested in the Bjerklie et al. (2010) study:

$$\mathbf{EIA} = \mathbf{0.0001} \times (\mathbf{TIA})^3 - \mathbf{0.005} \times (\mathbf{TIA})^2 + \mathbf{0.2287} \times (\mathbf{TIA}) \quad (3)$$

where TIA is expressed as a percent. This equation is appropriate for rural Connecticut watersheds and is called the “Rural method of estimating EIA” for the remainder of this study.

HYDROLOGICAL STATISTICS USED, SOFTWARE AND DATA SOURCES

The Nash-Sutcliffe Efficiency (NSE) index (Nash & Sutcliffe, 1970) is commonly used to evaluate surface water model simulations (Schaeffli & Gupta, 2007). The NSE was the main model performance evaluation method used in this study. Low flow time periods occur when a river has its lowest discharge amounts. Flow duration curves and the 7-day, 10 year low flow (7Q10) were used to assess flow exceedances and their frequencies. A flow duration is the probability that specified stream discharges are exceeded over a given period (Searcy, 1959), which provides a historical estimate of streamflow characteristics. A flow-duration curve (FDC) is a graph of these exceedance probabilities (Ahearn, 2008; Flynn, 2003; Suro & Gazoorian, 2011). A 7Q10 value corresponds to a 7 consecutive days low flow average that has a 10 percent chance of non-exceedance in a given year (Ahearn, 2008).

The various versions of software and programs, as well as sources of data, used in this study are listed within Appendix A in Table A-1 and Table A-2, respectively.

STUDY OBJECTIVES

The intention of this thesis was to study the effects that changes in impervious surface area have on the water balance of watersheds. The specific spatial effects of these change in development were incorporated into the study's design. This study's objectives included the following: 1) calibrate an updated PRMS model for the Pomperaug River watershed, 2) fully parameterize and calibrate a PRMS model for the Hockanum River watershed based on previously reported parameterization schemes and hydrogeological and land use data available in Geographic Information Systems, and 3) evaluate the relative impacts of development scenarios and methods of estimating EIA in the two watersheds. The second chapter discusses in detail the methods used to satisfy these objectives.

METHODS

STUDY AREA OVERVIEW

The two study areas of interest are located in the state of Connecticut within the conterminous United States. The Pomperaug River watershed is located in western Connecticut and the Hockanum River watershed is located in north central Connecticut (Figure 3).

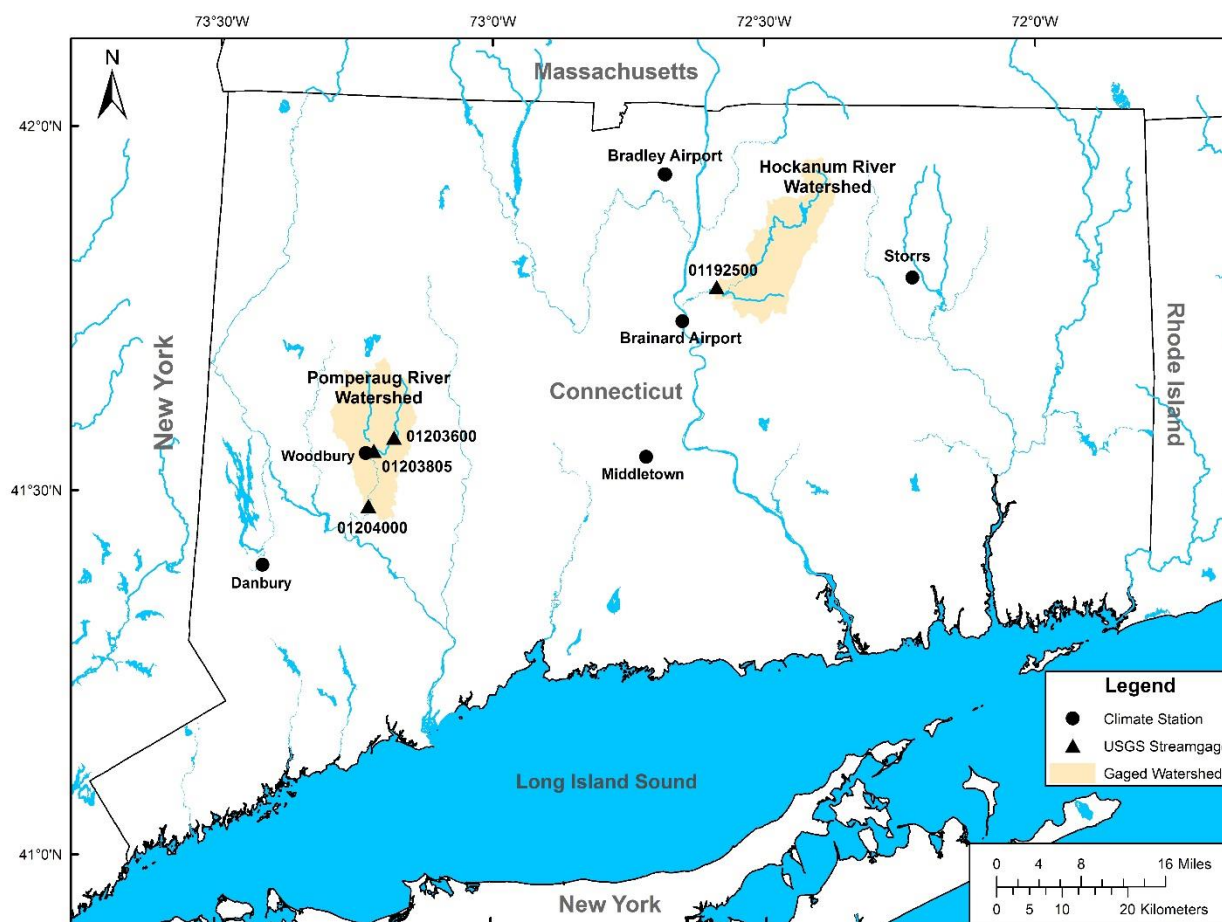


Figure 3. Map of Connecticut delineating the two study areas.

POMPERAUG RIVER WATERSHED

The Pomperaug River is formed at the confluence of the Weekepeemee and Nonnewaug Rivers and discharges into the Housatonic River. The Pomperaug River watershed is located in portions of the following eight Connecticut towns: Southbury, Woodbury, Middlebury, Roxbury,

Washington, Bethlehem, Morris, and Watertown. The USGS streamgage number for the Pomperaug River is 012404000; the drainage area for the gage is 195.8 km² (75.6 mi²). The total contributing watershed area that discharges into the Housatonic River is 230.5 km² (89 mi²) (Figure 4). Both the Weekeepemee and Nonnewaug Rivers have USGS streamgages, which are station numbers 01203805 and 01203600, respectively. Both gages have complete records from 2003 to 2015 that were used in this study. Above the Weekeepemee gage, which is located near the confluence with the Nonnewaug River, the watershed area is 70.1 km² (27.1 mi²). The Nonnewaug gage is located farther upstream of the confluence so the watershed area above it is 45.7 km² (17.7 mi²), while the total Nonnewaug watershed area is 70.2 km² (27.1 mi²).

Elevation in the gaged watershed ranges from approximately 30 m (100 ft) to 352 m (1155 ft) above mean sea level (Figure 5). The Pomperaug streamgage has been continuously monitored from 1933 to 2015. The mean daily streamflow during the 83 year period of record was 3.75 m³ s⁻¹ (132.6 ft³ s⁻¹), and from 1980 to 2015 the mean daily streamflow was 3.94 m³ s⁻¹ (139.0 ft³ s⁻¹). These flows are equivalent to an

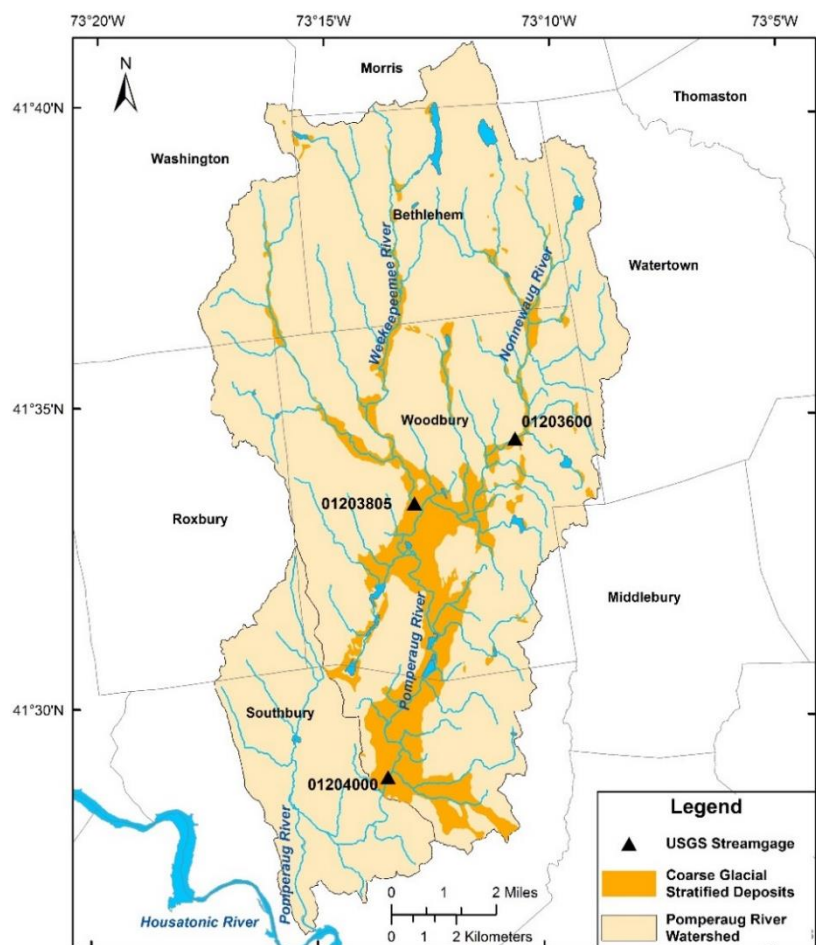


Figure 4. Pomperaug River watershed including ungaged area.

average annual runoff of 610 mm (24.0 in) and 638 mm (25.1) inches, respectively. March has had the greatest average streamflow, and the lowest flows for the year typically occur in July, August, or September. Peak streamflow can occur at any time during the year, but generally is associated with rain and snowmelt, large storms, or hurricane floods.

POMPERAUG RIVER WATERSHED CLIMATE

Average annual precipitation within the Pomperaug River has been reported from 47 to 51 inches depending on gage location and the period of record examined (Bjerklie et al., 2010). For example, the Water Resources Inventory of Connecticut reported an average annual precipitation of 1194 mm (47 in) from 1931 to 1960 (Wilson et al., 1974). Three National Oceanic and Atmospheric Administration (NOAA) Cooperative Observer Network (COOP) weather stations outside of the watershed at Bradley International Airport in Windsor, Danbury, and Middletown (Figure 3) reported an average of 1280 mm (50.4 in) of annual precipitation from 1980 to 2015; Bradley International Airport is located in Connecticut's Central Valley and averaged 1184 mm (46.6 in) of annual precipitation, which is less than the other stations. The only COOP station inside the watershed, located in Woodbury, had an average annual precipitation of 1288 mm (50.7 in) from 1980 to 2015. In general, precipitation is evenly distributed throughout each month. However, local variation in precipitation may occur with elevation and randomly distributed isolated storm events. Snowfall varies from year to year but averages 1016 mm (40 in) annually in the Pomperaug River watershed (Miller et al., 2002).

From 1980 to 2015, the average daily minimum and maximum temperatures for a year range from 4.4 to 15.6 °C (40 to 60 °F), respectively. January and February in general are the coolest months, while July and August have had the warmest temperatures. Potential evapotranspiration (PET) is a function of solar radiation, air temperature, cloud cover, wind

speed, and humidity. Therefore, PET is greatest in the summer and very small or trivial during winter months. Actual evapotranspiration (AET) is determined by PET, available soil moisture, and vegetation. If soil moisture is low or not available, AET would be reduced. This may occur in summer months when PET is high but precipitation is low for a period of time. Therefore, AET is complex process that will vary spatially and topographically depending on specific atmospheric and ground conditions. AET in the Pomperaug River watershed was estimated at 50 percent of the annual precipitation, or about 635 (25 in) (Wilson et al., 1974) and estimated at 584 to 686 mm (23 to 27 in) per year by Bjerklie et al. (2010).

POMPERAUG RIVER WATERSHED GEOLOGY

Across Connecticut, the two main aquifers types are coarse glacial stratified drift deposits or glacial till and bedrock. In the Pomperaug River Watershed, the surficial geology consists mostly of glacial till and lesser amounts stratified drift deposits along the main rivers (Figure 4). The stratified deposits allow for larger groundwater withdrawals by higher capacity production wells. The Pomperaug River watershed consists of mostly crystalline bedrock, an important source of well water for individual homes. There is also an approximately 28.5 km² (11 mi²) area of sedimentary and volcanic bedrock in the southern section of the Pomperaug River Basin (Wilson et al., 1974).

POMPERAUG RIVER WATERSHED LAND USE

This watershed has had an issue of concern for local resource managers since the area experienced a population growth in the 2000's (Bjerklie et al., 2010). The southern portion of the watershed in Southbury is the most urbanized portion of the watershed, along with some areas in Woodbury (Figure 6). The majority of the watershed is a sporadic mix of forest, single

residential homes, and agricultural land (Figure 7). Although fragmented, the watershed remains relatively rural.

The Pomperaug River Watershed Coalition (PRWC) formed to aid sustainable development and protect the health of the watershed from increases in populations and changes in land use. As a result, a comprehensive study by the USGS, the PRWC, and the Town of Woodbury led to the development of a PRMS model to evaluate land-use change on streamflow and groundwater availability to assist future water and ecological resource management (Bjerklie et al., 2010). The authors of this study provided their PRMS model that served as a partial basis for this thesis.

POMPERAUG RIVER WATERSHED WATER USE

Primary water use in the watershed is domestic supplied by individual groundwater wells (Bjerklie et al., 2010). The largest water public supply systems with documented diversions are the Watertown Fire District, Heritage Village, and United Water (Bjerklie et al., 2010). The Watertown Fire District diverts water entirely out of the watershed, along with portions of the Heritage Village withdrawals. Therefore, these are consumptive water uses in regards to the watershed. A detailed list of water diversions in the watershed are documented in the Bjerklie et al. report (2010). The Bronson-Lockwood Reservoir augments water supply to the Nonnewaug River and subsequently the Watertown Fire District well field, but releases are poorly documented. Another feature in the Pomperaug watershed are three abandoned gravel pit ponds that store water during flood events and then slowly release surface water back to the river (Bjerklie et al., 2010).

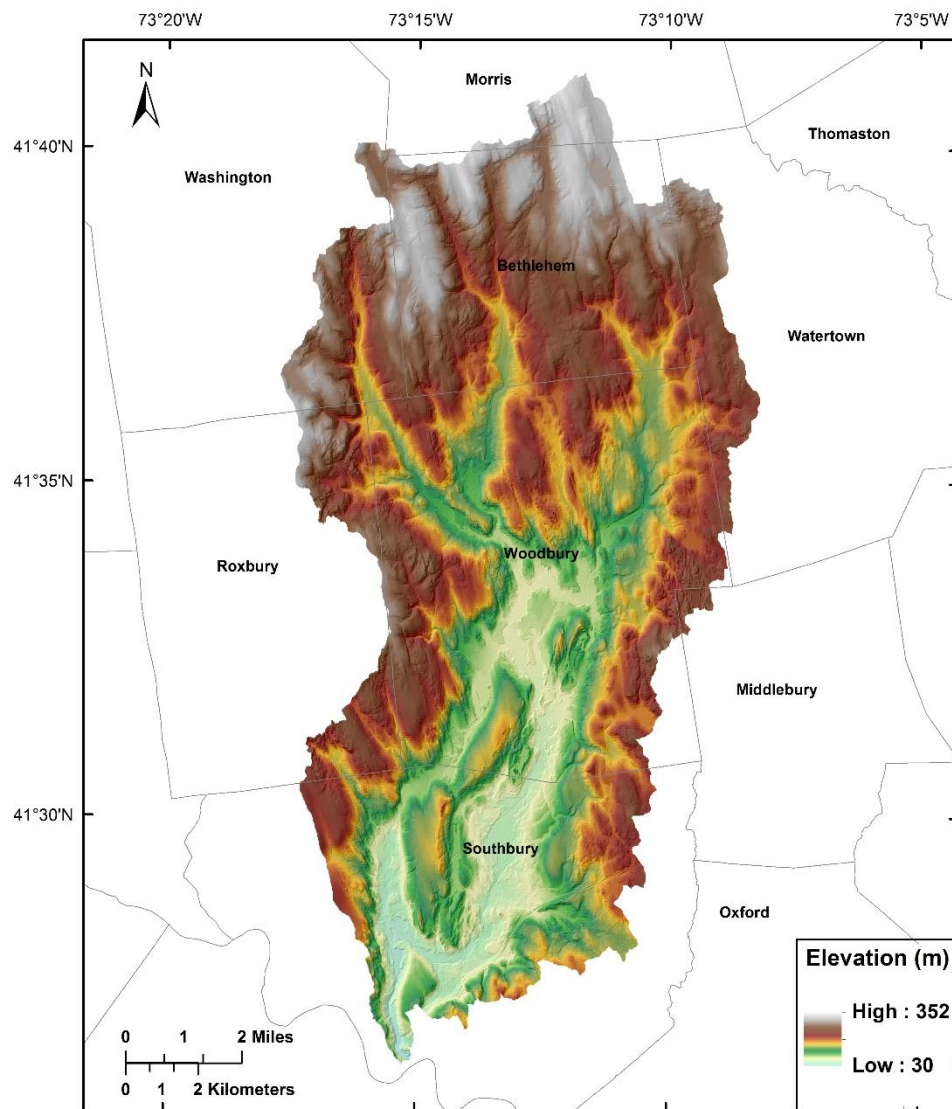


Figure 5. Digital elevation model of the Pomperaug River watershed.

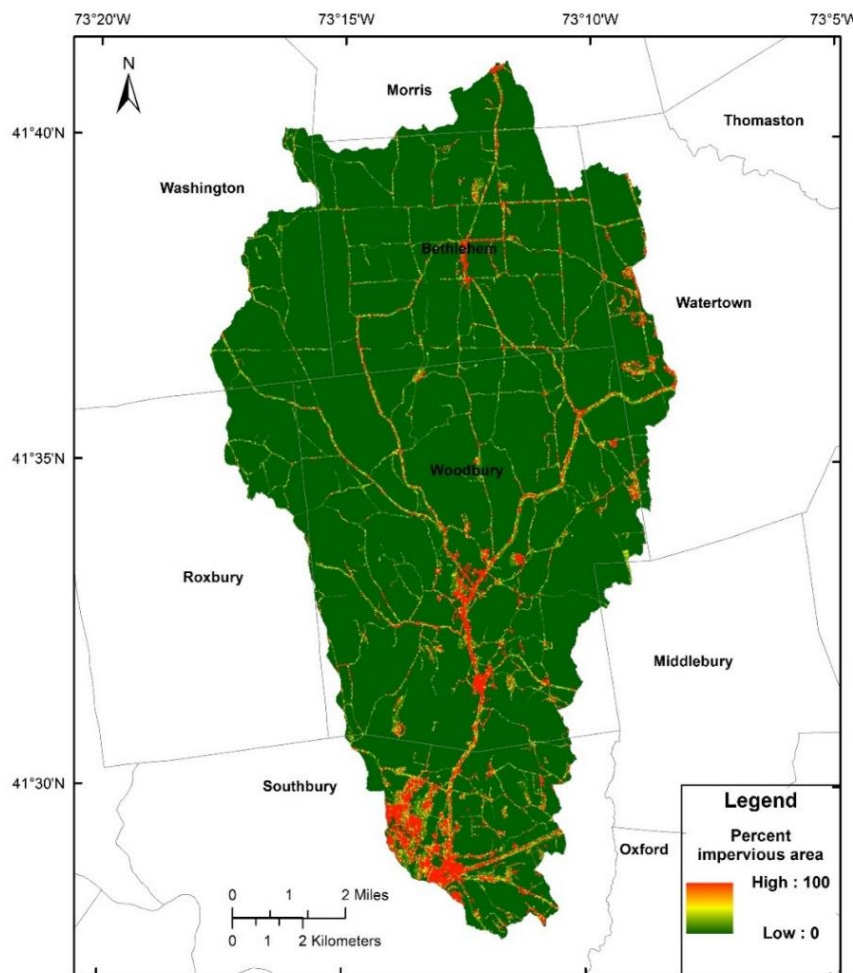


Figure 6. Percent impervious surface area in the Pomperaug River watershed. GIS data from the NLCD.

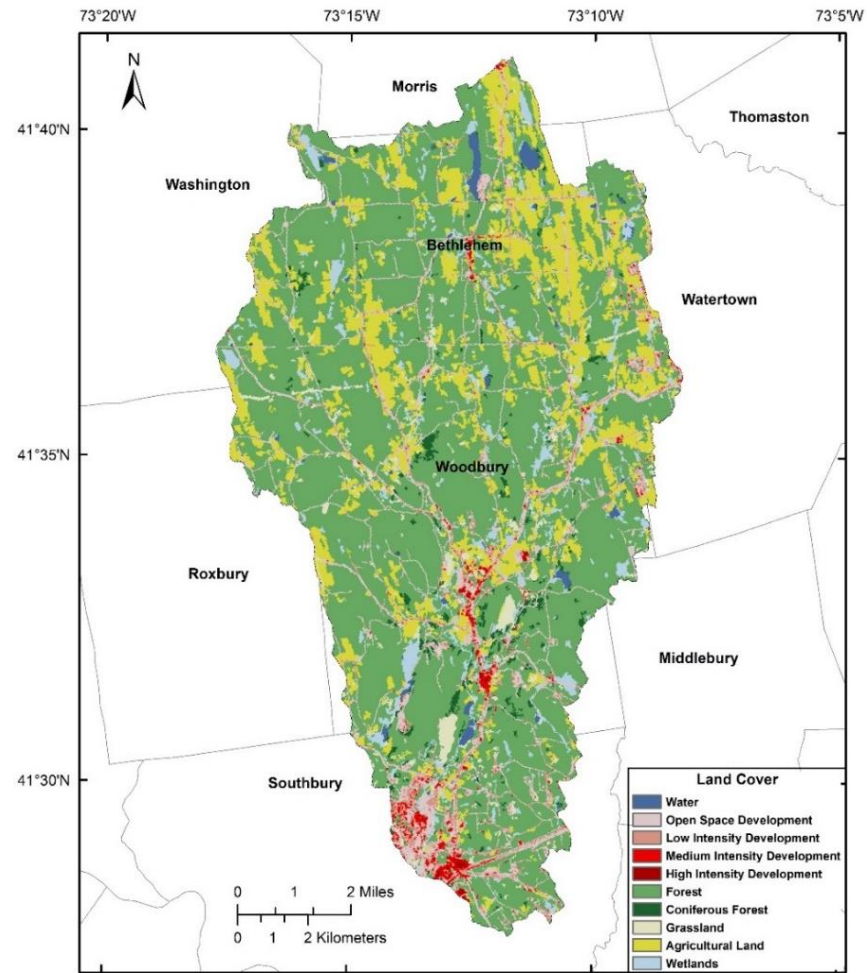


Figure 7. Land cover for the Pomperaug River watershed. GIS data modified from the NLCD.

PARAMETERIZATION OF THE POMPERAUG PRMS MODEL

The majority of parameterization and calibration of the Pomperaug River model had occurred in the original Bjerklie et al. study in 2010. Some data were outdated or needed to be updated to fit a new study period or the new PRMS software. Due to a lack of access to the previous version of PRMS, replication of the previous study's results were not exact. Adjustments had to be made to various parameters to recalibrate the model. A sensitivity analysis helped optimization. A full list of parameters are available digitally in Appendix G.

HYDROLOGIC RESPONSE UNIT (HRU) DELINEATION

Of the 64 previously delineated HRU's by Bjerklie et al. (2010), only 55 HRU's representing the watershed upstream of the USGS streamgauge were used in this study (Figure 8). The HRU's were delineated using right and left hillslopes as similar to the GIS Weasel's methodology (Viger & Leavesley, 2007) along with some modifications (Bjerklie et al., 2010). This method can be thought of as an HRU consisting of either the left or right land area of the associated river that exists until the next drainage divide.

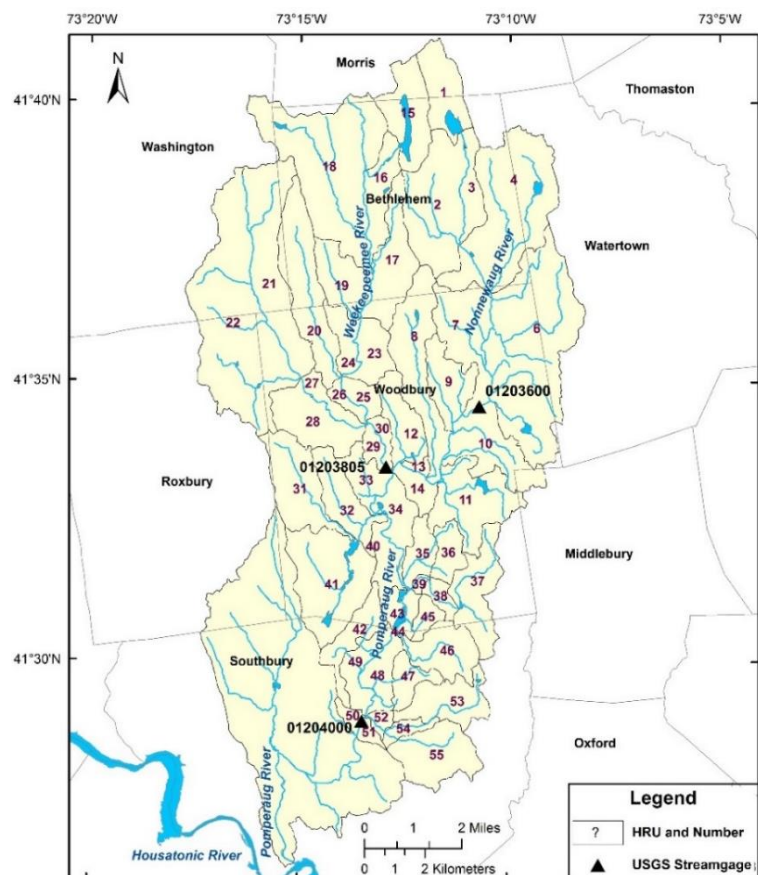


Figure 8. Pomperaug River study area with previously delineated HRUs (Bjerklie et al., 2010).

CLIMATIC MODULES

In PRMS, the long-term water balance is determined by climatic modules, some of which have multiple sub-options. Of the modules listed in Table B-1 of Appendix B, six control the climate. The modules that control distribution of solar radiation (*soltab*), snowmelt (*snowcomp*), and interception of precipitation by vegetation (*intcp*) have only one module option each. In the Pomperaug PRMS model, the modules *xyz_dist*, *ddsolrad*, and *potet_jh* control daily precipitation and temperature, magnitude of solar radiation, and potential evapotranspiration, respectively. Mathematical relationships between climate processes and inputted location parameters of the watershed, such as elevation and latitude, are used by these modules to more accurately portray local weather patterns.

The *xyz_dist* climate distribution module was used in the Pomperaug River watershed because it had been used previously in the Bjerklie et al. study (2010). This module distributes daily precipitation and maximum and minimum daily temperature to each HRU using a multiple linear regression method with measured climate station data (Markstrom et al., 2015). The module adjusts its distribution based around spatially determined x, y, and z values for each weather station. Four previously discussed NOAA COOP stations were used as data inputs into the PRMS model (Figure 3). The climate data inputs of daily precipitation, minimum, and maximum temperatures were updated from the previous report of 10/1/1975 to 9/30/2005 to 10/1/1980 to 9/30/2015 for this study. The overlapping datasets matched entirely. This new time period also matches the data that were available for the Hockanum River.

RUNOFF MODULES

The total streamflow is determined in PRMS via the summation of the three different runoff processes. Runoff is distributed as groundwater, subsurface, and land surface flow to the

stream network via the following three modules: *gwflow*, *soilzone*, and *srunoff_smidx*, respectively. The long-term water balance is controlled by the climate modules and transfer of water through the soil zone modules. The timing and magnitude of the daily hydrograph is controlled by the release of water from the different zones' conceptual storage reservoirs described in the PRMS Overview section. This is determined by parameters that characterize physical processes of watershed hydrology.

From the previous PRMS version used in the Bjerklie et al. study in 2010, the *soilzone* module was updated for PRMS-IV to include a preferential flow reservoir (Markstrom et al., 2015). Although it was not used in this study, it is suspected that some replication errors incurred were a result of a more complex *soilzone* module that had not been previously parameterized.

IMPERVIOUS SURFACE

The *srunoff_smidx* module computes Hortonian runoff from impervious surfaces by subtracting impervious surface depressions, **imperv_stor_max**, from available precipitation and multiplied by the fraction of impervious surface, **hru_percent_imperv**, in a given HRU (Markstrom et al., 2015). This portion of Hortonian runoff is directly routed to and contributes to streamflow volume. Since the Pomperaug is a rural watershed, the Rural method of estimating EIA (Equation 3) was used in both the Bjerklie et al. study (2010) and this thesis to set the parameter **hru_percent_imperv**.

FULL BUILDOUT

A comprehensive full buildout analysis was conducted by the Naugatuck Valley Council of Governments for the Bjerklie et al. study (2010) to assist in projecting future impervious coverage in the Pomperaug River watershed. These estimations of TIA and subsequent EIA

(Appendix G) were used in this study as part of developmental scenarios. The full-buildout process is described further in the Hockanum River watershed methods section.

STREAMFLOW ROUTING

Streamflow is computed by several different modules in PRMS. The simplest option is to use the *strmflow* module that calculates discharge leaving the model domain, i.e. exits the watershed, as a summation of surface, subsurface, and groundwater runoff from each HRU (Markstrom et al., 2015). This module assumes that all water that enters the stream network exits the watershed in a day, which is reasonable for smaller watersheds. Another option is to add in a storage component to the hydrologic model via streamflow routing. In PRMS, the Muskingum routing module (*muskingum*) can add storage and vary flow travel times (Markstrom et al., 2015). Muskingum routing distributes storm event surface runoff over time as opposed to in one day. This is most beneficial for larger river basins in which water in the stream network exits the watershed longer than in a daily time-step. Muskingum routing can be used to simulate reservoirs, dam discharge, and diversions (Markstrom et al., 2015) and help simulate large storm events that occur between two days, which PRMS may have trouble with because it operates on a daily time-step.

According to the PRMS-IV Manual, Muskingum routing is conceptualized as “a single-direction sequence of connected stream segments” in which one segment is often associated with an HRU (Markstrom et al., 2015). There are four additional parameters that are required for Muskingum routing compared to the streamflow module. The parameter **hru_segment** is the index to determine which stream segment an HRU contributes to. The parameter **tosegment** is an index number of each downstream segment to which the segment streamflow flows. The **K_coef** is the travel time is of a flow wave from one segment to its corresponding downstream

segment. The **x_coef** is the amount of attenuation for a flow wave from 0 to 0.5, in which 0 represents storage in a reservoir and 0.5 represents little or no flood attenuation (Elbashir, 2011).

The following equation was used to determine the **K_coef** in hours (LaFontaine et al., 2013):

$$\mathbf{K_coef} = \frac{L \text{ (m)}}{V \left(\frac{\text{m}}{\text{s}} \right)} \times \frac{1 \text{ min}}{60 \text{ s}} \times \frac{1 \text{ hour}}{60 \text{ min}} \quad (4)$$

where L is the length of the stream segment in meters, and V is the stream velocity in m s^{-1} . The stream segments (Figure C-1 of Appendix C) and length of each stream segment were determined in ArcGIS. The stream velocity was estimated at 0.76 m s^{-1} (2.5 ft s^{-1}) for a year round average based on a sensitivity analysis and the Bjerklie et al. study (2010). The calculated **K_coef** values for each stream segment are listed in Appendix G. The **x_coef** was estimated at 0.2 for each of the stream segments in the Pomperaug River watershed and subsequently not calibrated further.

HOCKANUM RIVER WATERSHED

The Hockanum River's headwaters form at Shenipsit Lake in Rockville (Vernon) and ultimately discharges in to the Connecticut River (Figure 9). The towns with the most drainage area in the watershed are Ellington, Manchester, Tolland, and Vernon, while Bolton, East Hartford, Glastonbury, Somers, South Windsor, and Stafford have small contributing areas. Some of the larger tributaries to the Hockanum River include the Tankerhoosen River, Charters Brook, Marsh Brook, South Fork Hockanum River, and Bigelow Brook. Shenipsit Lake is the largest waterbody in the watershed and is a large public water supply reservoir.

Elevation of the Hockanum River watershed ranges from approximately 1 to 314 m (3 to 1030 ft) above mean sea level (Figure 10). The Hockanum River watershed encompasses a drainage area of

approximately 199 km² (77 mi²), and about 192 km²

(74.1 mi²) of the watershed

is monitored by USGS

streamgage number

01192500. The gage is

located in East Hartford

(Figure 9). There are no

other gages in the

watershed, except for gage

01192050, which is an

occasionally used chemical and

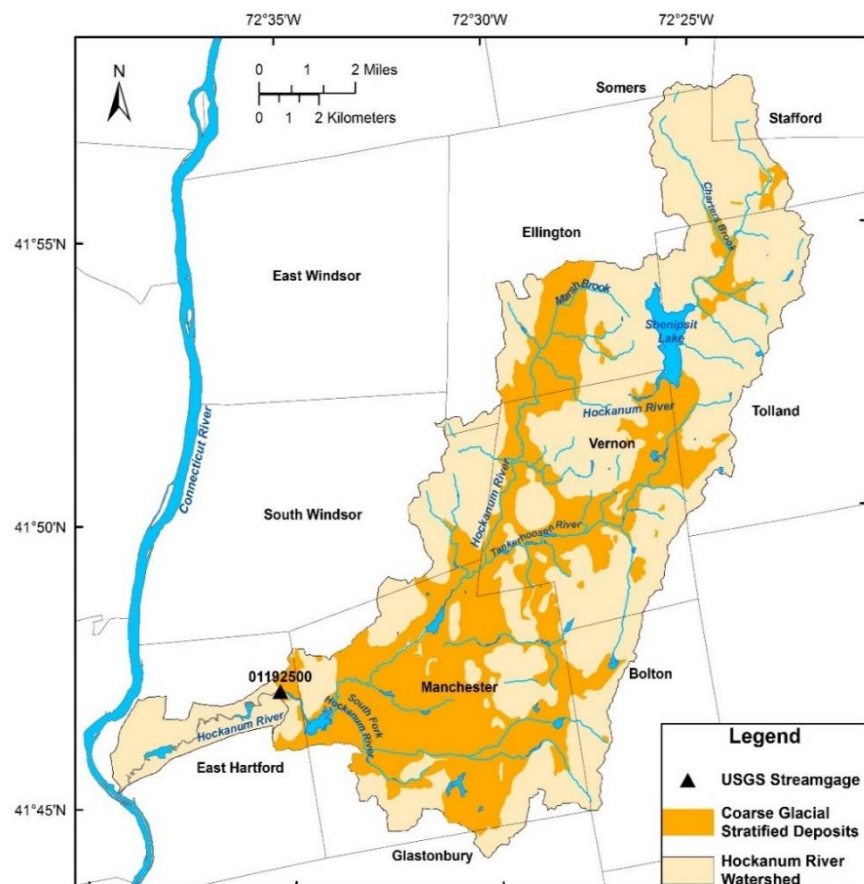


Figure 9. Hockanum River watershed including ungaged area.

microbial water quality monitoring station. It has been monitored for 84 of 96 years of record from 1919 to 2015. From 1919 to 2015, the mean daily discharge in the Hockanum River was $3.41 \text{ m}^3 \text{ s}^{-1}$ ($120.3 \text{ ft}^3 \text{ s}^{-1}$) and from 1980-2015, the mean daily discharge was $3.67 \text{ m}^3 \text{ s}^{-1}$ ($129.5 \text{ ft}^3 \text{ s}^{-1}$). These streamflows are equivalent to 559 and 602 mm yr⁻¹ (22.0 and 23.7 in yr⁻¹) of runoff for the gaged watershed. March and April have historically had the greatest average streamflows, and the lowest flows for the year can occur in July, August, or September. Peak streamflow can occur during any month but is usually associated with rain and snowmelt, large storms, or hurricane floods.

HOCKANUM RIVER WATERSHED CLIMATE

Climate in the Hockanum River watershed varies slightly when compared to the Pomperaug River basin. The reported average annual precipitation from 1930 to 1960 in Hartford was 1123 mm yr⁻¹ (44.2 in yr⁻¹) and was evenly distributed throughout each month (Ryder et al., 1981). For an updated comparison from 1980 to 2015, three COOP weather stations with complete records were evaluated. Bradley International Airport in Windsor Locks, Brainard Airport in Hartford, and the University of Connecticut weather station in Storrs are located just outside of the watershed (Figure 3); there are no continuously monitored or reported rain gages inside the watershed. The average annual observed precipitation between the three stations was 1250 mm yr⁻¹ (49.2 in yr⁻¹), lower than the precipitation in the Pomperaug River watershed. Isolated and randomly distributed storms will cause localized variations in precipitation from year to year. Snowfall varies from year to year but averages 1016 mm (40 in) annually in the Hockanum River watershed (Miller et al., 2002).

From 1980 to 2015, the average daily minimum and maximum temperatures for a year at the three weather stations range from 4.4 to 15.6 °C (40 to 60 °F), respectively. January and

February are also the coolest months and July and August are the warmest months in the watershed. PET will be greatest in the summer months due to high solar radiation and temperatures. PET and AET are often negligible during the winter. Evapotranspiration is estimated to be about half of the annual precipitation ranging from 509 to 558 mm (20 to 22 in) depending on the year (Ryder et al., 1981). Ryder et al. estimated the remainder of the water balance to be mostly runoff (1981).

HOCKANUM RIVER WATERSHED GEOLOGY

Geologically, the Hockanum River watershed is divided by the Eastern Border Fault so it is made up of both the Central Valley and Eastern Uplands (Ryder et al., 1981). When the fault formed about 200 million years ago, the Central Valley was downset from the land east of the fault. The valley filled with erodible sediment from the highlands. Glacial rivers and lakes and the present day Connecticut River further eroded the valley and deposited fluvial sediments and stratified drift throughout. The bedrock in the valley is mostly sedimentary and igneous and consists of red and brown sandstones. East of the border fault consists mainly of metamorphic crystalline bedrock, such as the Hebron Gneiss and Bolton Schists, igneous rocks, and glacial till (Aitken, 1955). The topography in the Eastern Uplands is much steeper than in the valley. The rivers and streams in the Hockanum River watershed generally flow west with occasional sharp angle turns north or south before flowing west again towards the Connecticut River (Aitken, 1955).

Manchester is located in the Central Valley and is underlain by large amounts of coarse stratified drift (Figure 9). This is important for aquifer recharge, groundwater contribution to rivers, and water quality. The remainder of the watershed's surficial geology is glacial till. The Central Valley bedrock is sedimentary rock, which allows for groundwater dissolution of the

rock. Therefore, the stream network in the Central Valley naturally has greater concentrations of dissolved solids than in the Eastern Uplands (Ryder et al., 1981).

HOCKANUM RIVER WATERSHED LAND USE

Historically, Native Americans cultivated fertile floodplains of the Hockanum River and used the area for hunting and fishing (Fuss & O'Neill, 2005). However, European settlers during the Revolutionary War clear cut the land for wide-scale agricultural use. When the majority of the agricultural industry left Connecticut, factories and mills along rivers became the primary economic market. The steep gradient of the Hockanum and its tributaries were well-suited for waterpower and led to the development of many textile and paper industries through the 1950's (Fuss & O'Neill, 2005). Although most of these businesses no longer exist, many of their antiquated river impoundment structures remain. Industrial work declined in Manchester and Vernon in the through the 1970's coinciding with a rapid population growth and commercial development. According to the United States 2010 Census, the population within the boundaries of the Hockanum River watershed is approximately 120,000, with Manchester and Vernon having the greatest populations in the watershed.

About half of the Hockanum River watershed is urbanized, especially in East Hartford, Manchester, and Vernon (Figure 11). As the Hockanum flows from the Shenipsit Lake downstream, it becomes increasingly developed with medium and high density housing as well as commercial and industrial land use. Some areas of the Hockanum River watershed are highly developed, but do not have a large population. For example, Interstate-84 (I-84) and Interstate-384 (I-384), Buckland Hills Mall (Manchester), the historic section of Rockville (Vernon), and their immediate surrounding areas have considerable impervious surface, but lower population densities. In Ellington, much of the land is still agriculture and relatively flat west of Shenipsit

Lake. Upstream areas north and east of Shenipsit Lake in Ellington and Tolland are mostly forested or have rural single family residential homes (Figure 12).

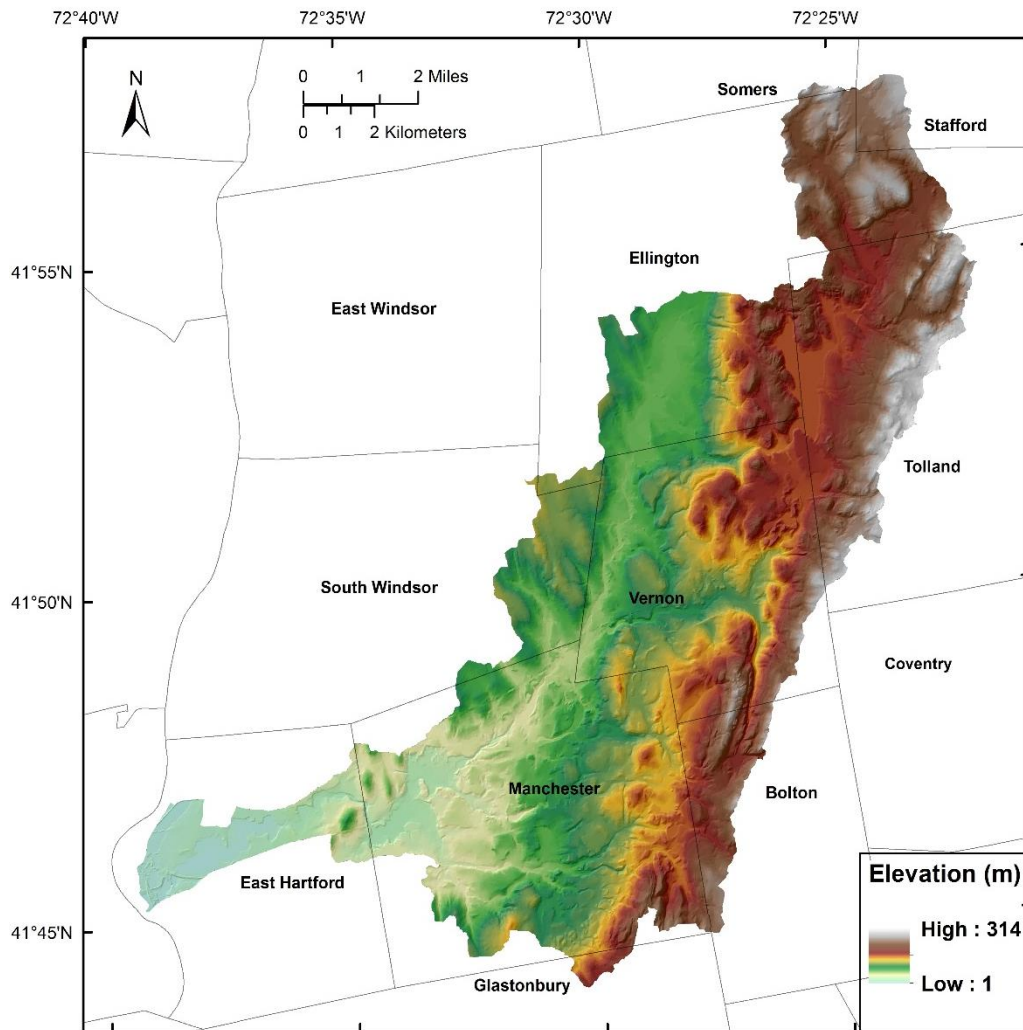


Figure 10. Digital elevation model of the Hockanum River watershed.

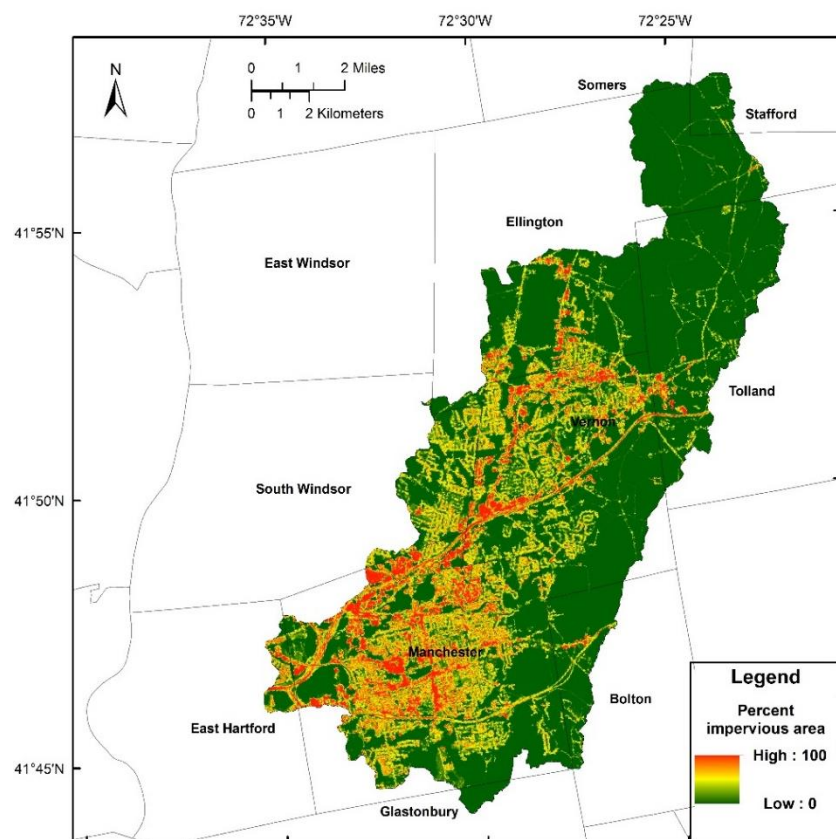


Figure 11. Percent impervious surface area in the Hockanum River watershed. GIS data from the NLCD.

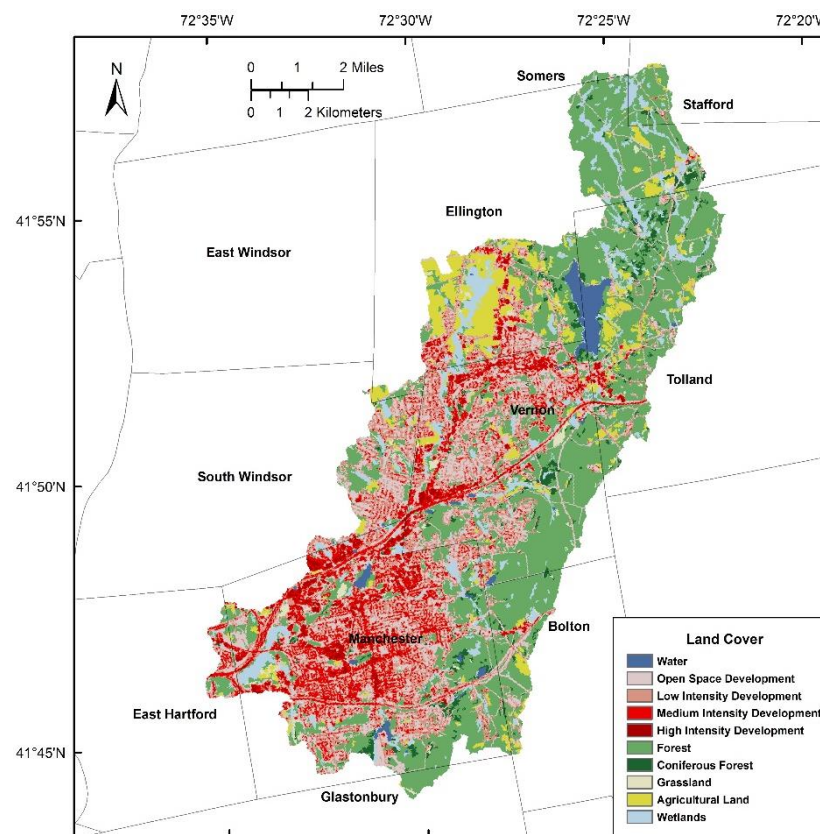


Figure 12. Land cover for the Hockanum River watershed. GIS data modified from the NLCD.

HOCKANUM RIVER WATERSHED WATER USE

Public water supply from surface water predominates over private wells in the lower Hockanum River watershed because of Shenipsit Lake and the Town of Manchester's water system. The Shenipsit Lake reservoir has been operated for public water supply since 1847 when the Rockville Aqueduct Company was founded. The company merged with Rockville Water Power Company in 1893. The Rockville Water and Aqueduct Company managed the reservoir until the city of Rockville acquired operations in 1957 (Pierce, 2017). Shenipsit Lake is currently controlled by the Connecticut Water Company (CWC) as part of its Northern-Western water system. Storage in the reservoir was estimated at 13,741,000 m³ (3.63 billion gallons) (Ryder et al., 1981).

Facilitated through the Northern-Western system, CWC provides water to customers in East Granby, East Windsor, Ellington, Enfield, Somers, South Windsor, Suffield, Tolland, Vernon, and Windsor Locks (Figure 13). The majority water source for the system is from Shenipsit Lake, with supplemental water blended in by various groundwater wells located throughout the serviced towns. Therefore, there is a daily transfer of water from the Hockanum River watershed to other river basins since the water is not returned. Average daily production of water for supply was estimated at 17,034 m³ day⁻¹ (4.5 millions of gallons per day, Mgd), but this number will vary seasonally (Connecticut Water Company, personal communication, 2017). In order to start supplying water to the University of Connecticut in 2017, the Rockville water treatment plant at Shenipsit Lake was upgraded from a maximum production capacity of 24,227 m³ day⁻¹ (6.4 Mgd) to 34,069 m³ day⁻¹ (9.0 Mgd). These changes post-date the study period of 1980-2015 and will be disregarded quantitatively, but they are considerations for future studies of the Hockanum River watershed.

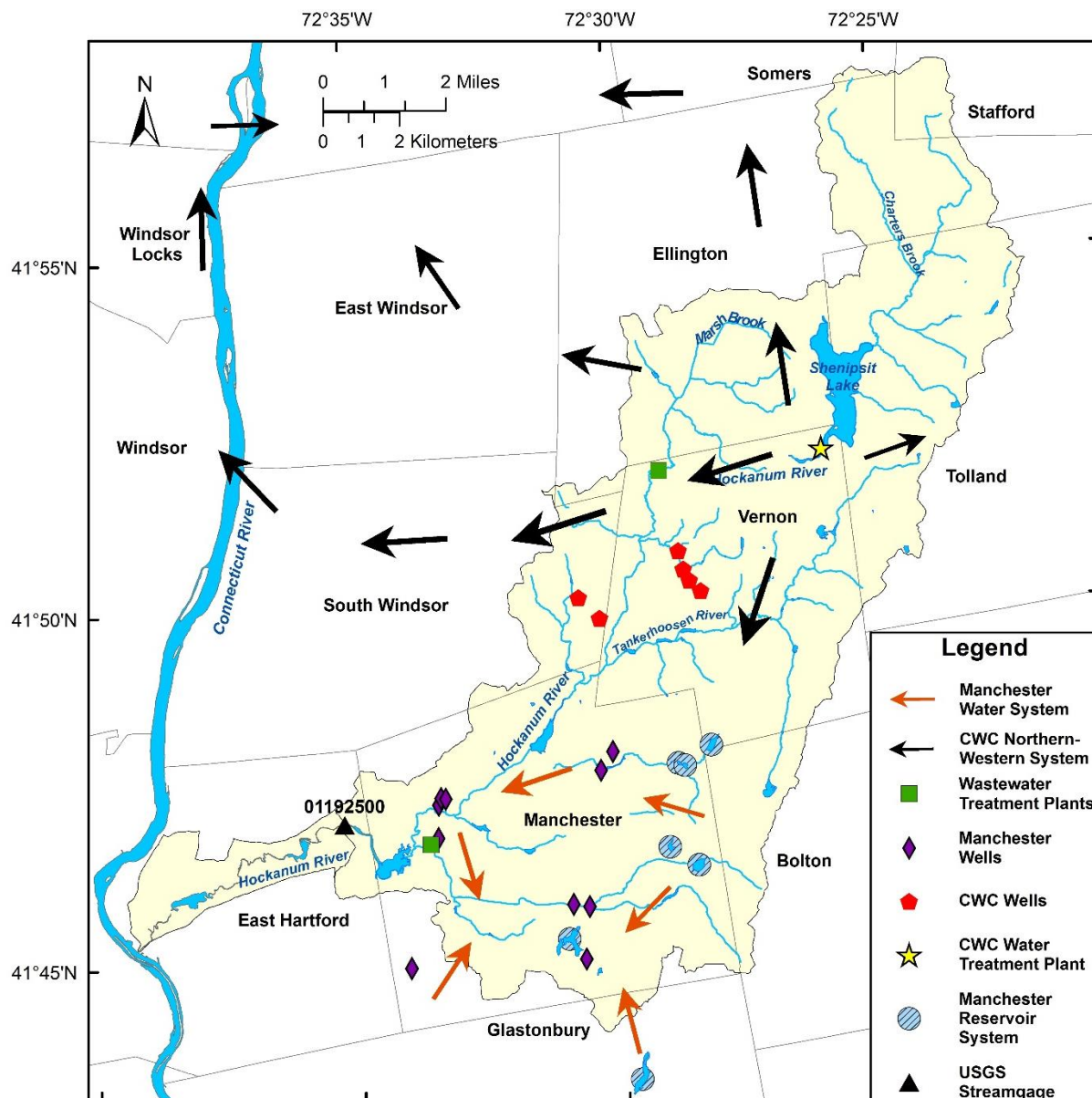


Figure 13. Depiction of water usage affecting the Hockanum River watershed. The arrows represent the generalized location of public water supply distribution by the Town of Manchester and CWC's Northern Western System. The arrows do not represent any quantitative data. The Town of Manchester consists of ten groundwater wells and seven surface water reservoirs. The CWC's system consists of six groundwater wells and the Shenipsit Lake surface reservoir. The locations of water supply wells are not exact due to protection of this information. Day-to-day data were not available for water supply distribution or wastewater treatment discharges.

Releases from Shenipsit Lake are required by the State of Connecticut Department of Energy and Environmental Protection (DEEP) to maintain safe ecological streamflows in the Hockanum River (Connecticut Department of Environmental Protection, 2015a). This

legislation from DEEP sets a daily release target from Shenipsit Lake at $7,949 \text{ m}^3 \text{ day}^{-1}$ (2.1 Mgd). However, there is an allowance for lesser discharges depending on the lake level because it is a public water supply source. There is an additional spring freshet requirement of $141,953 \text{ m}^3 \text{ day}^{-1}$ (37.5 Mgd). These releases cannot be quantified in the PRMS and would have to be accounted for outside of the model, but daily data are not available. Beginning in approximately 2025, new release requirements will be adopted for Shenipsit Lake that involve specific bioperiod releases (Connecticut Department of Environmental Protection, 2015b).

Manchester has its own town water supply within the Hockanum River watershed separate from CWC's Northern-Western system. The Manchester system consists of a series of seven surface water reservoirs and ten groundwater wells. Only the Buckingham reservoir is located outside the boundaries of the Hockanum River watershed and is a transfer of water into the basin. The Globe Hollow Reservoir is where the town's water treatment plant is located and is gravity fed by the other six reservoirs. This reservoir is the main source of water for the town during the winter. During peak demand in the summer water is supplied to customers by both the reservoir and the ten groundwater wells (Figure 13). A relatively small amount of this public water is provided to localized areas outside of the Hockanum River watershed.

There are two sewer treatment plants within the Hockanum River watershed, one in Vernon and one in Manchester (Figure 13). Sewer treatment plants are another water use consideration when hydrologically modeling a watershed because they discharge daily into a river, which might alter a daily hydrograph that a simulation might not capture. The Vernon sewer treatment plant was permitted to discharge $26,876 \text{ m}^3 \text{ day}^{-1}$ (7.1 Mgd) (Connecticut Department of Environmental Protection, 2004), while the Manchester sewer treatment plant was permitted to discharge $31,040 \text{ m}^3 \text{ day}^{-1}$ (8.2 Mgd) (Connecticut Department of Environmental

Protection, 2006), a combined maximum $0.67 \text{ m}^3 \text{ s}^{-1}$ ($23.7 \text{ ft}^3 \text{ s}^{-1}$) discharged to the river.

However, daily discharge data are not available. Also, the sources to the sewer treatment plant are not strictly from inside the basin. For example, the Vernon treatment plant discharges into the Hockanum River, but its sources are from Vernon, Ellington, Manchester, South Windsor, and Tolland, which may include customers that are using water from a different river basin.

Water diversions are either registered (prior to 1983) or permitted through the Connecticut DEEP. All of the documented registrations and permits during the study the period are listed in Table D-1 of Appendix D. Registrations are difficult for water planning because they do not always represent realistic water capacity or use amounts, but they legally allow for diverting that much water. For example, Shenipsit Lake is registered for a $56,781 \text{ m}^3 \text{ day}^{-1}$ (15 Mgd) diversion even though the water treatment plant cannot operate at that capacity. Although some of these companies no longer exist or have changed names, the registrations can transfer companies or be used at a later time. The number of diversions in the watershed and the potentially false maximum usage create complexity for hydrological simulations. Therefore, only the major diversion of Shenipsit Lake was considered for this study

This discussion highlights the some of the considerations and complications of interbasin transfers when hydrologically modeling a watershed.

PARAMETERIZATION OF THE HOCKANUM RIVER WATERSHED MODEL

The Hockanum River is a complex watershed that has not been modeled before in PRMS. Through prior experience with the Pomperaug River PRMS model and help from USGS manuals and its staff, a new model was parameterized and calibrated for the Hockanum River. The following describes parameterization and calibration of the model. Additional in depth

information regarding specific calculations is provided in Appendix E. All final parameters are available digitally in Appendix G.

HYDROLOGIC RESPONSE UNIT (HRU) DELINEATION

Numerous input parameters and climate data were required to create a hydrologic model of the Hockanum River watershed in PRMS. The initial set of steps involved delineation of the watershed and subdivision into HRU's. First, the digital elevation model (DEM) for an area fully encompassing the potential watershed was downloaded from the Natural Resources Conservation Service's (NRCS) National Elevation Dataset (NED). The resolution of the DEM used was 10 meter and was imported into ESRI's geographic information systems (GIS) software ArcMap. The DEM was re-projected to the North American Datum (NAD) 83-2011 Connecticut State Plane coordinate system in meters.

Within ArcMap there is a Hydrology "toolbox" that contains a set of tools to determine hydrologic characteristics of a watershed. In addition, ESRI offers another toolbox available for download called ArcHydro that is used in ArcMap. Along with other spatial analyst tools, both of the aforementioned hydrology toolboxes were necessary for delineating HRU's. First, the "Fill" tool raised sinks in the DEM by increasing the sink's z-coordinate value to reduce the vertical difference from that of the surrounding cells. These sinks were holes in the raster dataset which do not exist or were much lower than the surrounding eight raster cells; therefore, there could be no hydrologic flow from those cells. Once the DEM was filled, the "Flow Direction" tool determined the direction flow to each adjacent cell based on the steepest elevation. A flow direction raster can create a watershed with the selection of a drain point; any water flowing to the drain point due to topography would be included in the watershed area. The "Watershed" tool used the flow direction raster and the USGS streamgage as a drain point to delineate the

Hockanum River watershed. The area draining to the streamgage created by the Watershed tool was 192 km² (74.1 mi²).

The DEM and flow direction rasters were clipped to the extent of this newly delineated watershed; this area was used for all further watershed processing. Next, the “Flow Accumulation” tool processed the DEM and flow direction rasters to calculate accumulated flow into each cell from all upslope cells. The “Stream Definition” tool in the Terrain Preprocessing subset of ArcHydro used the flow accumulation raster to compute a stream grid based a defined threshold. All cells from the flow accumulation raster that have a value greater than the threshold are designated as part of the stream grid, and other cells are designated no data. Therefore, a smaller threshold will produce a denser stream network and vice-versa. A denser stream network will ultimately create more HRU’s. For the Hockanum River watershed, a 20,000 cell threshold was used to approximately represent 1% of maximum flow accumulation.

The “Stream Segmentation” tool assigned unique segment identification to the stream network based on inputted stream definition and flow direction grids. Finally, the “Catchment Grid Delineation” tool used the unique stream segments to create subwatersheds, which represent HRU’s. There were anomalies created with this tool that had be processed manually and reclassified to larger HRU’s. This completed the delineation of the 56 HRU’s (Figure 14), which range from 0.34 to 9.36 km² (84.5 to 2,314 acres). These HRU’s roughly match sub-watersheds of tributaries to the Hockanum River. This procedure differed from the Pomperaug study, which used left and right hillslopes to define HRU’s.

CLIMATIC MODULES

In the Hockanum River watershed, the climate-by-HRU (CBH) module, *climate_hru*, controlled daily precipitation, temperature, and solar radiation, while *potet_jh* controlled

potential evapotranspiration. Mathematical relationships between inputted location parameters of the watershed, such as elevation and latitude, and climate processes are used by these modules to more accurately portray local weather patterns.

The Climate-by-HRU distribution module was chosen for the Hockanum River watershed due to the complexity of setting up appropriate *xyz_dist* parameters and the ease of data access for each HRU from Daymet. A GIS shapefile of the 56 delineated HRU's was uploaded into the USGS's GeoDataPortal (GDP), which had climate variables from Daymet from 1980 to 2015 for the conterminous United States. This process provided daily precipitation,

solar radiation, and maximum and minimum temperature values distributed to each HRU (Thornton et al., 2017). These data were converted into usable CBH input files for PRMS.

Along with GIS determined physical characteristics of the watershed, these inputted climate data are assumed to be accurate and would not be subject to a calibration process. However, the results produced by the Daymet climate data were still compared with three other weather station observations to ensure the PRMS model was simulating the climatic water balance appropriately, e.g. precipitation, and minimum and maximum daily temperature. The

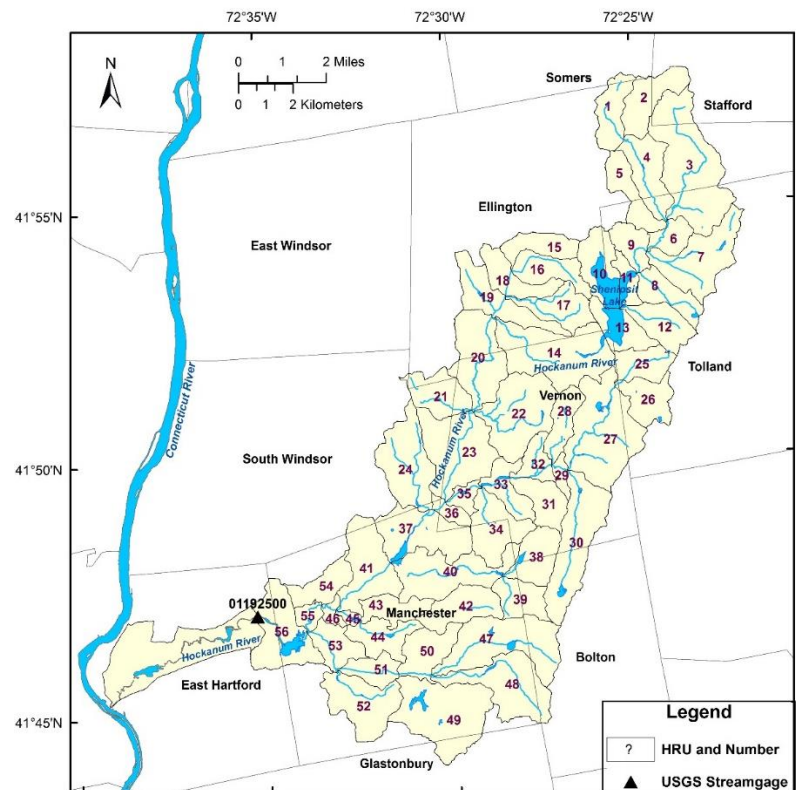


Figure 14. Hockanum River study area with delineated HRUs.

three weather stations used were located at Bradley Airport, Brainard Airport, and Storrs, Connecticut (Figure 3). There are inherent inconsistencies in climate data within individual and amongst the Daymet and weather stations due to differences in who and how the data were collected. In general the data are considered appropriate for usage and comparison.

RUNOFF

Runoff in the Hockanum River model was calculated with the same modules as in the Pomperaug River model. However, the Hockanum River model required full parameterization to simulate these processes as opposed to using a previously developed model. Further detail beyond the impervious coverage calculations are described in Appendix E.

IMPERVIOUS SURFACE

NLCD impervious surface raster data from 2011 was used to determine the mean percent of impervious coverage in each HRU. The “Tabulate Area” spatial analyst tool in ArcMap outputted a table of the percent imperviousness for each HRU. However, these data are considered the TIA and subsequent calculation of EIA was required. The Transitional method of estimating EIA from TIA was applied to the Hockanum River PRMS model (Equation 2) to set the parameter **hru_percent_imperv**.

FULL BUILDOUT ANALYSIS

Full buildout analyses can project potential future developmental and land use conditions based on current town zoning regulations. These buildouts have been implemented to study impacts of growth on a state’s communities (Rozum et al., 2008). The buildouts can then in turn help a town’s planning with its future zoning decisions depending on its growth and economic goals. Buildout analyses vary in complexity and accuracy depending on its goals, techniques,

and data availability. Therefore, thorough documentation of a buildout analysis is imperative to interpreting its results.

A buildout analysis was conducted in this study for the Hockanum River to estimate future impervious coverage. This provides a method of determining maximum development in the watershed based on zoning regulations and undevelopable land. The data available were more limited in the Hockanum River watershed than for the Pomperaug study. Therefore, the full-buildout analysis for this thesis was conducted with a number of assumptions made and should be considered limited in its applications outside of this study.

Certain data are required to conduct the buildout analysis such as land cover, the watershed boundaries, unsuitable areas for development including steep slopes or previously developed land, and local zoning regulations (Giannotti & Prisloe, 1998; Rozum et al., 2008). Table 2 lists the data that were removed as potential development sites for the Hockanum River buildout scenarios. The following was the procedure conducted to determine the maximum development extent for each HRU based on zoning regulations in Manchester, Vernon, South Windsor, Tolland, Ellington, and Bolton. These towns were used because they encompass the majority of the gaged watershed area.

Table 2. Lands considered undevelopable and were removed from the buildout analysis.

| Undevelopable Land |
|---------------------------|
| Slopes >20% |
| Wetlands |
| Hydrography |
| Previously Developed Land |

Table 3. Urban and rural impervious area coefficients that were multiplied by developable land to determine the additional extent of impervious surface coverage.

| Impervious Area Coefficients | | |
|------------------------------|-------|-------|
| Zone | Urban | Rural |
| Residential | 0.35 | 0.25 |
| Commercial | 0.85 | 0.75 |
| Industrial | 0.72 | 0.65 |
| Mixed Use | 0.75 | - |

DETERMINATION OF DEVELOPMENTAL EXTENT

First, the slope as percentage rise was determined from the DEM for each town that makes up the Hockanum River watershed. These data were reclassified so that slopes less than 20% were NoData. This created a raster with slopes greater than 20%. Starting from a polygon inclusive of all Hockanum River watershed towns, slopes greater than 20%, areas classified as wetlands, and all hydrography were erased. It should be noted that an assumption was made to leave protected open spaces as developable land in order to maximize the buildout. This new polygon represented lands that were developable. The NLCD land use data were then reclassified so that water, developed land (open space, low, medium, & high intensities), and all wetlands were considered NoData. This developable land use raster was clipped to the extent of the polygon of developable lands to further remove undevelopable land that may have existed in the land use data.

The “Identity” analysis tool in ArcMap was used to apply the Capitol Region Council of Governments (CRCOG) regionalized zoning, which was associated to each town, to every HRU in the watershed. This provided zoning by town by HRU within the polygon. The “Tabulate Intersection” tool was run with the identity tool result as zone features, the zone fields as each HRU, CRCOG zone, and town, and developable lands polygon as the input class features. This process calculated the amount of developable land by zoning category by town by HRU.

Often a town will set a maximum impervious lot coverage in its zoning regulations for new developments. For the purposes of this study, lot coverages from Manchester, South Windsor, and Vernon were considered more urbanized than Bolton, Ellington, and Tolland. Therefore, generalized impervious surface coefficients (Table 3), determined by the towns’ relative urban or rural zoning status, were multiplied by the developable land area in each HRU

to calculate additional impervious coverage. Zoning from the three urban towns were applied to East Hartford, which has minimal area in the gaged watershed, and zoning from the three rural towns were applied to the minimal areas of Glastonbury, Somers, and Stafford. This additional impervious coverage was added to the current impervious surface extent in each HRU to determine the maximum extent of TIA from a full buildout. The TIA was then subjected to the aforementioned EIA Equation 2 so that it could be used for **hru_percent_imperv**. The results are provided in Appendix G.

STREAMFLOW ROUTING

Similar to the Pomperaug River PRMS model, Muskingum Routing was implemented on the Hockanum River watershed. The stream segments are depicted in Figure C-2 of Appendix C, while the stream length and **K_coef** were calculated with the previously described methods and their results are listed in Appendix G. An **x_coef** of 0.2 was used for flow wave attenuation, the same value that was used in the Pomperaug River watershed model. It is important to note that an **x_coef** of 0 was used to simulate the major reservoir storage occurring at Shenipsit Lake.

DEVELOPMENT SCENARIOS

Entire watershed and local, specific HRU development scenarios were conducted in both models. Four entire basin scenarios were run in both watersheds. Of the four, each model was run with current land cover conditions to calibrate the model and provide baseline results for each watershed. Also, parameter files with fully undeveloped and entirely forested land cover were created for each watershed to determine what the water balance may have been prior to impervious surface or agricultural land development. For each watershed two scenarios were implemented to assess full buildout relative to what current zoning regulations allow, with

appropriate methods of estimating EIA and minimizing and maximizing stormwater collection for each scenario.

Along with the four basin-wide scenarios, four scenarios in the Pomperaug and three scenarios in the Hockanum were designed to analyze any locational effects of increased impervious coverage on the components of streamflow for each watershed. These scenarios academically ignored zoning regulations.

To test the three methods of estimating EIA from TIA in each watershed, sets of TIA values were applied throughout both watersheds. All parameters that were changed for each of the scenarios described are provided digitally in Appendix G.

SPECIFIC POMPERAUG RIVER WATERSHED DEVELOPMENT SCENARIOS

Two full buildout scenarios were evaluated in the Pomperaug River. The first scenario represents a full buildout that has limited stormwater collection, which used the Rural method of estimating EIA (Equation 3). The second scenario represents development in a watershed that has maximum stormwater collection, which increases the EIA relative to the first method. The Transitional method of estimating EIA was applied to simulated maximum stormwater collection (Equation 2). The full buildout total impervious area values determined in the Bjerklie et al. (2010) study were used to reflect current zoning regulations.

The first three local development scenarios involved individually building out the three main subbasins (Figure 15). The Nonnewaug and Weekeepeemee River watersheds are upstream development, while the Pomperaug subbasin is downstream development. The fourth scenario developed both the Nonnewaug and Weekeepeemee River watersheds in order to determine if there any additional downstream impacts.

Each of these localized buildout scenarios were developed beyond what is allowed by zoning regulations. This is strictly an academic assumption to reflect the question, “If a town wanted to facilitate economic and resident growth, what impacts would the increased impervious coverage have on the water balance?”. In order to answer this question, the town of Manchester, Connecticut was used as a template for development because of its suburban housing with large commercial or industrial areas. Manchester’s overall TIA of 24.7% was converted into EIA and inputted into each HRU for a given subbasin’s development scenario. Equation 2, the Transitional method of estimating EIA, was used to calculate EIA for developed HRU’s because Manchester has stormwater collection systems. Current TIA values were used for HRU’s not subjected development.

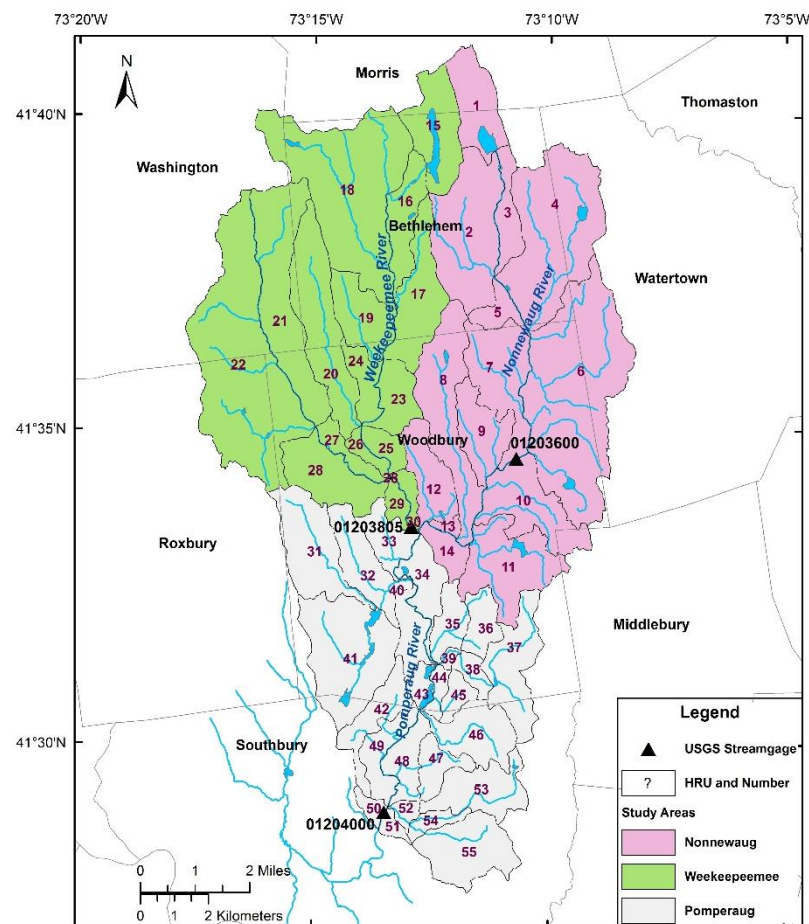


Figure 15. The three subbasins that make up the Pomperaug River watershed. These subbasins were used as study areas.

SPECIFIC HOCKANUM RIVER WATERSHED DEVELOPMENT SCENARIOS

Two full buildout scenarios were evaluated in the Hockanum River. The first scenario represents a full buildout that has current stormwater collection, which used the Transitional method of estimating EIA (Equation 2); this will be considered minimum stormwater collection because it is relative to the next scenario and independent of the Pomperaug’s “minimum stormwater collection”. The second scenario represents full buildout of the Hockanum with maximum stormwater collection. The Urban method of estimating EIA was applied to simulated maximum stormwater collection (Equation 1). The full buildout TIA values determined in the previously discussed full buildout analysis were used to estimate EIA.

The next three local development scenarios involved individually building out three subbasins (Figure 16). The geography of the Hockanum River watershed is different than in the Pomperaug River watershed. Therefore, the Hockanum River watershed was broken up into three approximately equal study areas. The Upper, Middle, and Lower watershed study areas follow stream network drainage, but are not exact

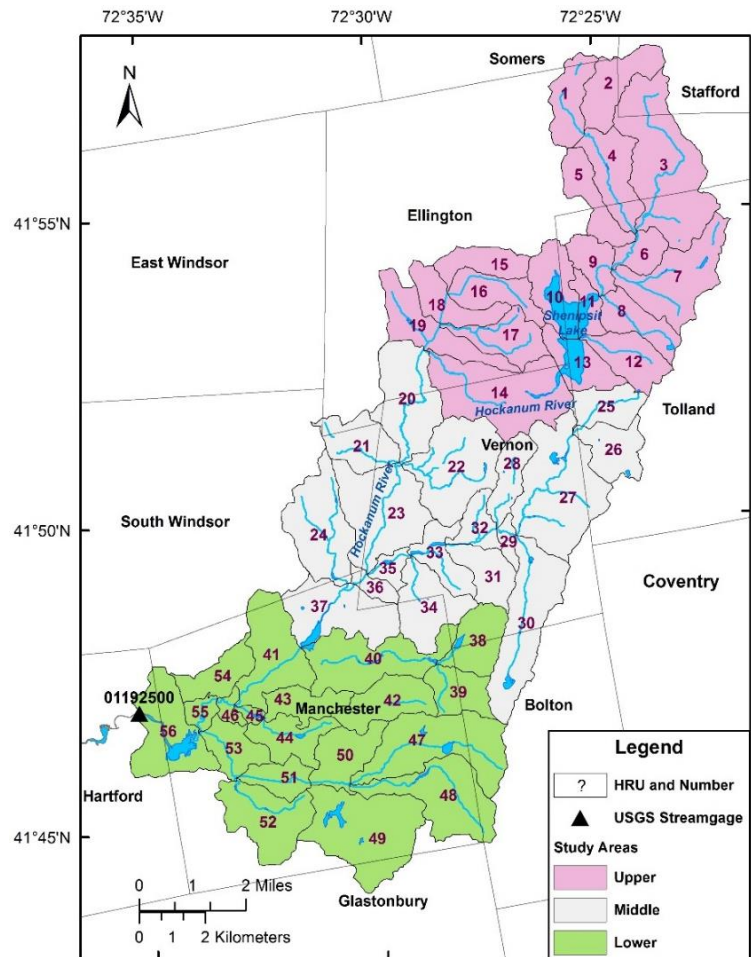


Figure 16. The three study areas used in the Hockanum River watershed. These areas were delineated following the stream network, but are not specific subwatersheds like in the Pomperaug watershed.

subbasins. They are 63.2 km² (24.4 mi²), 65.0 km² (25.1mi²), and 63.7 km² (24.6 mi²), respectively.

Just like in the Pomperaug, each of these buildout scenarios were developed beyond what is allowed by zoning regulations. HRU 44, which has the largest percentage of TIA at 43.0%, was used to estimate EIA and inputted into each HRU for a given study area's development scenario. Equation 2, the Transitional method of estimating EIA, was used to calculate EIA for developed HRU's and non-developed HRU's. Current TIA values were used for HRU's not subjected development.

TEST OF EFFECTIVE IMPERVIOUS ESTIMATION METHODS

Different TIA's of 12.5%, 25%, 50%, 75%, and 100% were used to test the relative effects that the various EIA estimation methods had on the two watersheds. Each of these TIA's were applied throughout both watersheds regardless of current TIA. A value of 12.5% was chosen as the lowest TIA to test because 12 to 13% TIA has shown to significantly reduce water quality downstream of the impervious surface (Bellucci, 2007). The other TIA values were chosen arbitrarily and were a method of observing the impacts of increased TIA, i.e. how do the methods of estimating EIA handle urbanization? In total, 30 PRMS outputs were created between the two watersheds; five TIA's for three different methods of estimating EIA in each watershed.

PRMS OUTPUT VARIABLES UTILIZED

The primary PRMS output variables used for this study are listed in Table 4. These outputs represent the components of streamflow and some of the climatic variables that govern a watershed's overall water balance. The appropriate HRU variable counterparts were also used in addition to the basin-wide variables described below.

Table 4. List of the primary output variables from PRMS used in this study.

| Output Parameter | Description | Output Units |
|-------------------------|--|--------------|
| <i>streamflow_cfs</i> | Observed daily streamflow at basin outflow gage station | CFS |
| <i>basin_cfs</i> | Simulated daily streamflow leaving the basin through the stream network | CFS |
| <i>basin_sroff_cfs</i> | Simulated daily basin area-weighted average surface runoff to the stream network | CFS |
| <i>basin_ssflow_cfs</i> | Simulated daily basin area-weighted average subsurface flow to the stream network | CFS |
| <i>basin_gwflow_cfs</i> | Simulated daily basin area-weighted average groundwater flow to the stream network | CFS |
| <i>basin_potet</i> | Simulated daily basin area-weighted average potential evapotranspiration | Inches |
| <i>basin_actet</i> | Simulated daily basin area-weighted average actual evapotranspiration | Inches |
| <i>basin_ppt</i> | Simulated daily basin area-weighted average precipitation | Inches |
| <i>basin_tmax</i> | Simulated daily basin area-weighted maximum air temperature | °F |
| <i>basin_tmin</i> | Simulated daily basin area-weighted minimum air temperature | °F |

MODEL PERFORMANCE EVALUATION: NASH-SUTCLIFFE EFFICIENCY

In order to properly communicate hydrologic modeling results, model performance must be evaluated. The Nash-Sutcliffe Efficiency (NSE) index (Nash & Sutcliffe, 1970) is one of the most common methods of evaluating surface water modeling performance (Schaepli & Gupta, 2007). The NSE is a normalized measurement of model accuracy that compares mean square error for a model simulation to the variance of the target output (Schaepli & Gupta, 2007). The NSE index is calculated by the following Equation 5:

$$NSE = 1 - \frac{\sum_{t=1}^N [Q_{obs}(t) - Q_{sim}(t)]^2}{\sum_{t=1}^N [Q_{obs}(t) - \bar{Q}_{obs}]^2} \quad (5)$$

where Q_{sim} is the model simulated streamflow, Q_{obs} is the observed streamflow, and \bar{Q}_{obs} is the average observed streamflow for the time reference (daily, monthly, etc...) examined. The NSE ranges from $-\infty$ to 1, of which an NSE less than 0 occurs when the observed average is a better predictor itself than what is simulated by the model. An NSE closer to 1 indicates a more

accurate simulation, and greater than 0.5 is generally used as an indicator of a well performing hydrologic model (Moriiasi et al., 2007).

The NSE is limited due to the sensitivity for a greater squared difference between observed and simulated values with larger discharge events. Inherently, a handful of large storms throughout the record could distort the NSE value. Therefore the Log NSE, which requires taking the Log transform of each individual value and calculating the result with the same method as Equation 5, is a useful measure that can help reduce the effects large discharge events have on the NSE. If a Log NSE value is greater than the NSE value, it is indicative of a model that is simulating lower flows better than higher flows. Both the NSE and Log NSE are used in this study.

RESULTS AND DISCUSSION OF THE PRMS INVESTIGATIONS

RESULTS OF THE POMPERAUG RIVER CURRENT CONDITIONS MODEL

Despite having the previous Pomperaug River watershed model available for the majority of parameters required for PRMS, the model needed to be adjusted slightly to account for the new PRMS software and to fit a new study time period. Therefore, the following describes the results from the current condition, baseline model to ensure that the water balance was simulated correctly. This includes calibration of both the long-term water balance and daily streamflow conditions.

LONG-TERM WATER BALANCE

The long-term water balance in the natural world is controlled by climate and is thereby calibrated first in the model. It is imperative that these processes are simulated accurately to best predict streamflow and its components throughout the entirety of the study period. A model's streamflow could be calibrated by curve matching, but this does not necessarily portray natural conditions. The model itself and any changes in the model, such as developmental or climate change scenarios, would not be realistic and have limited applications.

Input data with respect to climate for the Pomperaug River PRMS model included four NOAA COOP weather stations (Danbury, Middletown, Woodbury, and Bradley Airport) and their daily precipitation, maximum temperature, and minimum temperatures from 1980 to 2015. To ensure that this input data, along with relevant model parameters, were simulated correctly, the observed climate station data were compared to the simulated outputs from the current conditions and baseline PRMS model. Figure 17 a, b, & c depict the average observed precipitation and temperature data from the four weather stations used as inputs along with PRMS simulations. The data were organized by month to ensure correct simulation of

seasonality. The PRMS model for the Pomperaug River outputted temperatures and precipitation accurately on a monthly basis (Figure 17 a, b, & c).

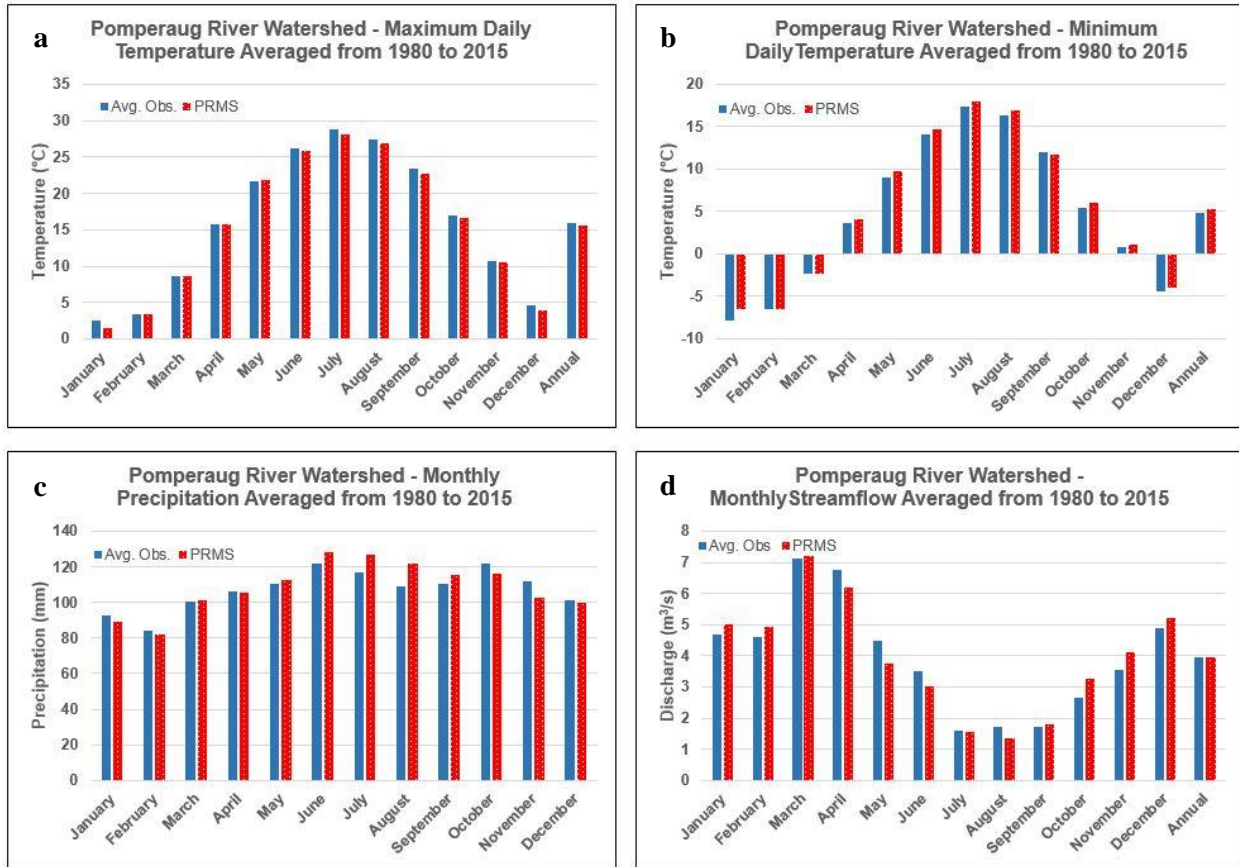


Figure 17. Observed versus simulated water balance data in the Pomperaug River. **a.** Maximum daily temperature averaged by month from between four observed weather stations and PRMS’s simulated output; **b.** Minimum daily temperature averaged by month between four observed weather stations and PRMS’s simulated output; **c.** Monthly precipitation averaged between four observed weather stations and PRMS’s simulated output; **d.** Daily streamflow averaged by month between the USGS streamgage and PRMS’s simulated output.

Annual climate conditions were evaluated in addition to seasonality. Average annual precipitation was simulated at 1311 mm (51.6 in), slightly greater than the previously reported 1168 to 1270 mm yr⁻¹ (46 to 50 in yr⁻¹). Actual evapotranspiration (AET) was estimated by the model to be 670 mm yr⁻¹ (26.4 in yr⁻¹) during the study period, which falls within the expected 584 to 686 mm yr⁻¹ (23 to 27 in yr⁻¹) range. This is 51% of the estimated annual precipitation and is similar to previous predictions.

Over long timescales the net change in storage in a watershed should approximate 0. The annual change in storage is calculated using Equation 6.

$$\Delta S = P - Q - AET - q \quad (6)$$

where ΔS is the change in storage, P is the precipitation, Q is the area weighted streamflow, AET is the actual evapotranspiration, and q is the export from diversions or withdrawals from the watershed, all of which are annual values in millimeters. The annual changes in storage are then summed to calculate the net storage. The net storage in the Pomperaug River approximated an increase of 37.7 mm (1.5 in) over 34 years of record excluding the first warmup year (Table 5). This is reasonable given variations in annual precipitation. No major exports were expected on a long-term scale; exports were accounted for in the Bjerklie et al. study (2010).

The simulated streamflow can be compared to collected streamgauge data. In the Pomperaug River, average daily streamflow from water year 1982 to 2015 recorded at USGS gage 01204000 was $4.00 \text{ m}^3 \text{ s}^{-1}$ ($141.2 \text{ ft}^3 \text{ s}^{-1}$). During the same time period, PRMS simulated discharge at the Pomperaug River to be $3.97 \text{ m}^3 \text{ s}^{-1}$ ($140.3 \text{ ft}^3 \text{ s}^{-1}$). Average contribution to total streamflow was $0.48 \text{ m}^3 \text{ s}^{-1}$ ($17.1 \text{ ft}^3 \text{ s}^{-1}$) from surface runoff, $1.01 \text{ m}^3 \text{ s}^{-1}$ ($35.8 \text{ ft}^3 \text{ s}^{-1}$) from subsurface flow, and $2.48 \text{ m}^3 \text{ s}^{-1}$ ($87.4 \text{ ft}^3 \text{ s}^{-1}$) from groundwater flow. It can be seen that the seasonality of streamflow was partitioned accurately in Figure 17d.

In the Pomperaug River, groundwater contribution to streamflow has been estimated at anywhere from 40 to 50% (Meinzer & Stearns, 1929) to 60 to 70% (Bjerklie et al., 2010). The baseline model in this study outputted a 62% contribution. To ensure that PRMS was estimating groundwater contribution correctly, it was verified using the Partition (PART) baseflow separation method within USGS's software Groundwater Toolbox (Barlow et al., 2015). Groundwater Toolbox estimated around 68% contribution from both the observed and simulated data (Table 6.), which is still within the expected range.

Table 5. Change in storage by year for the Pomperaug River watershed as simulated by PRMS.

| Water Year | Annual Precipitation (mm) | Annual AET (mm) | Daily Average Simulated Streamflow (mm) | Change in Storage (mm) | Daily Average Observed. Streamflow (mm) |
|------------------------------------|----------------------------------|------------------------|--|-------------------------------|--|
| 1982 | 1386.7 | 644.5 | 744.3 | -2.1 | 698.1 |
| 1983 | 1407.8 | 589.6 | 820.4 | -2.2 | 766.3 |
| 1984 | 1610.4 | 622.9 | 995.7 | -8.2 | 948.5 |
| 1985 | 1088.4 | 744.5 | 293.2 | 50.7 | 316.9 |
| 1986 | 1067.5 | 641.9 | 490.4 | -64.7 | 473.8 |
| 1987 | 1315.3 | 590.2 | 661.7 | 63.4 | 702.3 |
| 1988 | 994.2 | 606.7 | 450.2 | -62.7 | 394.2 |
| 1989 | 1475.9 | 739.8 | 665.4 | 70.8 | 681.1 |
| 1990 | 1357.9 | 697.9 | 705.9 | -45.8 | 784.2 |
| 1991 | 1421.8 | 688.5 | 651.5 | 81.8 | 621.5 |
| 1992 | 1247.8 | 741.3 | 576.9 | -70.3 | 539.8 |
| 1993 | 1278.0 | 564.7 | 666.7 | 46.6 | 628.5 |
| 1994 | 1466.4 | 727.5 | 731.2 | 7.7 | 789.2 |
| 1995 | 946.9 | 557.3 | 450.3 | -60.7 | 501.0 |
| 1996 | 1565.0 | 667.5 | 825.3 | 72.1 | 803.9 |
| 1997 | 1351.6 | 649.0 | 781.5 | -78.9 | 831.3 |
| 1998 | 1326.8 | 662.4 | 643.1 | 21.3 | 612.6 |
| 1999 | 1297.4 | 547.4 | 672.8 | 77.2 | 548.7 |
| 2000 | 1268.1 | 760.4 | 587.6 | -79.9 | 622.4 |
| 2001 | 1103.4 | 597.3 | 474.5 | 31.6 | 526.5 |
| 2002 | 929.8 | 659.4 | 309.5 | -39.1 | 289.7 |
| 2003 | 1503.4 | 754.3 | 667.3 | 81.8 | 674.2 |
| 2004 | 1360.8 | 687.4 | 675.8 | -2.5 | 694.1 |
| 2005 | 1059.3 | 580.6 | 580.4 | -101.7 | 531.7 |
| 2006 | 1723.9 | 763.6 | 933.1 | 27.2 | 897.9 |
| 2007 | 1217.3 | 606.2 | 649.5 | -38.3 | 659.1 |
| 2008 | 1624.0 | 803.8 | 719.4 | 100.9 | 696.4 |
| 2009 | 1288.8 | 745.1 | 611.2 | -67.5 | 740.2 |
| 2010 | 1242.0 | 579.1 | 637.8 | 25.1 | 655.3 |
| 2011 | 1844.1 | 781.6 | 975.2 | 87.3 | 1054.8 |
| 2012 | 1206.8 | 739.1 | 556.8 | -89.1 | 575.8 |
| 2013 | 1271.9 | 761.6 | 529.8 | -19.5 | 622.3 |
| 2014 | 1156.0 | 625.9 | 548.7 | -18.6 | 546.8 |
| 2015 | 1181.8 | 665.3 | 472.2 | 44.3 | 458.9 |
| Net Change in Storage (mm): | | | | 37.7 | |

Table 6. Estimated groundwater contribution to streamflow in the Pomperaug River.

| Groundwater Contribution to Streamflow | | Method |
|---|-------|---------------|
| Observed | 68.1% | GW Toolbox |
| Simulated | 68.7% | GW Toolbox |
| Simulated | 62.3% | PRMS |

DAILY DISCHARGE TIMING AND BASE-FLOW RECESSION

The magnitude of the daily fluxes in streamflow and its components and the hydrograph are calibrated after the long-term water balance and was aided by sensitivity analyses of parameters. The calculated daily Nash-Sutcliffe Efficiency (NSE) coefficients for the Pomperaug model were 0.65 with a Log NSE of 0.77 (Table 7). This indicates good model performance and that the model is generally simulating lower flows better than higher flows. The model performance increased in the monthly and annual NSE calculations, which demonstrates that the model handles streamflow better when aggregated on longer timescales. Seasonally, the model also performed well, except during July, August, and September, months that are subject to thunderstorms and hurricanes. The year 1999 is an example of the limitation of the NSE measurement due to Hurricane Floyd (Table 7). If the day of precipitation and successive two days (September 16th – 18th) are removed from the NSE calculation, the coefficient increases from -0.10 to over 0.7. Thus the model performed well for the remainder of the 362 days, i.e. after exclusion of the large hurricane event.

Of the three components of streamflow, only groundwater flow can be evaluated with certainty based on observed data. Streamflow recession can be monitored after the completion of a precipitation event and occurrence of the river's peak discharge. This is known as a base-flow recession curve. The model should be simulating the rate of streamflow recession accurately even if the exact discharges are slightly off. For example, Figure 18 depicts a precipitation event where the Pomperaug River's discharge increases and then recedes back to contribution from only groundwater flow. The model is simulating the rate of decrease and post-precipitation groundwater flow correctly.

Table 7. Daily, monthly, annual, individual month, and individual year NSE and Log NSE values for the Pomperaug River current conditions PRMS model.

| | NSE | Log NSE | Water Year | NSE | Log NSE | Water Year | NSE | Log NSE |
|------------------|------|---------|-------------|------|---------|-------------|-------|---------|
| Daily | 0.65 | 0.77 | 1982 | 0.63 | 0.53 | 1999 | -0.10 | 0.82 |
| Monthly | 0.81 | 0.82 | 1983 | 0.87 | 0.84 | 2000 | 0.35 | 0.42 |
| Annual | 0.90 | 0.91 | 1984 | 0.84 | 0.88 | 2001 | 0.77 | 0.69 |
| January | 0.68 | 0.71 | 1985 | 0.75 | 0.81 | 2002 | 0.61 | 0.75 |
| February | 0.58 | 0.69 | 1986 | 0.35 | 0.27 | 2003 | 0.55 | 0.64 |
| March | 0.70 | 0.79 | 1987 | 0.77 | 0.85 | 2004 | 0.80 | 0.89 |
| April | 0.60 | 0.86 | 1988 | 0.51 | 0.85 | 2005 | 0.80 | 0.90 |
| May | 0.73 | 0.73 | 1989 | 0.21 | 0.79 | 2006 | 0.61 | 0.85 |
| June | 0.80 | 0.79 | 1990 | 0.67 | 0.86 | 2007 | 0.72 | 0.92 |
| July | 0.35 | 0.58 | 1991 | 0.74 | 0.88 | 2008 | 0.61 | 0.79 |
| August | 0.40 | 0.70 | 1992 | 0.65 | 0.84 | 2009 | 0.52 | 0.33 |
| September | 0.33 | 0.77 | 1993 | 0.69 | 0.83 | 2010 | 0.76 | 0.82 |
| October | 0.60 | 0.72 | 1994 | 0.77 | 0.79 | 2011 | 0.52 | 0.73 |
| November | 0.55 | 0.57 | 1995 | 0.62 | 0.75 | 2012 | 0.69 | 0.81 |
| December | 0.67 | 0.77 | 1996 | 0.82 | 0.91 | 2013 | 0.70 | 0.70 |
| | | | 1997 | 0.62 | 0.83 | 2014 | 0.71 | 0.88 |
| | | | 1998 | 0.73 | 0.85 | 2015 | 0.50 | 0.76 |

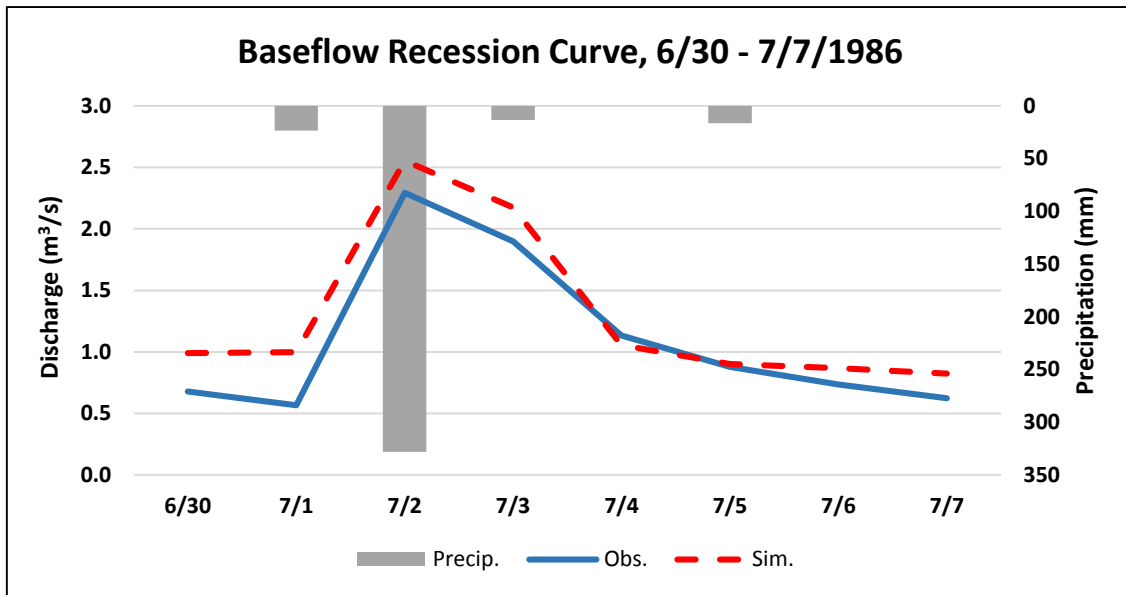


Figure 18. Example of a baseflow recession curve for the Pomperaug River current conditions model.

In addition to comparing the observed streamflow at the Pomperaug River gage and the entire river basin's simulation efficiency, the Nonnewaug and Weekepeemee River subbasins were briefly evaluated because observed streamflow data were available from Water Year's 2003

to 2015. Since the Nonnewaug's streamgage is upstream of the confluence, only the simulated discharges from HRU's 1 to 7 were calculated for comparison to the gage. Table 8 lists the NSE and Log NSE coefficients for the two subbasins. These coefficients show that the model is performing satisfactory on local scales. Therefore, the model was not calibrated further.

Table 8. Observed and simulated streamflow for the Nonnewaug and Weekeepeemee Rivers, and calculated NSE and Log NSE based on streamgage data from water years 2003 to 2015.

| | Observed Streamflow (m³/s) | Simulated Streamflow (m³/s) | NSE | Log NSE |
|---------------------------|--|---|------------|----------------|
| Nonnewaug River | 1.01 | 1.11 | 0.43 | 0.70 |
| Weekeepeemee River | 1.61 | 1.47 | 0.37 | 0.69 |

FLOW DURATION AND EXCEEDANCES

Figure 19 depicts the flow duration curve for both the observed and simulated discharges. This curve does not reflect timing accuracy but does show that PRMS model is under predicting some of the highest flows greater than a 1% exceedance and over predicting the lowest flows below the 99% exceedance, i.e. the extreme values. Under prediction of the highest flows can be attributed to Muskingum routing attenuation. The observed low flows are slightly lower than the simulated values, which might be a result of out of basin water exports not captured in the model. It should be noted that the log scale exaggerates the differences on the low discharge end of the flow duration curve graph.

Table 9 lists the Q_{99} and 7Q10 for both observed and simulated values in the Pomperaug River current conditions, baseline model:

Table 9. Observed and simulated 7Q10 and Q_{99} for the Pomperaug River.

| | 7Q10 (m³/s) | Q_{99} (m³/s) |
|-------------------------------------|-------------------------------|--|
| Observed | 0.16 | 0.19 |
| Simulated Current Conditions | 0.19 | 0.23 |

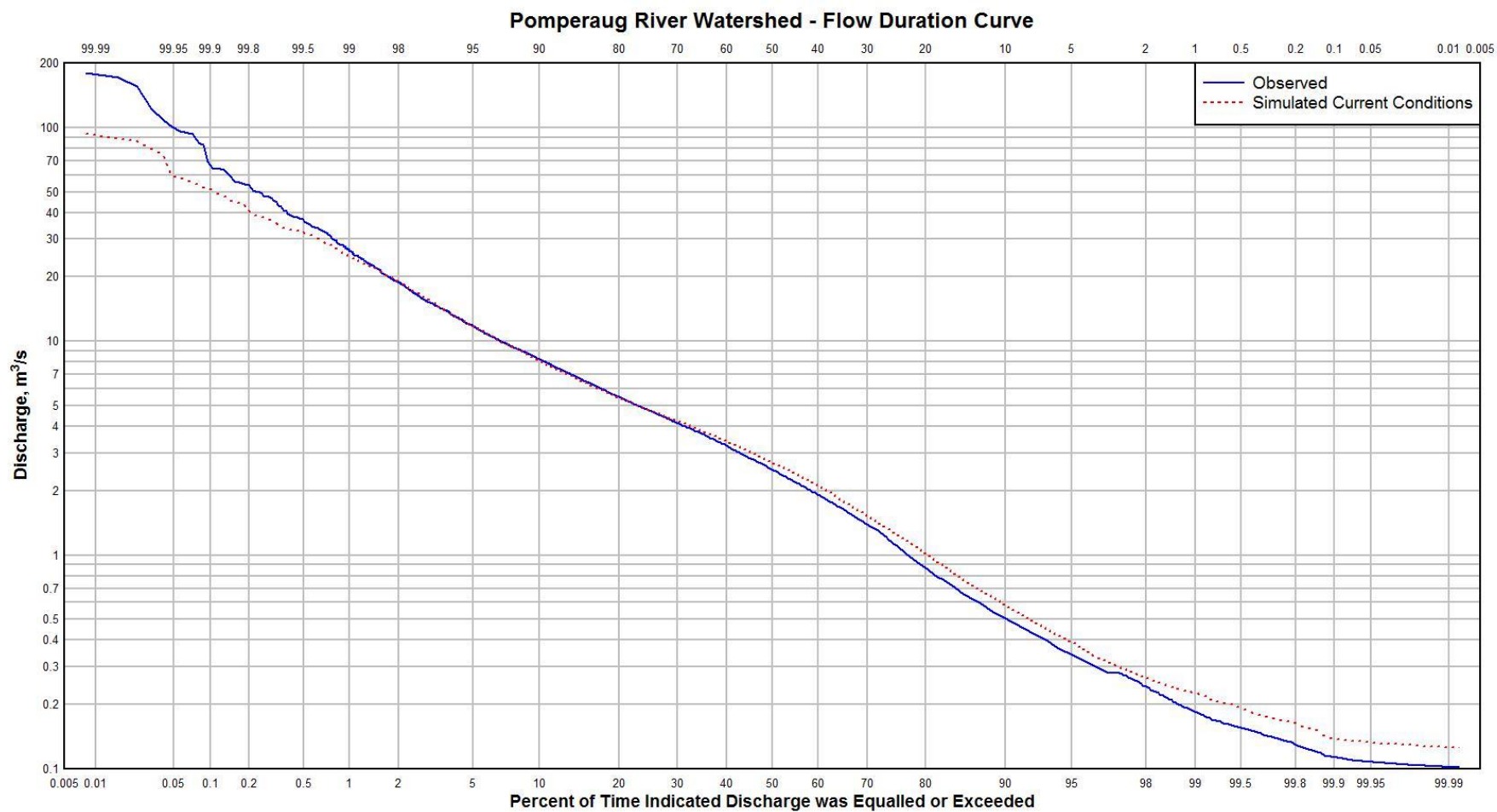


Figure 19. Flow duration curve comparing observed and simulated streamflows for the current conditions Pomperaug River PRMS model.

BUILDOUT OF THE POMPERAUG RIVER WATERSHED

The Pomperaug River watershed was subjected to various scenarios of development to assess the relative impacts of effective impervious area on different components of the water balance. The following two sections describe the results of these scenarios.

DEVELOPMENT SCENARIOS IN THE POMPERAUG RIVER WATERSHED

The first scenario tested for the Pomperaug was the undeveloped version of the watershed (Table 10). The resultant changes were expected considering the parameters that were altered to reflect an undeveloped watershed. The average annual actual evapotranspiration increased from 670 to 676 mm yr⁻¹ (26.4 to 26.6 in yr⁻¹) due to the increase in tree canopy cover and interception. The increase in actual evapotranspiration reduced average streamflow from 3.97 to 3.94 m³ s⁻¹ (140.2 to 139.1 ft³ s⁻¹). The contribution to streamflow decrease from surface runoff and increased from groundwater flow; this occurred because the reduction of impervious surface created a greater infiltration capacity for the soil layers. The increase in average groundwater flow occurred in winter and spring months. This explains why the Q₉₉, for which flows would generally occur in the summer or fall, still decreased from 0.23 to 0.22 m³ s⁻¹ (8.1 to 7.8 ft³ s⁻¹) due to increased evapotranspiration in the summer.

Two zoning based buildout scenarios were evaluated for the Pomperaug River watershed. The first involved full buildout of the watershed with minimum stormwater collection (using the Rural method of estimating EIA) and the second involved full buildout with maximum stormwater collection (using the Transitional method of estimating EIA). As expected, the average streamflow increased from current conditions at 3.97 m³ s⁻¹ (140.2 ft³ s⁻¹) to 4.02 m³ s⁻¹ (142.0 ft³ s⁻¹) with buildout that had minimum stormwater collection and further increased to

Table 10. Simulated components of the water balance and high and low flow values for different development scenarios in the Pomperaug River watershed.

| Buildout | Streamflow (m ³ /s) | Surface Runoff (m ³ /s) | Interflow (m ³ /s) | Groundwater Flow (m ³ /s) | AET (mm/yr) |
|--|-----------------------------------|---------------------------------------|----------------------------------|---|----------------|
| Observed | 4.00 | - | - | - | - |
| Current Conditions | 3.97 | 0.48 | 1.01 | 2.48 | 670 |
| Undeveloped | 3.94 | 0.42 | 1.01 | 2.51 | 676 |
| Minimum Stormwater Collection ¹ | 4.02 | 0.57 | 1.00 | 2.45 | 663 |
| Maximum Stormwater Collection ¹ | 4.06 | 0.64 | 0.99 | 2.43 | 657 |
| Nonnewaug ² | 4.10 | 0.73 | 0.97 | 2.41 | 650 |
| Weekeepeemee ² | 4.10 | 0.73 | 0.95 | 2.42 | 650 |
| Nonnewaug and Weekeepeemee ² | 4.23 | 0.97 | 0.91 | 2.35 | 629 |
| Pomperaug ² | 4.07 | 0.66 | 0.99 | 2.42 | 655 |

| Buildout | Maximum Discharge (m ³ /s) | Minimum Discharge (m ³ /s) | 7Q10 (m ³ /s) | Q ₉₉ (m ³ /s) | Q ₁ (m ³ /s) |
|--|--|--|-----------------------------|--|---------------------------------------|
| Observed | 180.1 | 0.10 | 0.16 | 0.19 | 26.4 |
| Current Conditions | 93.6 | 0.13 | 0.19 | 0.23 | 24.7 |
| Undeveloped | 93.4 | 0.13 | 0.19 | 0.22 | 24.4 |
| Minimum Stormwater Collection ¹ | 93.9 | 0.12 | 0.19 | 0.22 | 25.1 |
| Maximum Stormwater Collection ¹ | 94.2 | 0.12 | 0.19 | 0.22 | 25.3 |
| Nonnewaug ² | 94.4 | 0.12 | 0.20 | 0.22 | 25.6 |
| Weekeepeemee ² | 94.2 | 0.12 | 0.20 | 0.23 | 25.4 |
| Nonnewaug and Weekeepeemee ² | 95.0 | 0.12 | 0.20 | 0.22 | 27.1 |
| Pomperaug ² | 94.6 | 0.12 | 0.19 | 0.22 | 25.6 |

4.06 m³ s⁻¹ (143.4 ft s⁻¹) with buildout that had maximum stormwater collection (Table 10).

These increases are attributed to statistically significant increases in average surface runoff (Table 11). In the maximum stormwater collection scenario, the decreases in average groundwater flow was statistically significant.

Table 11. Statistical significance of increase or decrease in the water balance due to buildout based on a P Value of 0.05.

| Buildout | P Values | | | |
|-------------------------------|------------|----------------|-----------|------------------|
| | Streamflow | Surface Runoff | Interflow | Groundwater Flow |
| Undeveloped | 0.278 | 0.018 | 0.438 | 0.074 |
| Minimum Stormwater Collection | 0.236 | 0.003 | 0.368 | 0.131 |
| Maximum Stormwater Collection | 0.099 | 0.000 | 0.290 | 0.017 |

Although the Q_{99} only decreased from 0.23 to 0.22 $\text{m}^3 \text{s}^{-1}$ (8.1 to 7.8 $\text{ft}^3 \text{s}^{-1}$) in both scenarios, this trend would continue with further development in the future. It also does not account for increased water usage or exports due to population growth, which could have significant localized impacts on streamflow. The flow duration curve (Figure 20) depicts little change in any of the simulated high or flow percent exceedances. This is consistent with the results found in the Bjerklie et al. study (2010), which explored similar scenarios. The overall resiliency and lack of changes in the water balance could be explained by limited impervious surface increases because of zoning regulations.

The next four scenarios ignored zoning regulations to determine the impacts from significant developmental growth upstream and downstream in the watershed. The TIA was increased in the Nonnewaug River, Weekeepeemee River, both of the upstream rivers, and the Pomperaug River subbasins to 24.7%, or the average TIA in the town of Manchester, Connecticut. The watersheds' outputted water balances are listed in Table 10. As expected, the same trends of increased streamflow and decreased groundwater flow that occurred in the zoning based buildout scenarios were evident in all of these subbasin developments. It was observed that the changes in streamflow that occurred in the Nonnewaug and Weekeepeemee development scenarios were summed when development occurred in both watersheds at the time. In other words, discharge increased 0.13 $\text{m}^3 \text{s}^{-1}$ (4.6 $\text{ft}^3 \text{s}^{-1}$) in both of the individual subbasins, and the discharge increased 0.26 $\text{m}^3 \text{s}^{-1}$ (9.0 $\text{ft}^3 \text{s}^{-1}$) when both watersheds were developed simultaneously (Table 10). Overall, the Nonnewaug and Weekeepeemee River development scenarios produced roughly the same changes in the entire basin's water balance.

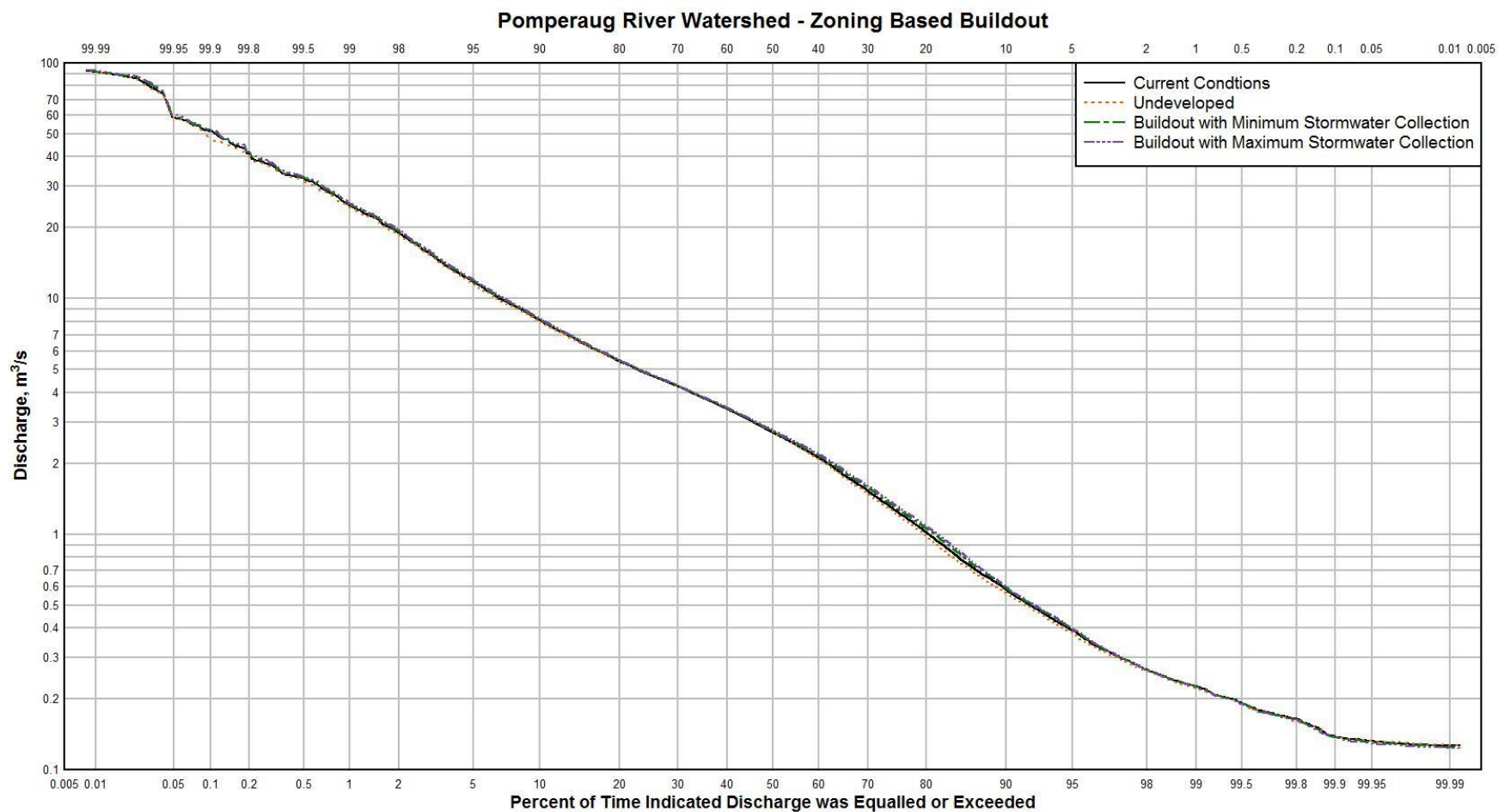


Figure 20. Flow duration curve comparing simulated streamflows among the current conditions, undeveloped, and buildout with minimum and maximum stormwater collection scenarios in the Pomperaug River watershed.

The Pomperaug River subbasin development produced the same trends, but in lesser quantities. For example, compared to current conditions, the average streamflow and surface runoff increased $0.13 \text{ m}^3 \text{ s}^{-1}$ ($4.6 \text{ ft}^3 \text{ s}^{-1}$) and $0.25 \text{ m}^3 \text{ s}^{-1}$ ($8.8 \text{ ft}^3 \text{ s}^{-1}$), respectively, in the Nonnewaug and Weekepeemee, while they only increased $0.10 \text{ m}^3 \text{ s}^{-1}$ ($3.5 \text{ ft}^3 \text{ s}^{-1}$) and $0.18 \text{ m}^3 \text{ s}^{-1}$ ($6.4 \text{ ft}^3 \text{ s}^{-1}$), respectively, in the Pomperaug River development (Table 10).

In addition to these basin-wide changes, localized effects were evaluated to determine if these development scenarios had larger relative impacts on a given subbasin. However, the changes in streamflow that were seen on the basin-wide scale were the exact same changes seen on a local scale (Table 12), e.g. $0.13 \text{ m}^3 \text{ s}^{-1}$ ($4.6 \text{ ft}^3 \text{ s}^{-1}$) in the Nonnewaug and Weekepeemee subbasin, and $0.10 \text{ m}^3 \text{ s}^{-1}$ ($3.5 \text{ ft}^3 \text{ s}^{-1}$) in the Pomperaug subbasin. This suggests that PRMS is additive and that the water balance changes are translated through the watershed from the upper basins to the lower basin. It is noted that the largest relative decrease in the Q_{99} occurred in the Pomperaug subbasin. This could be explained because the coarse stratified drift deposits are greater in this portion of the watershed.

Table 12. Relationships between changes in streamflow due to development and subbasin area within the Pomperaug River watershed.

| | Gaged Area Simulated Streamflow (m ³ /s) | Entire Subbasin Simulated Streamflow (m ³ /s) | Change in Discharge (m ³ /s) | Percent of Total Change in Discharge | Percent of Watershed Area | Entire Subbasin Q_{99} (m ³ /s) |
|-----------------------------------|--|---|---|---|---------------------------------|--|
| Nonnewaug Current Conditions | 0.95 | 1.44 | 0.13 | 35.8 | 35.8 | 0.059 |
| Nonnewaug Developed | 1.03 | 1.57 | | | | 0.056 |
| Weekepeemee Current Conditions | Same as "Entire" | 1.43 | 0.13 | 36.3 | 35.9 | 0.053 |
| Weekepeemee Developed | Same as "Entire" | 1.56 | | | | 0.051 |
| Pomperaug Current Conditions | Same as "Entire" | 1.10 | 0.099 | 28.0 | 28.3 | 0.087 |
| Pomperaug Developed | Same as "Entire" | 1.20 | | | | 0.081 |

As previously discussed, the Pomperaug River subbasin development produced less change in the water balance than the Nonnewaug and Weekepeemee development scenarios, which had similar water balance changes to each other. The Nonnewaug and Weekepeemee subbasins are approximately the same size at 70.1 km² (27.1 mi²) and 70.2 km² (27.1 mi²), while the Pomperaug subbasin is only 55.5 km² (21.4 mi²). When the total change in discharge was summed for the three watershed development scenarios, the percentages of change in discharge were approximately equal to the percentage of watershed area a given subbasin consisted of (Table 12). For example, the Pomperaug River subbasin is 28.3% of the entire watershed's area, and its change in discharge was 28.0% when compared to each other subbasin. This suggests that basin drainage area might have a stronger influence on changes in the Pomperaug River watershed than other characteristics such as location of development or land cover characteristics. This effect was also observed in the Ahearn study on regional regression equations to estimate flow-duration in Connecticut (2010).

ESTIMATING EIA WITHIN THE POMPERAUG RIVER WATERSHED

Three different methods of estimating EIA were tested in the Pomperaug River on a variety of TIA values because impervious surface is a sensitive parameter. Figures 21 and 22 depict two of the flow duration curves produced by the three different methods; the other flow duration curves produced are provided in Figure 23, Figure 24, and Figure 25. When the TIA was set to 12.5% for the entire Pomperaug River watershed, the three methods of estimating EIA produced very little differences in the flow duration curve (Figure 21). However, as TIA increased to 25%, the three methods produced more divergent flow duration curves (Figure 22). The percentage exceedances begin to vary more with increased TIA, a trend that can be seen with the remainder of the flow duration curves in Figure 23, Figure 24, and Figure 25. This

suggests that PRMS is more sensitive to the method chosen to estimate EIA at higher TIA. In other words, at greater TIA, the method chosen to estimate EIA becomes more important to accurately produce peak discharges and surface runoff fluxes due to precipitation events. For additional comparisons, Figures F-1, F-2, and F-3 of Appendix F depict the resultant flow duration curves for each TIA produced by one of the three individual methods of estimating EIA.

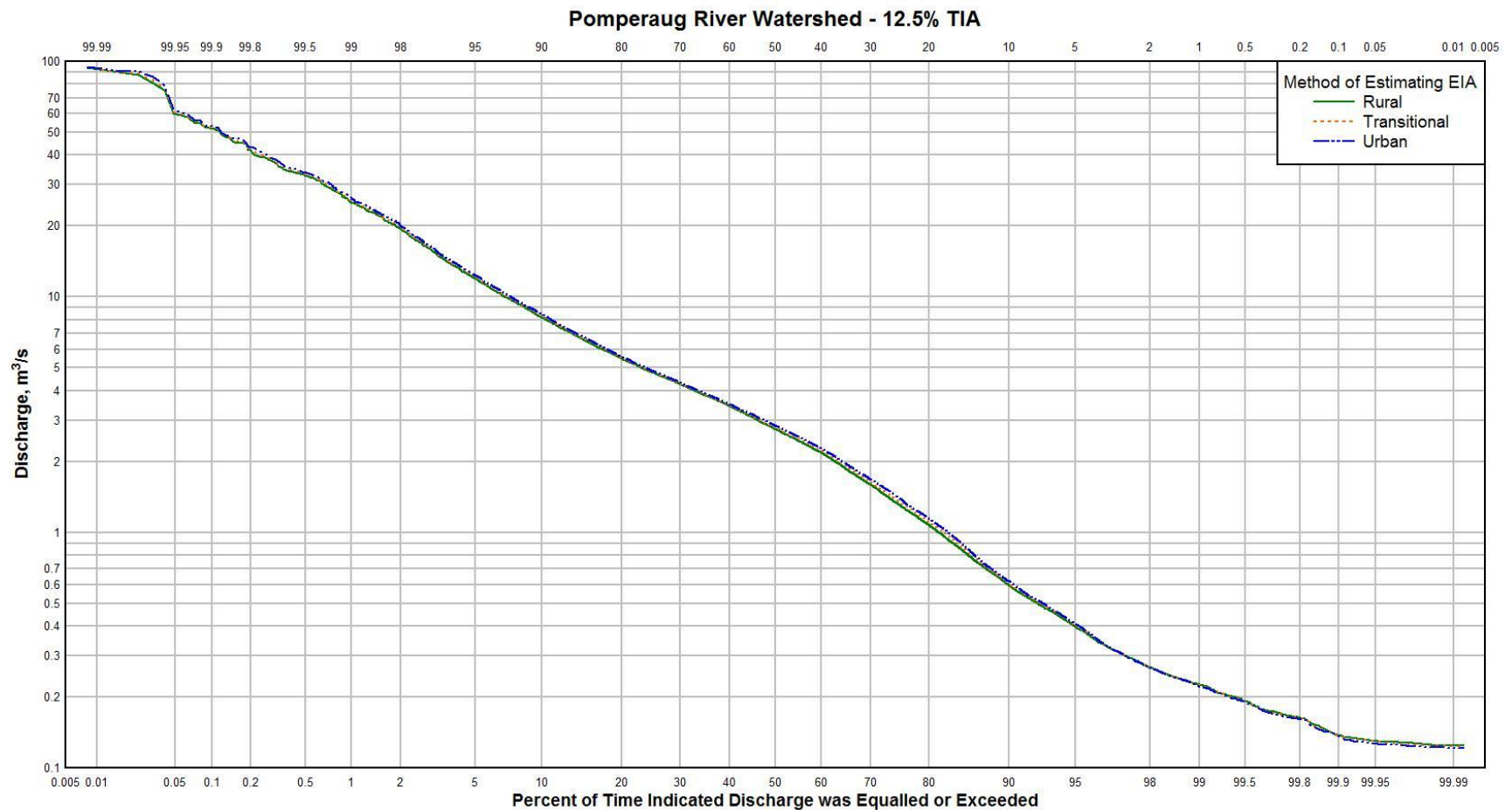


Figure 21. Flow duration curve for the Pomperaug River watershed comparing the three methods of estimating EIA based on 12.5% TIA. This percentage TIA was applied throughout the entire watershed, regardless of current conditions, and translated into an EIA via each method.

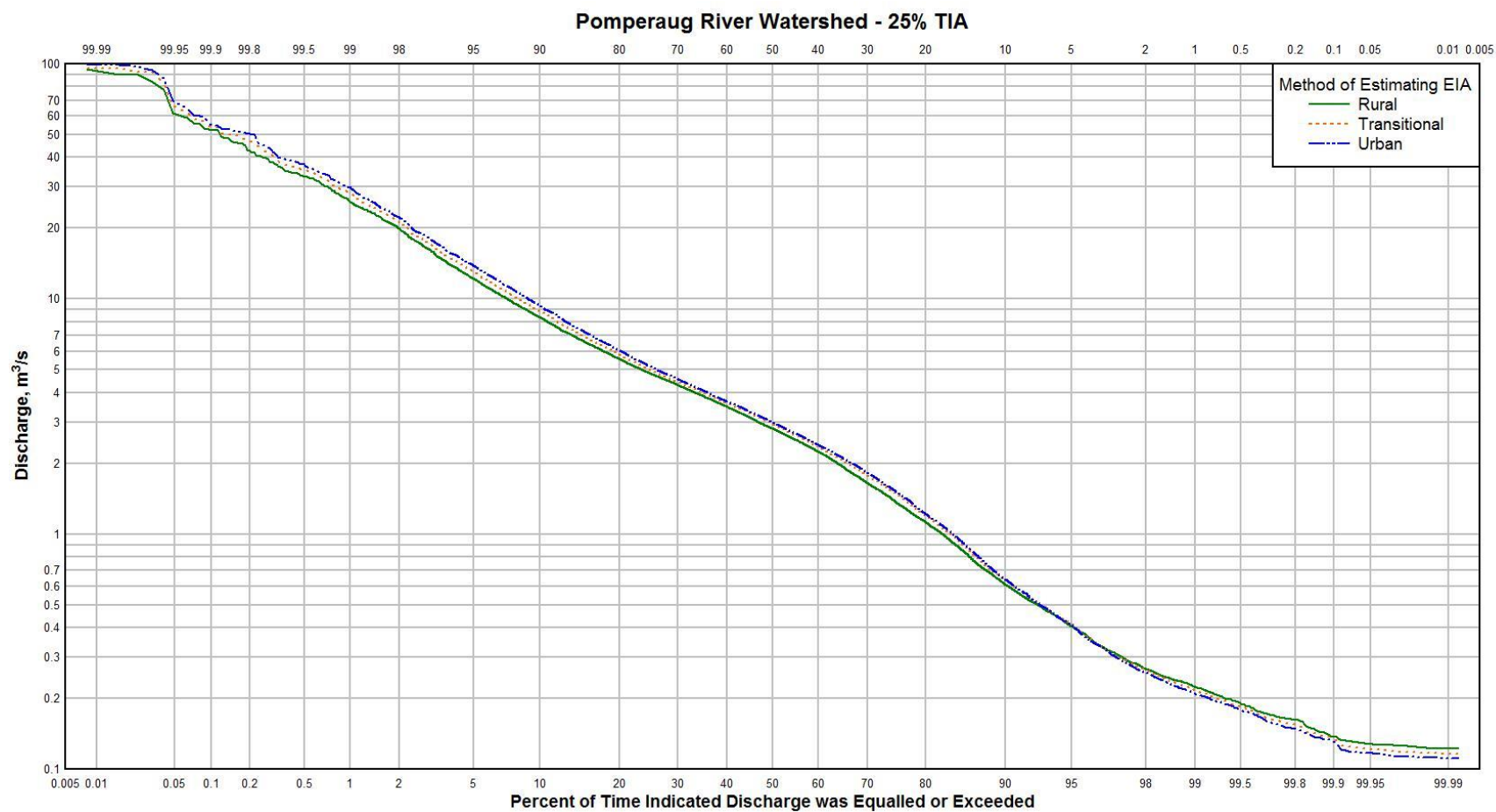


Figure 22. Flow duration curve for the Pomperaug River watershed comparing the three methods of estimating EIA based on 25% TIA. This percentage TIA was applied throughout the entire watershed, regardless of current conditions, and translated into an EIA via each method.

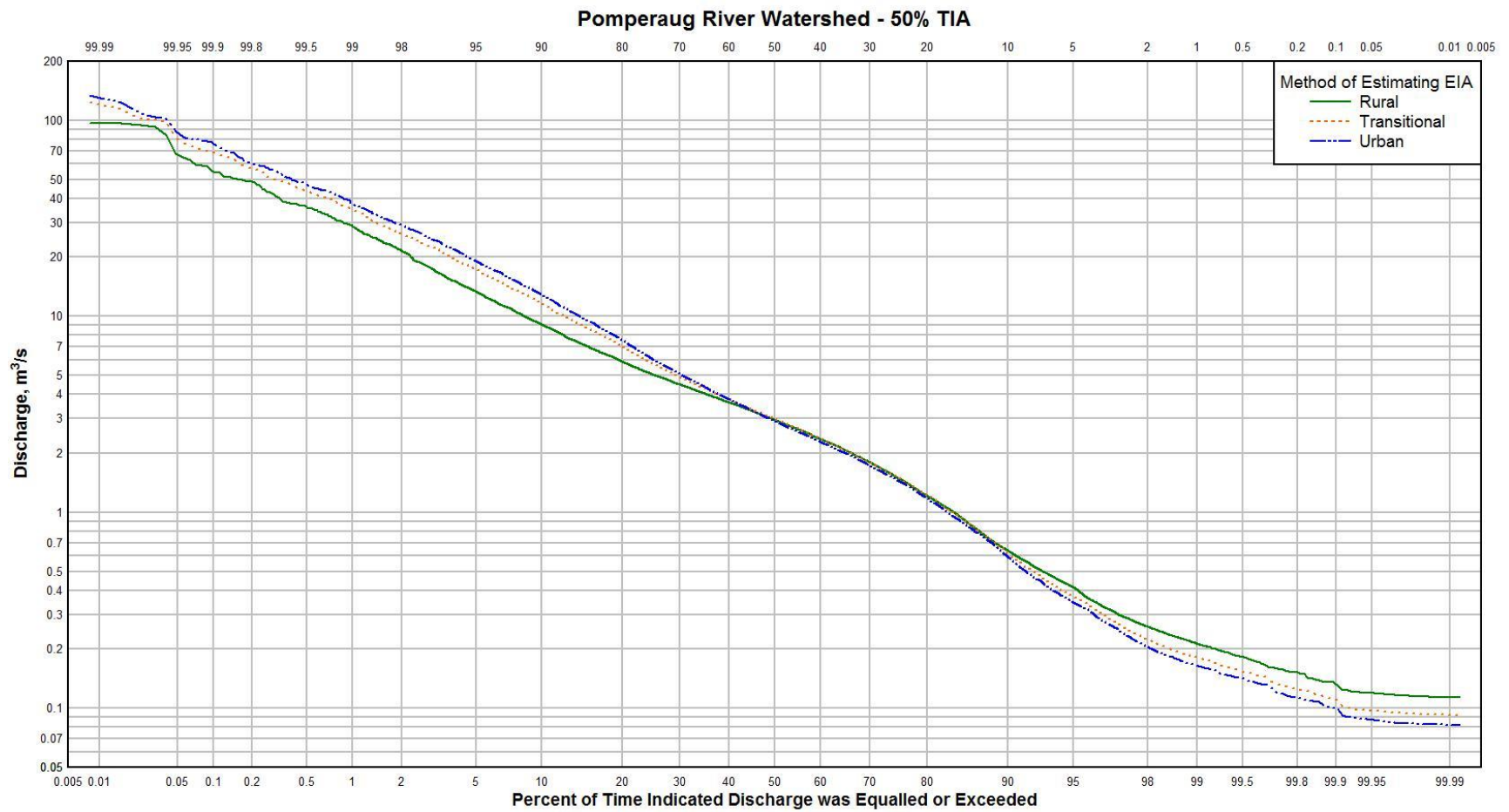


Figure 23. Flow duration curve for the Pomperaug River watershed comparing the three methods of estimating EIA based on 50% TIA. This percentage TIA was applied throughout the entire watershed, regardless of current conditions, and translated into an EIA via each method.

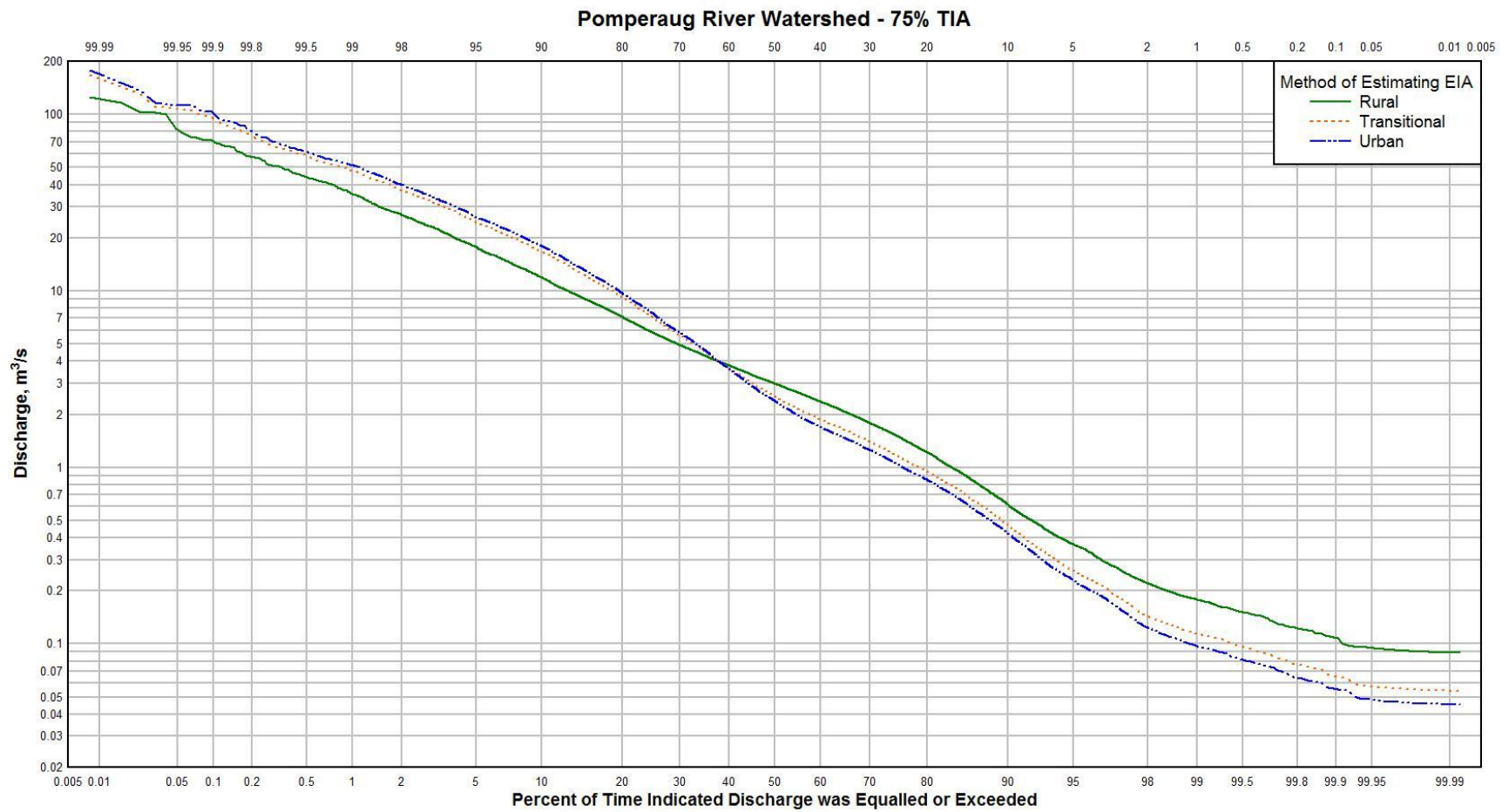


Figure 24. Flow duration curve for the Pomperaug River watershed comparing the three methods of estimating EIA based on 75% TIA. This percentage TIA was applied throughout the entire watershed, regardless of current conditions, and translated into an EIA via each method.

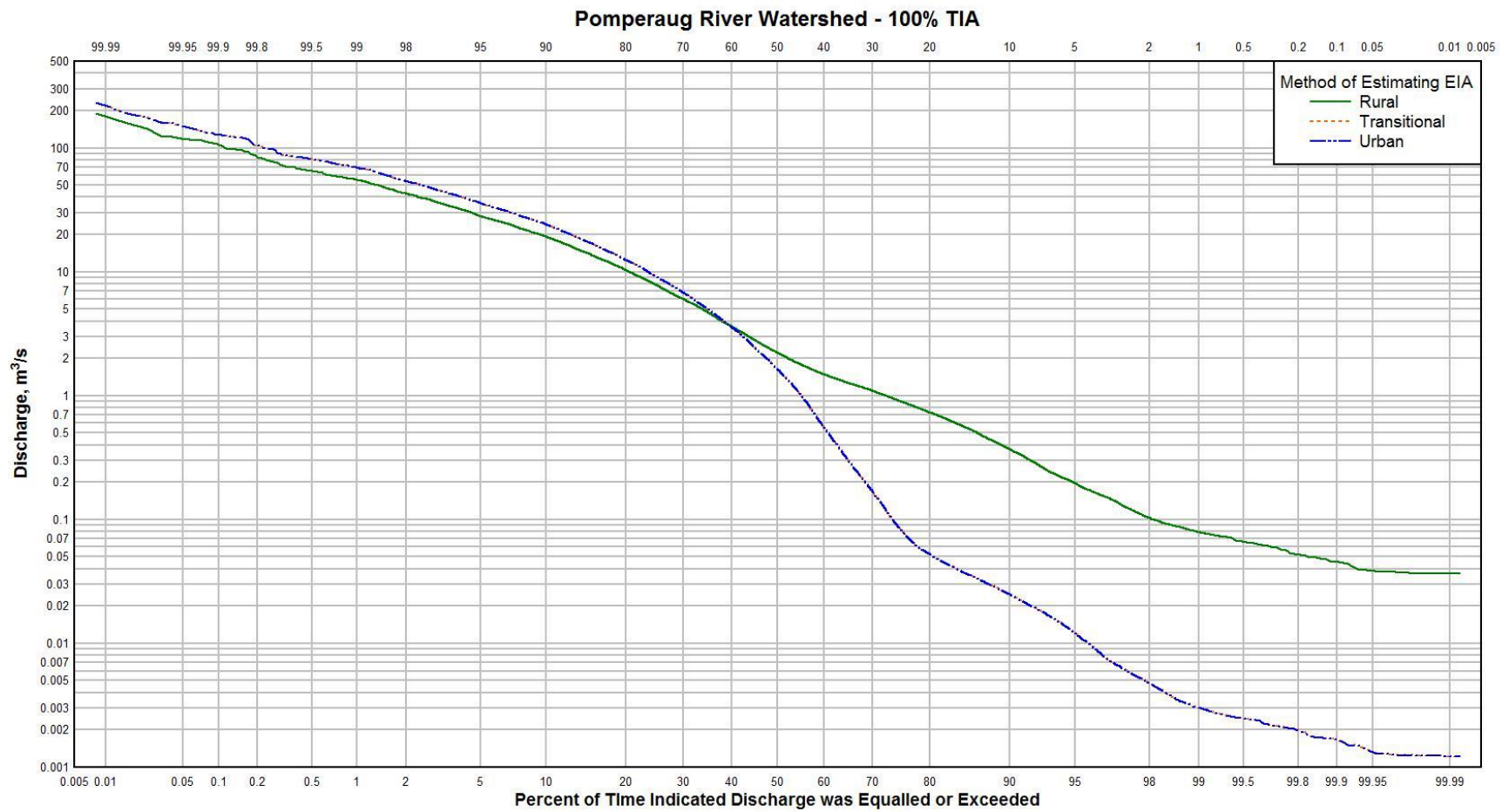


Figure 25. Flow duration curve for the Pomperaug River watershed comparing the three methods of estimating EIA based on 100% TIA. This percentage TIA was applied throughout the entire watershed, regardless of current conditions, and translated into an EIA via each method.

CALIBRATION OF THE HOCKANUM PRMS MODEL

Similar to the Pomperaug River model, the Hockanum River model was subject to calibration and optimization. However, there were no prior PRMS models or data for the Hockanum River. The following results of the long-term and daily water balance are from the current conditions, baseline model.

LONG-TERM WATER BALANCE

The input climate data for the Hockanum River PRMS model originated from Daymet from the Geo Data Portal. The output of these data from PRMS was compared against three weather stations (Bradley Airport, Brainard Airport, and Storrs) for accuracy of daily precipitation, maximum temperature, and minimum temperatures from 1980 to 2015. Figure 26 a, b, & c depict the average observed precipitation and temperature data from the three weather stations along with the outputted Daymet data from the PRMS simulation. The data were organized by month to ensure correct simulation of seasonality. The PRMS model for the Hockanum River outputted temperatures and precipitation accurately on a monthly basis (Figure 26 a, b, & c). Observed precipitation was generally slightly greater from the observed weather stations, but this is due to the Storrs weather station being at a higher elevation than the other weather stations and the watershed itself.

Annual climate conditions were evaluated in addition to seasonality for the basin. Average annual precipitation was simulated at 1179 mm yr⁻¹ (46.4 in yr⁻¹), which is higher than the previously reported 1123 mm yr⁻¹ (44.2 in yr⁻¹) in the Connecticut Water Resources Inventory (Ryder et al., 1981). Considering variation amongst years and an average annual precipitation between the three weather stations of 1250 mm yr⁻¹ (49.2 in yr⁻¹), the simulation is a reasonable value. The AET was simulated at 553 mm yr⁻¹ (21.8 in yr⁻¹). This is less than the

expected value of 50% of precipitation, but it falls within the estimated 509 to 558 mm (20 to 22 in) range (Ryder et al., 1981).

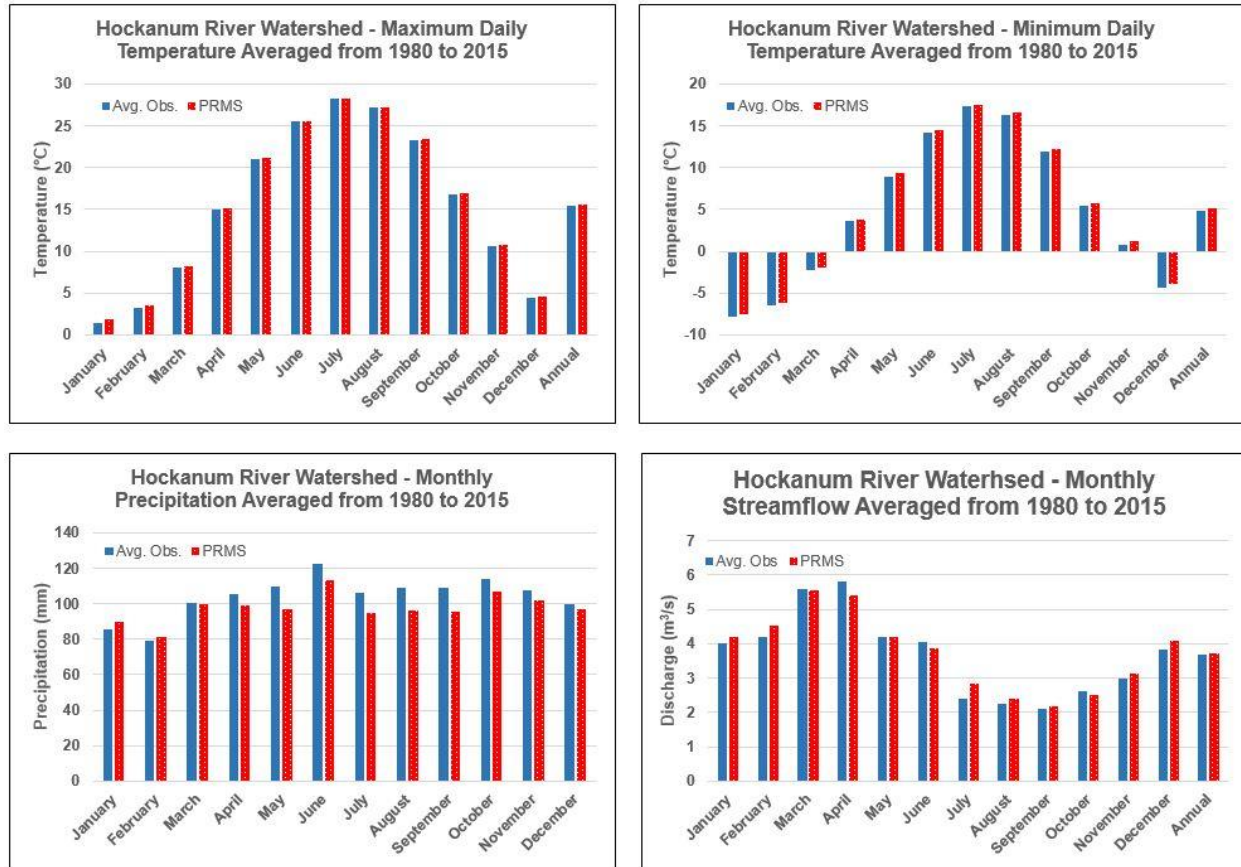


Figure 26. Observed versus simulated water balance data in the Hockanum River watershed. **a.** Maximum daily temperature averaged by month from between three observed weather stations and PRMS’s simulated output; **b.** Minimum daily temperature averaged by month between three observed weather stations and PRMS’s simulated output; **c.** Monthly precipitation averaged between three observed weather stations and PRMS’s simulated output; **d.** Daily streamflow averaged by month between the USGS streamgauge and PRMS’s simulated output.

An issue with the Hockanum River model was that when it was initially calibrated, net storage approximated an increase of 2083 mm (82 in) when calculated with Equation 6 over 34 years of record excluding the first warmup year. After a sensitivity analysis, parameters governing maximum available water holding capacity of the capillary reservoir and recharge

zone (**soil_moist_max** and **soil_rechr_max**), evapotranspiration and interception (**jh_coef_hru** and **cov_type**), and groundwater flow (**gwsink_coef** and **gwflow_coef**) were adjusted to reduce the net storage while maintaining an accurate water balance. Regardless of how these parameters and others were adjusted, the lowest net storage change achieved without disturbing the water balance accuracy was an increase of 178 mm (7 in) over 34 years of record. This indicated that an average export from the watershed of approximately 5.1 mm (0.2 in) was most likely occurring each year, which could potentially be explained by out of basin diversions from the Shenipsit Lake. With this assumption, the estimated net change was a decrease of 18.7 mm (0.74 in) during the study period (Table 13).

The simulated streamflow was compared to observed streamgage data. In the Hockanum River, average daily streamflow from water year 1982 to 2015 recorded at USGS gage 01192500 was $3.72 \text{ m}^3 \text{ s}^{-1}$ ($131.4 \text{ ft}^3 \text{ s}^{-1}$). For the same time period, PRMS simulated discharge to be the same at $3.78 \text{ m}^3 \text{ s}^{-1}$ ($133.5 \text{ ft}^3 \text{ s}^{-1}$). A greater simulated average discharge is reasonable given the previous assumption of 5.1 millimeters of exported water and that observed streamflow would reflect the actual export. Average contribution to total streamflow was $0.57 \text{ m}^3 \text{ s}^{-1}$ ($20.1 \text{ ft}^3 \text{ s}^{-1}$) from surface runoff, $0.22 \text{ m}^3 \text{ s}^{-1}$ ($7.9 \text{ ft}^3 \text{ s}^{-1}$) from subsurface flow, and $2.99 \text{ m}^3 \text{ s}^{-1}$ ($105.5 \text{ ft}^3 \text{ s}^{-1}$). Seasonality of the streamflow was also partitioned accurately by the PRMS model (Figure 26d).

Groundwater contribution to streamflow in the Hockanum River watershed has not been estimated previously. Due to greater percentages of glacial coarse stratified drift deposits than in the Pomperaug River watershed, it would be expected to have a greater contribution in this watershed. PRMS estimated 78.9% contribution from groundwater to total streamflow. The PART base-flow separation method from Groundwater Toolbox estimated 79% contribution based upon observed streamflow and 82.4% from the simulated PRMS streamflow (Table 14).

Table 13. Change in storage by year for the Hockanum River watershed as simulated by PRMS.

| Water Year | Annual Precipitation (mm) | Annual AET (mm) | Daily Average Simulated Streamflow (mm) | Expected Watershed Export (mm) | Change in Storage (mm) | Daily Average Observed. Streamflow (mm) |
|-------------------------------|----------------------------------|------------------------|--|---------------------------------------|-------------------------------|--|
| 1982 | 1314.5 | 542.7 | 696.5 | 5.1 | 70.1 | 749.4 |
| 1983 | 1169.3 | 460.8 | 699.8 | 5.1 | 3.6 | 659.3 |
| 1984 | 1409.7 | 509.9 | 854.5 | 5.1 | 40.3 | 812.4 |
| 1985 | 994.2 | 664.6 | 373.0 | 5.1 | -48.4 | 359.9 |
| 1986 | 921.0 | 517.5 | 437.2 | 5.1 | -38.7 | 519.0 |
| 1987 | 1158.9 | 467.4 | 597.4 | 5.1 | 88.9 | 572.3 |
| 1988 | 915.0 | 529.3 | 456.7 | 5.1 | -76.1 | 393.5 |
| 1989 | 1325.1 | 590.1 | 617.0 | 5.1 | 112.9 | 568.3 |
| 1990 | 1291.6 | 580.8 | 765.4 | 5.1 | -59.8 | 696.0 |
| 1991 | 1220.4 | 559.3 | 613.1 | 5.1 | 43.0 | 604.5 |
| 1992 | 1056.7 | 601.8 | 528.0 | 5.1 | -78.2 | 513.6 |
| 1993 | 1150.3 | 463.7 | 625.0 | 5.1 | 56.6 | 613.0 |
| 1994 | 1328.5 | 595.4 | 689.4 | 5.1 | 38.6 | 668.9 |
| 1995 | 883.5 | 478.3 | 490.1 | 5.1 | -89.9 | 476.9 |
| 1996 | 1359.3 | 552.0 | 748.4 | 5.1 | 53.7 | 718.9 |
| 1997 | 1148.3 | 515.9 | 692.0 | 5.1 | -64.7 | 696.2 |
| 1998 | 1242.9 | 520.3 | 687.4 | 5.1 | 30.1 | 648.5 |
| 1999 | 1143.9 | 481.2 | 594.6 | 5.1 | 63.0 | 509.3 |
| 2000 | 1251.4 | 613.3 | 690.6 | 5.1 | -57.6 | 601.5 |
| 2001 | 1020.2 | 476.2 | 553.6 | 5.1 | -14.6 | 465.6 |
| 2002 | 897.8 | 591.2 | 354.8 | 5.1 | -53.2 | 300.2 |
| 2003 | 1429.4 | 616.3 | 686.4 | 5.1 | 121.6 | 673.5 |
| 2004 | 1245.1 | 601.0 | 674.8 | 5.1 | -35.8 | 665.6 |
| 2005 | 967.9 | 463.7 | 592.0 | 5.1 | -92.9 | 652.8 |
| 2006 | 1531.5 | 604.3 | 880.4 | 5.1 | 41.8 | 1001.0 |
| 2007 | 1114.8 | 483.3 | 662.9 | 5.1 | -36.5 | 622.5 |
| 2008 | 1500.6 | 668.0 | 700.3 | 5.1 | 127.2 | 596.5 |
| 2009 | 1206.8 | 637.7 | 663.6 | 5.1 | -99.5 | 727.3 |
| 2010 | 1038.7 | 472.4 | 597.2 | 5.1 | -35.9 | 601.9 |
| 2011 | 1618.9 | 687.4 | 775.0 | 5.1 | 151.4 | 763.1 |
| 2012 | 1060.2 | 635.0 | 577.9 | 5.1 | -157.8 | 661.7 |
| 2013 | 1080.3 | 615.3 | 482.4 | 5.1 | -22.4 | 643.9 |
| 2014 | 1018.4 | 505.6 | 520.6 | 5.1 | -12.9 | 539.1 |
| 2015 | 1067.3 | 504.9 | 543.9 | 5.1 | 13.3 | 483.5 |
| Net Change in Storage: | | | | | -18.7 | |

Table 14. Estimated groundwater contribution to streamflow in the Hockanum River.

| Groundwater Contribution to Streamflow | | Method |
|---|-------|---------------|
| Observed | 79.0% | GW Toolbox |
| Simulated | 82.4% | GW Toolbox |
| Simulated | 78.9% | PRMS |

DAILY DISCHARGE TIMING AND BASE-FLOW RECESSION

The calculated daily NSE coefficients for the Hockanum River model were 0.72 with a Log NSE of 0.72 (Table 15) indicating that the model's simulation of daily streamflow fluxes performed well. Like the Pomperaug model, the Hockanum model's performance improved its NSE calculations on the long-term monthly and annual scales. Seasonally, the model performed well in all months except for July. For individual years, only 1985 had an NSE less than 0.5. Its NSE was 0.13 and its Log NSE was -0.52 (Table 15). It is a result of consistent underestimation from the PRMS simulations from approximately 8/1/1985 to 11/4/1985 (Figure 27), but the reason behind this poor performance is unknown. The simulated discharge values are inaccurate even though the rate of streamflow increases and recessions are consistent with observed streamflow.

Accurate peak discharge and rate of the base-flow recession after precipitation events were more difficult to predict in the Hockanum model. This was potentially caused by more hydrologic control in the watershed from the Shenipsit Reservoir storage and releases. An example of an accurate base-flow recession curve is depicted in Figure 28. The model predicts the peak discharge and base flow accurately and roughly estimates the recession rate correctly. PRMS simulates groundwater flow with linear routing, which is the recession curve is more linear for the simulated flow than the observed flow. This demonstrates that the PRMS model can simulate the daily discharge fluxes caused by precipitation events.

Table 15. Daily, monthly, annual, individual month, and individual year NSE and Log NSE values for the Hockanum River current conditions PRMS model.

| | NSE | Log NSE | Water Year | NSE | Log NSE | Water Year | NSE | Log NSE |
|------------------|------|---------|-------------|------|---------|-------------|------|---------|
| Daily | 0.72 | 0.72 | 1982 | 0.76 | 0.70 | 1999 | 0.53 | 0.74 |
| Monthly | 0.81 | 0.79 | 1983 | 0.76 | 0.76 | 2000 | 0.69 | 0.60 |
| Annual | 0.79 | 0.79 | 1984 | 0.69 | 0.78 | 2001 | 0.70 | 0.60 |
| January | 0.62 | 0.65 | 1985 | 0.13 | -0.52 | 2002 | 0.63 | 0.58 |
| February | 0.63 | 0.69 | 1986 | 0.71 | 0.21 | 2003 | 0.70 | 0.77 |
| March | 0.74 | 0.75 | 1987 | 0.83 | 0.74 | 2004 | 0.67 | 0.74 |
| April | 0.71 | 0.82 | 1988 | 0.67 | 0.72 | 2005 | 0.73 | 0.88 |
| May | 0.71 | 0.70 | 1989 | 0.74 | 0.70 | 2006 | 0.63 | 0.81 |
| June | 0.69 | 0.76 | 1990 | 0.77 | 0.77 | 2007 | 0.73 | 0.79 |
| July | 0.44 | 0.33 | 1991 | 0.63 | 0.78 | 2008 | 0.65 | 0.69 |
| August | 0.59 | 0.49 | 1992 | 0.61 | 0.60 | 2009 | 0.66 | 0.78 |
| September | 0.59 | 0.60 | 1993 | 0.74 | 0.71 | 2010 | 0.77 | 0.85 |
| October | 0.74 | 0.64 | 1994 | 0.71 | 0.73 | 2011 | 0.76 | 0.78 |
| November | 0.61 | 0.65 | 1995 | 0.81 | 0.83 | 2012 | 0.63 | 0.74 |
| December | 0.70 | 0.70 | 1996 | 0.71 | 0.79 | 2013 | 0.56 | 0.65 |
| | | | 1997 | 0.76 | 0.84 | 2014 | 0.74 | 0.80 |
| | | | 1998 | 0.86 | 0.82 | 2015 | 0.67 | 0.73 |

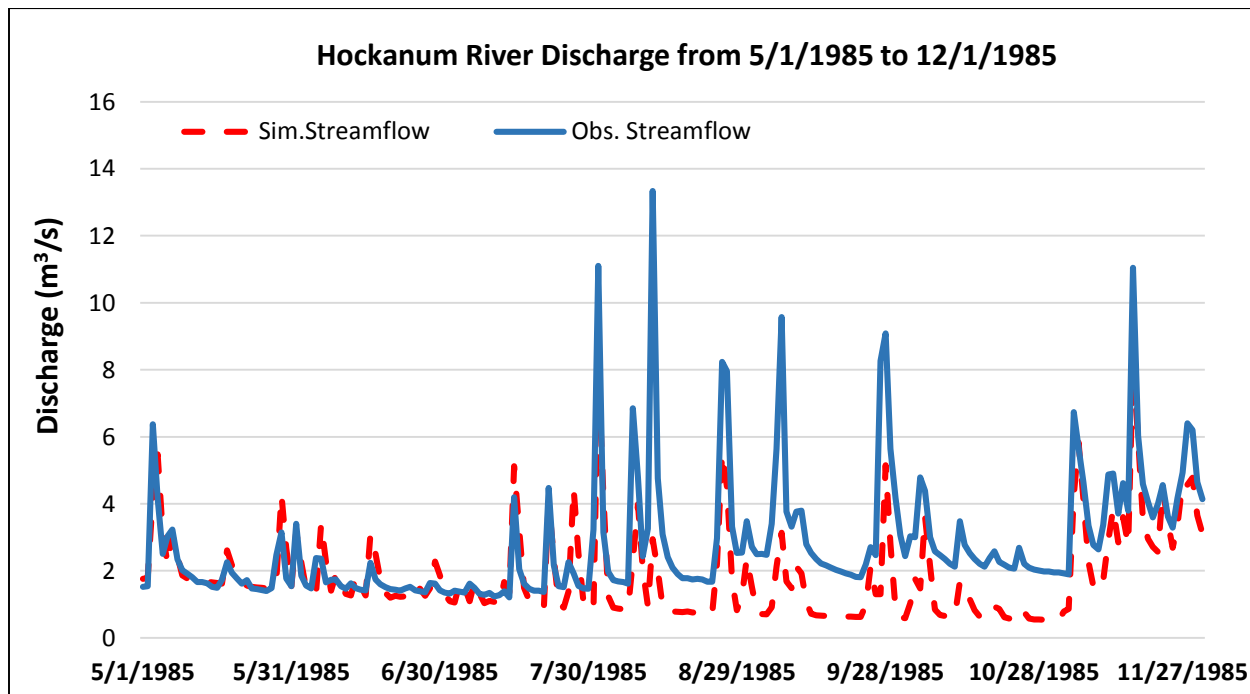


Figure 27. Observed and simulated hydrographs for the Hockanum River current conditions model depicting poor model performance.

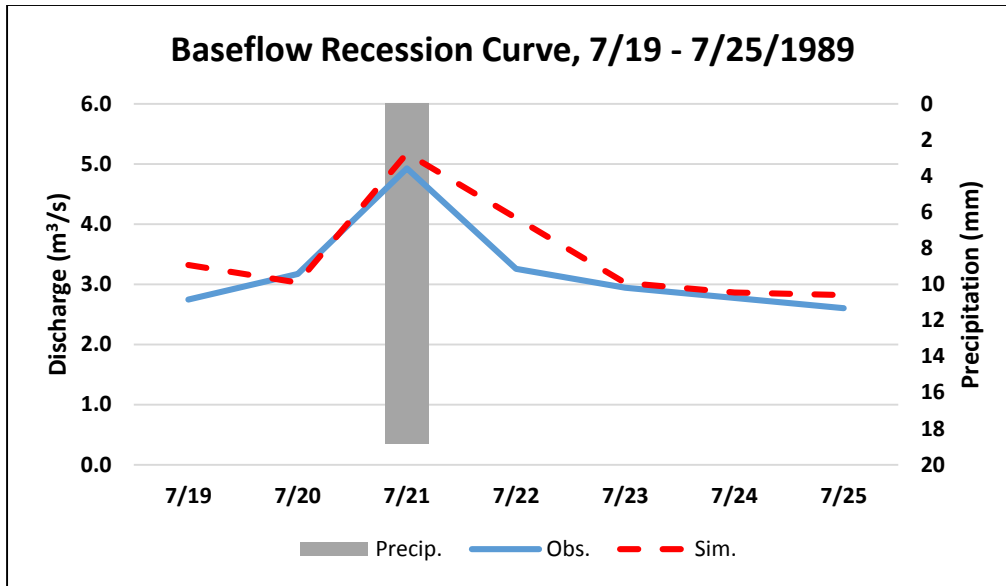


Figure 28. Example of a baseflow recession curve for the Hockanm River current conditions model.

FLOW DURATION AND EXCEEDANCES

Figure 29 depicts the flow duration curve for both the observed and simulated discharges. There is a lack of accuracy between the observed and simulated throughout most of the percentage exceedances. This could potentially be explained by real life streamflow manipulations that are not captured within the PRMS model. The observed low flows are probably greater than the modeled low flows due to the influence releases from the reservoir and wastewater treatment plants, especially the Manchester treatment plant because it is within a few kilometers of the USGS streamgage. The observed peak discharges are greater than simulated discharges, which is probably attributed to Muskingum routing attenuation in the PRMS model.

Table 16 lists the Q_{99} and 7Q10 for both observed and simulated values in the Hockanum River watershed:

Table 16. Observed and simulated 7Q10 and Q_{99} for the Hockanum River

| | 7Q10 (m3/s) | Q_{99} (m3/s) |
|-------------------------------------|-------------|-----------------|
| Observed | 0.84 | 0.97 |
| Simulated Current Conditions | 0.78 | 0.80 |

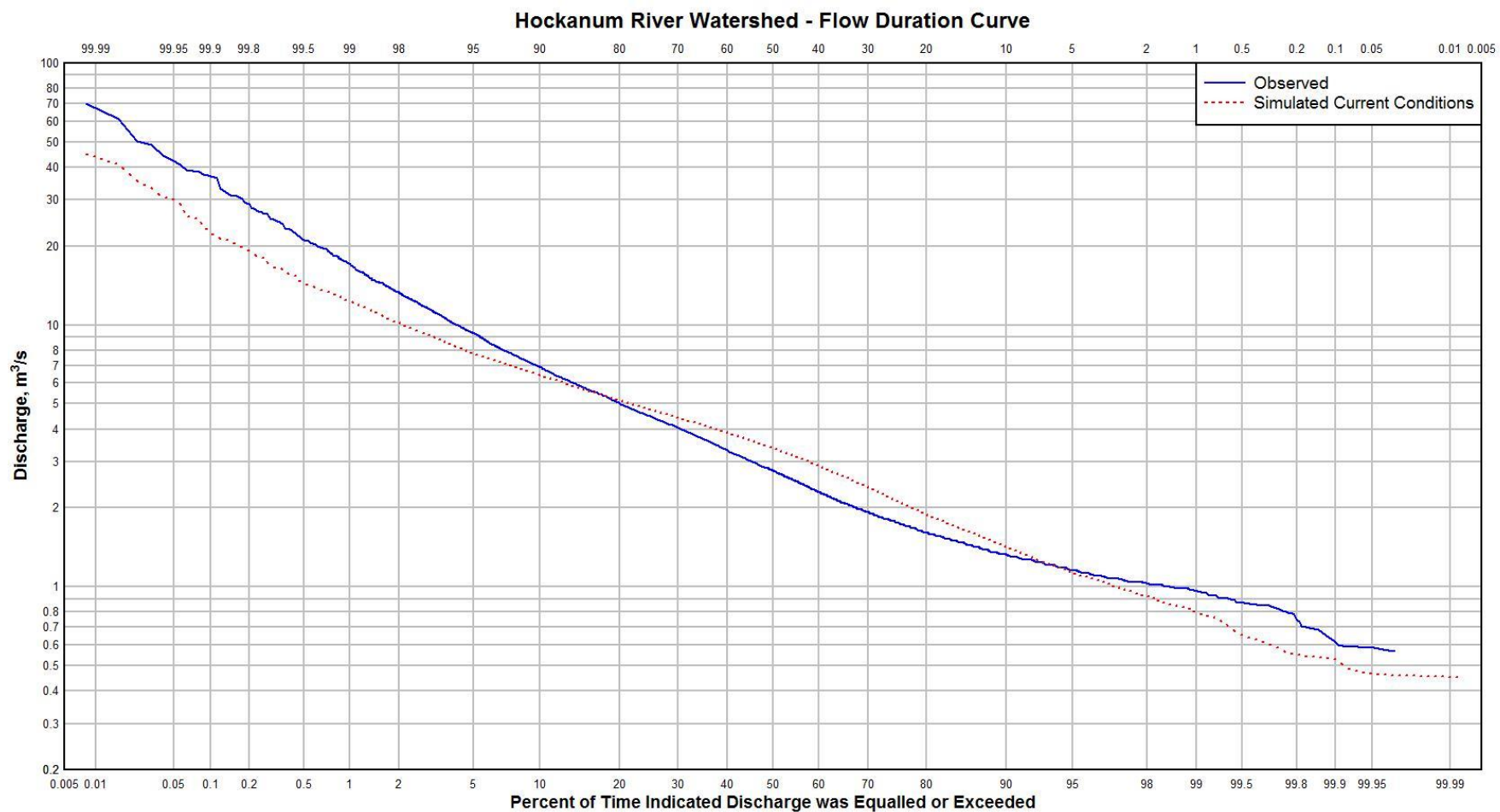


Figure 29. Flow duration curve comparing observed and simulated streamflows for the current conditions Hockanum River PRMS model.

BUILDOUT OF THE HOCKANUM RIVER WATERSHED

The Hockanum River watershed was subjected to various scenarios of development to assess the relative impacts of effective impervious area on different components of the water balance. The following two sections describe the results of these scenarios.

DEVELOPMENT SCENARIOS IN THE HOCKANUM RIVER WATERSHED

The first scenario tested for the Hockanum was an undeveloped version of the watershed (Table 17). The changes that occurred in the water balance were somewhat expected for an undeveloped watershed given the parameters that were altered. Average annual evapotranspiration increased from 553 to 576 mm yr⁻¹ (21.8 to 22.7 in yr⁻¹) due to large increases in tree canopy cover and interception, which does not currently exist in the highly developed portions of the watershed. Impervious surface decreased to 0% throughout the watershed, which would increase the infiltration capacity of the soil layers. Large decreases in average streamflow from 3.78 to 3.59 m³ s⁻¹ (133.5 to 126.8 ft³ s⁻¹) can be attributed to large decreases in surface runoff from 0.57 to 0.22 m³ s⁻¹ (20.1 to 7.8 ft³ s⁻¹) and groundwater flow from 2.99 to 2.49 m³ s⁻¹ (105.6 to 87.9 ft³ s⁻¹). The large decrease in groundwater flow is a result of the increased soil zone moisture storage capacity, which resulted in less water available to transfer to the groundwater reservoir within the model simulations. Therefore, less water in the groundwater reservoir resulted in less outflow. This same reasoning can be applied to why interflow increased from 0.22 to 0.87 m³ s⁻¹ (7.8 to 30.7 ft³ s⁻¹).

The maximum discharge increased from 45.2 to 46.2 m³ s⁻¹ (1596 to 1632 ft³ s⁻¹). This unexpected result occurred because there were two different events that produced the maximum streamflows. On June 6, 1982, the streamflow increased in the undeveloped scenario compared to the current conditions model because of timing surrounding the event with regards to the soil

zone storage capacity and subsequent interflow and groundwater flow. Minimum discharge and the 7Q10 and Q₉₉ all decreased for the same reason they did in the Pomperaug, increased evapotranspiration during the summer and fall months when low flows occur.

Table 17. Simulated components of the water balance and high and low flow values for different development scenarios in the Hockanum River watershed.

| Buildout | Streamflow (m³/s) | Surface Runoff (m³/s) | Interflow (m³/s) | Groundwater Flow (m³/s) | AET (mm/yr) |
|--|---|---|--|---|------------------------|
| Observed | 3.72 | - | - | - | - |
| Current Conditions | 3.78 | 0.57 | 0.22 | 2.99 | 553 |
| Undeveloped | 3.59 | 0.22 | 0.87 | 2.49 | 576 |
| Minimum Stormwater Collection¹ | 3.79 | 0.59 | 0.22 | 2.98 | 551 |
| Maximum Stormwater Collection¹ | 3.86 | 0.73 | 0.21 | 2.91 | 540 |
| Upper Watershed² | 3.97 | 0.97 | 0.18 | 2.83 | 521 |
| Middle Watershed² | 3.94 | 0.90 | 0.21 | 2.84 | 526 |
| Lower Watershed² | 3.90 | 0.83 | 0.21 | 2.87 | 533 |

| Buildout | Maximum Discharge (m³/s) | Minimum Discharge (m³/s) | 7Q10 (m³/s) | Q99 (m³/s) | Q1 (m³/s) |
|--|--|--|-----------------------------------|----------------------------------|---------------------------------|
| Observed | 70.2 | 0.54 | 0.84 | 0.97 | 17.0 |
| Current Conditions | 45.2 | 0.45 | 0.78 | 0.80 | 12.3 |
| Undeveloped | 46.2 | 0.38 | 0.68 | 0.70 | 14.2 |
| Minimum Stormwater Collection¹ | 45.5 | 0.45 | 0.78 | 0.80 | 12.4 |
| Maximum Stormwater Collection¹ | 47.5 | 0.44 | 0.76 | 0.78 | 13.5 |
| Upper Watershed² | 49.2 | 0.44 | 0.77 | 0.80 | 14.6 |
| Middle Watershed² | 49.9 | 0.43 | 0.75 | 0.77 | 14.7 |
| Lower Watershed² | 49.0 | 0.43 | 0.76 | 0.78 | 14.3 |

The two zoning based buildout scenarios designed for the Hockanum River watershed were evaluated. The first involved buildout of the watershed with minimum stormwater collection (using the Transitional method of estimating EIA) and the second involved full buildout with maximum stormwater collection (using the Urban method of estimating EIA). Average annual actual evapotranspiration decreased from 553 mm yr⁻¹ (21.8 in yr⁻¹) to 551 and 540 mm yr⁻¹ (21.7 and 21.3 in yr⁻¹) for the Transitional and Urban stormwater methods, respectively.

The average streamflow increased from current conditions at $3.78 \text{ m}^3 \text{ s}^{-1}$ ($133.5 \text{ ft}^3 \text{ s}^{-1}$) to $3.79 \text{ m}^3 \text{ s}^{-1}$ ($133.8 \text{ ft}^3 \text{ s}^{-1}$) with minimum stormwater collection methods but further increased to $3.86 \text{ m}^3 \text{ s}^{-1}$ ($136.3 \text{ ft}^3 \text{ s}^{-1}$) with buildout that maximized stormwater collection (Table 17). With the minimum stormwater collection, the full buildout scenario did not produce any significant changes in the components in streamflow (Table 18). However, maximizing stormwater collection created statistically significant increases in streamflow due to significant increases in surface runoff (Table 18). Groundwater flow also decreased significantly in the maximum stormwater collection scenario. This type of scenario could occur if the Hockanum River watershed had urban-like growth or if low impact developments were not considered.

Table 18. Statistical significance of increase or decrease in the water balance due to buildout based on a P Value of 0.05.

| Buildout | P Values | | | |
|--------------------------------------|-------------------|-----------------------|------------------|-------------------------|
| | Streamflow | Surface Runoff | Interflow | Groundwater Flow |
| Undeveloped | 0.000 | 0.000 | 0.000 | 0.000 |
| Minimum Stormwater Collection | 0.359 | 0.115 | 0.444 | 0.293 |
| Maximum Stormwater Collection | 0.007 | 0.000 | 0.209 | 0.000 |

The Q_{99} only decreased from 0.80 to $0.78 \text{ m}^3 \text{ s}^{-1}$ (28.3 to $27.5 \text{ ft}^3 \text{ s}^{-1}$) with maximum stormwater collection. The reality of this is difficult to assess from a modeling perspective because of release requirements from wastewater treatment plants and reservoir releases. However, it is presumed that natural low flows would decrease with increased development. It also does not account for increased water usage or exports due to population growth. For the Hockanum River, these pressures could also occur outside of the watershed because of the Shenipsit Lake reservoir's public water system. The flow duration curve (Figure 30) depicts a divergence and increase in the simulated peak flows greater than approximately a 10 percent exceedance (Q_{10}), but little change in the simulated low flow percent exceedances with any buildout.

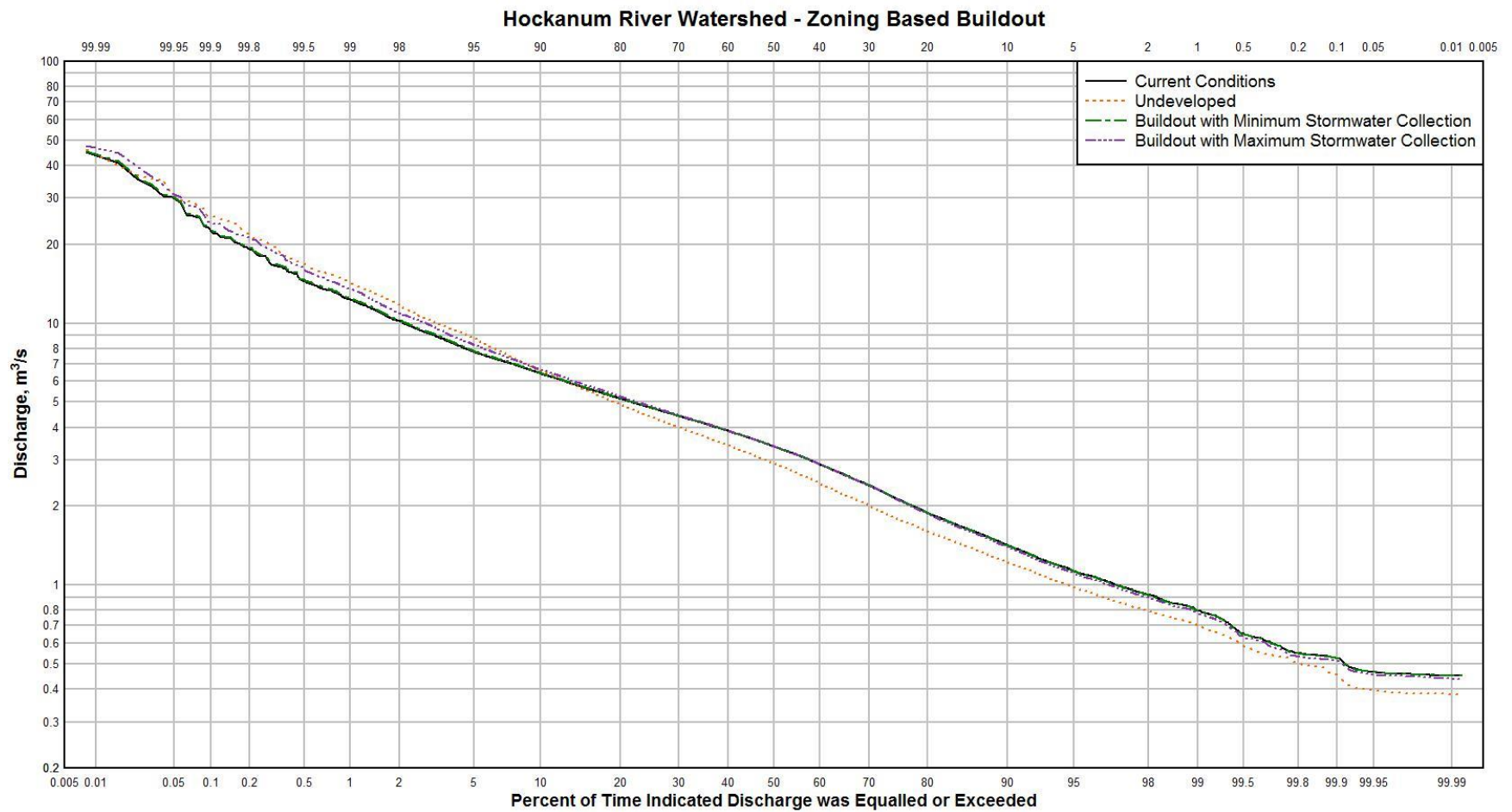


Figure 30. Flow duration curve comparing simulated streamflows among the current conditions, undeveloped, and buildout with minimum and maximum stormwater collection scenarios in the Hockanum River watershed.

The next three scenarios ignored zoning regulations and examined the impacts of significant developmental growth upstream and downstream in the watershed. The TIA was increased in the Upper, Middle, and Lower Watershed study areas to 43.0%, which is equivalent to the HRU with the greatest current impervious surface. The watersheds' outputted water balances are listed in Table 17. Since the changes in imperviousness were so large, the same trends that occurred with zoning buildout happened with these three scenarios.

At their current conditions, the Upper, Middle, and Lower Watershed study areas increase in order from lowest to greatest impervious surface. The changes in average streamflow that occurred from these development scenarios increased in the same order (Table 17). Streamflow increased 0.19, 0.16, and 0.12 m³ s⁻¹ in the Upper, Middle, and Lower study areas. Unlike in the Pomperaug River watershed where drainage area was good predictor of the change in streamflow, in the Hockanum River the current condition impervious areas are a better predictor (Table 19). The Q₉₉ decreases the most in the Upper study area, which could be attributed to the fact that has the least development currently. The Q₉₉ in the Lower study area decreased the least (Table 19); even though it has the greatest percentage of coarse stratified drift deposits, they are already mostly developed on.

Table 19. Relationships between changes in streamflow due to development and subbasin area within the Hockanum River watershed.

| | Study Area Simulated Streamflow (m ³ /s) | Change in Discharge (m ³ /s) | Percent of Total Change in Discharge | Percent of Watershed Area | Study Area Q ₉₉ (m ³ /s) |
|--|---|---|--|---------------------------------|---|
| Upper Watershed Current Conditions | 1.26 | 0.19 | 40.27 | 32.9 | 0.29 |
| Upper Watershed Developed | 1.45 | | | | 0.13 |
| Middle Watershed Current Conditions | 1.26 | 0.16 | 34.09 | 33.9 | 0.30 |
| Middle Watershed Developed | 1.42 | | | | 0.27 |
| Lower Watershed Current Conditions | 1.26 | 0.12 | 25.64 | 33.2 | 0.29 |
| Lower Watershed Developed | 1.38 | | | | 0.27 |

ESTIMATING EIA WITHIN THE HOCKANUM RIVER WATERSHED

The same three methods of estimating EIA that were tested in the Pomperaug River were tested in Hockanum River for the same TIA values. Figure 31 and Figure 32 depict two of the flow duration curves produced by the three different methods. When the TIA was set to 12.5% across the Hockanum River watershed, there were little differences in predicted low flow exceedances, but there were some differences in high flow exceedances among the three methods (Figure 31). These divergences in high flow predictions are more apparent with 25% TIA, as well as the three methods beginning to estimate low flow exceedances differently (Figure 32). These trends continue in the remainder of the flow duration curves in Figure 33, Figure 34, and Figure 35. Just as in the case with the Pomperaug River, the method chosen to estimate EIA was shown to be more important with greater TIA. For additional comparisons, Figures F-4, F-5, and F-6 of Appendix F depict the resultant flow duration curves for each TIA produced by one of the three individual methods of estimating EIA.

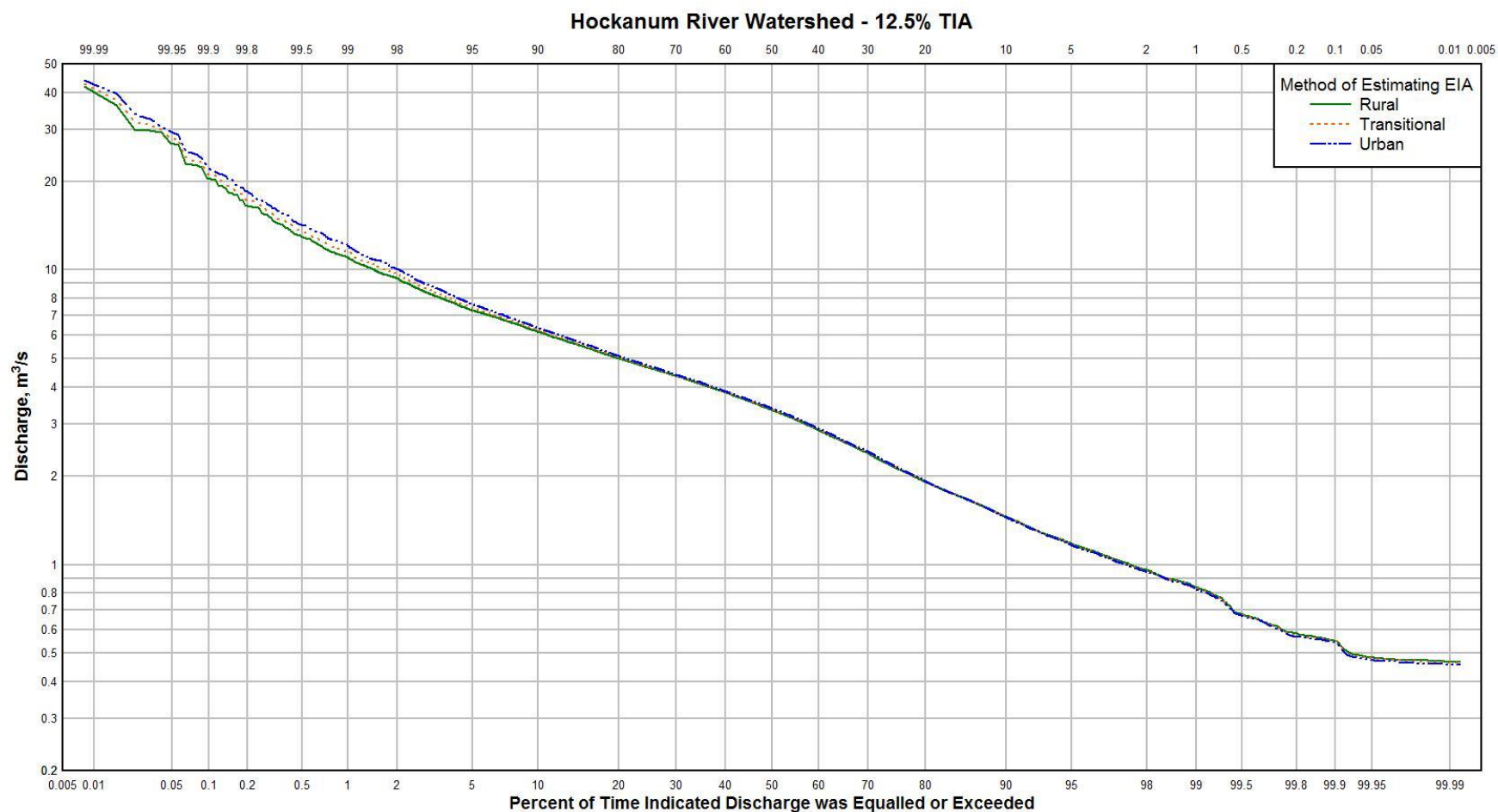


Figure 31. Flow duration curve for the Hockanum River watershed comparing the three methods of estimating EIA based on 12.5% TIA. This percentage TIA was applied throughout the entire watershed, regardless of current conditions, and translated into an EIA via each method.

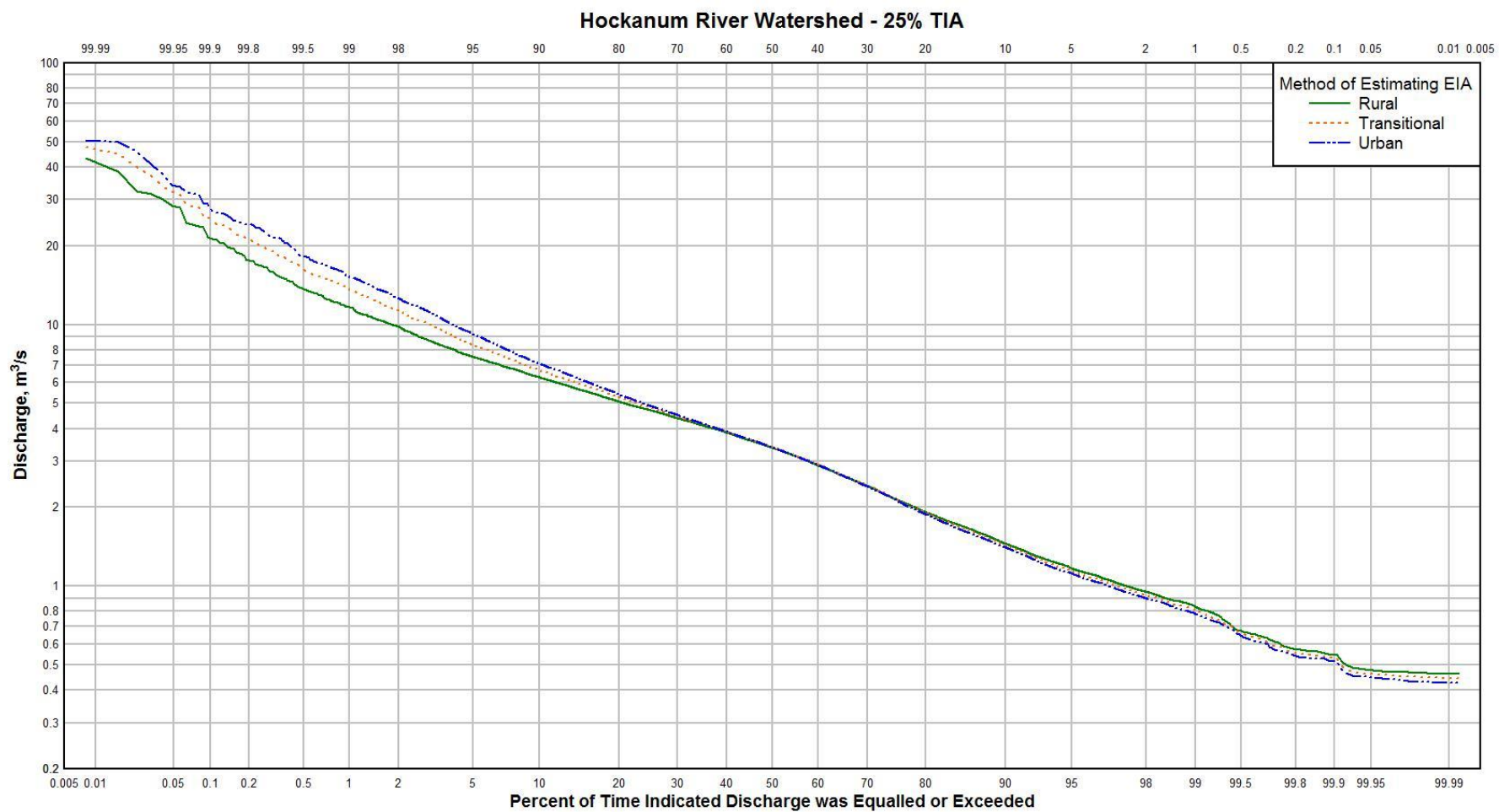


Figure 32. Flow duration curve for the Hockanum River watershed comparing the three methods of estimating EIA based on 25% TIA. This percentage TIA was applied throughout the entire watershed, regardless of current conditions, and translated into an EIA via each method.

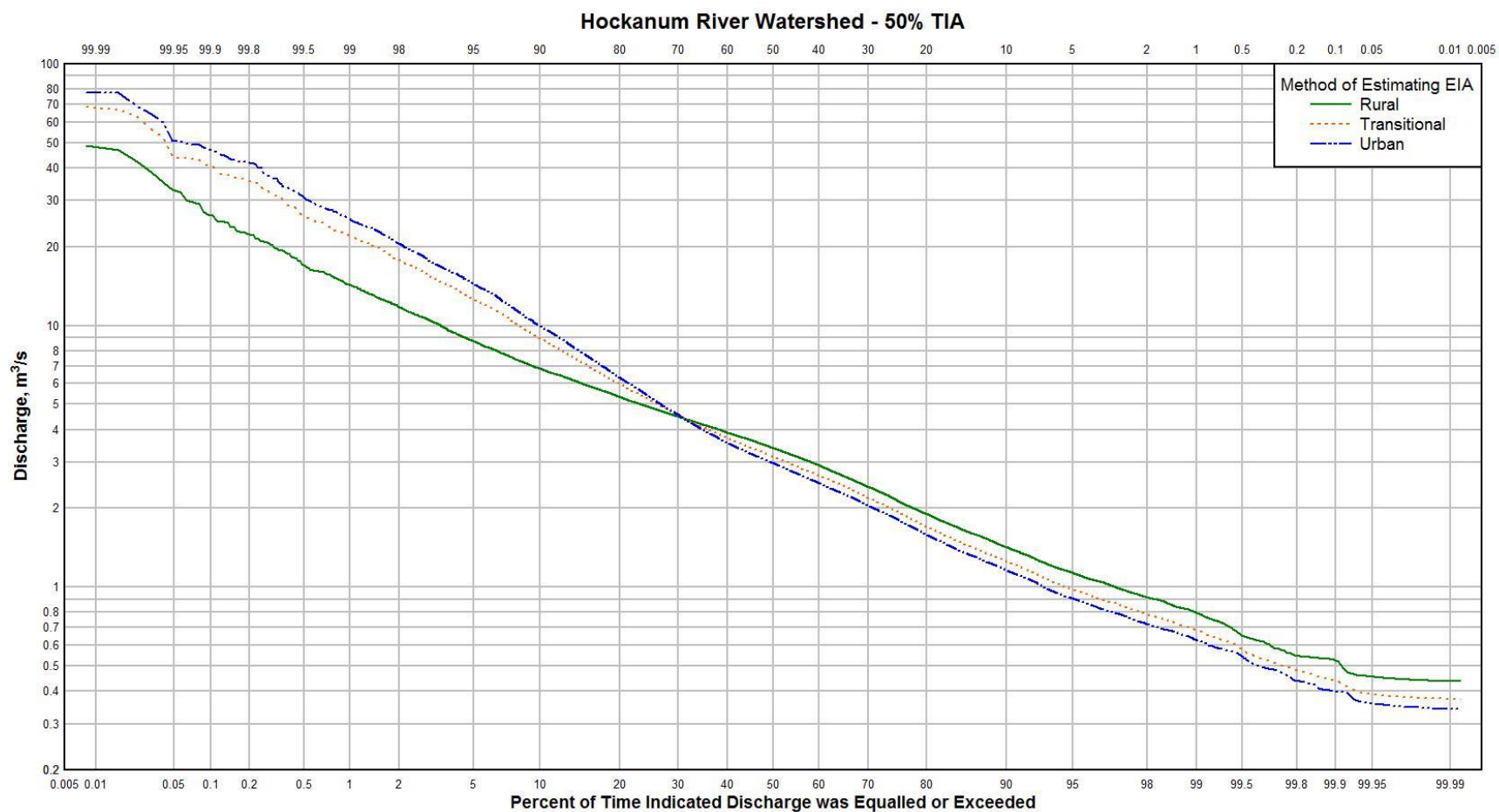


Figure 33. Flow duration curve for the Hockanum River watershed comparing the three methods of estimating EIA based on 50% TIA. This percentage TIA was applied throughout the entire watershed, regardless of current conditions, and translated into an EIA via each method.

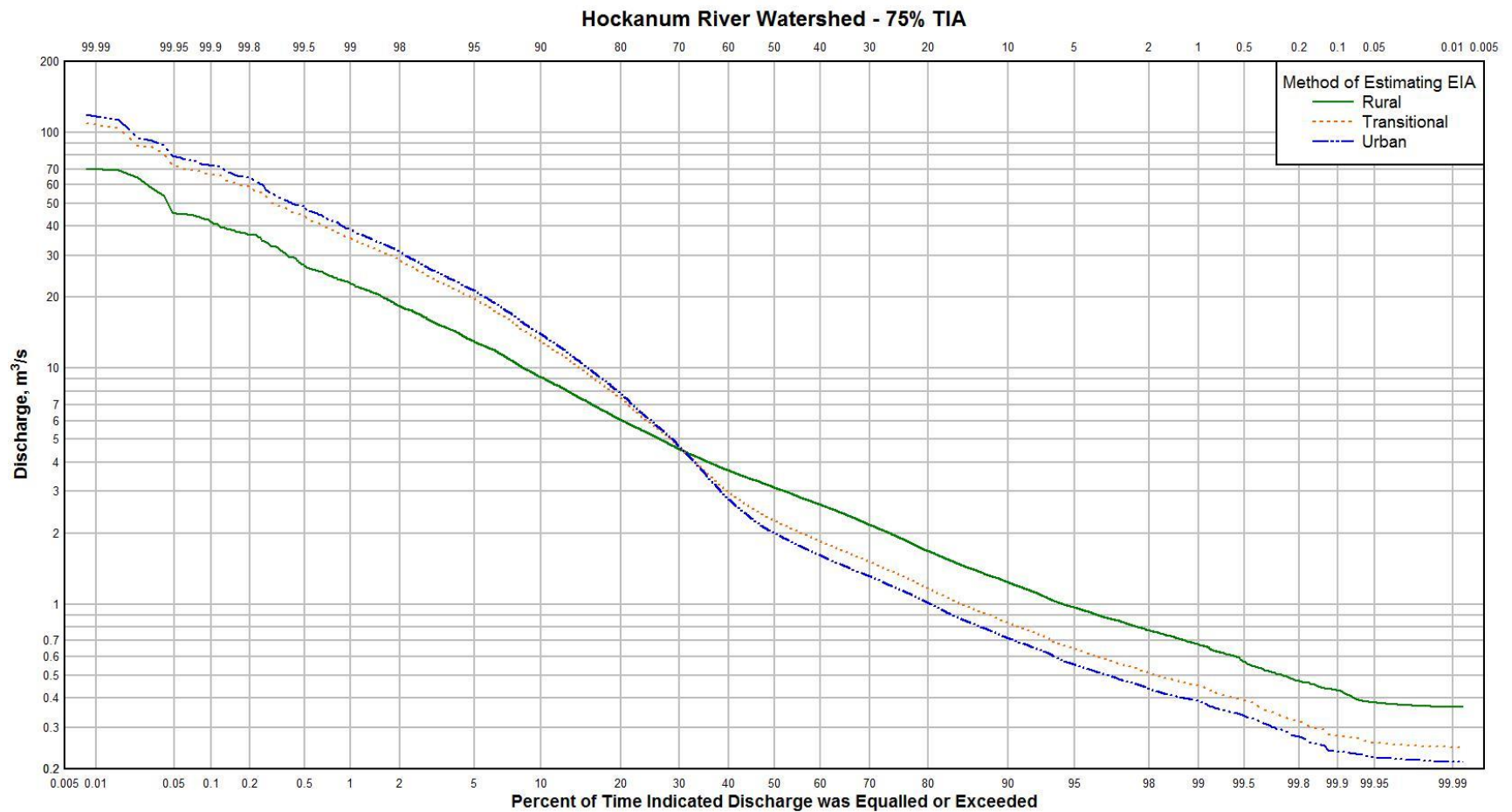


Figure 34. Flow duration curve for the Hockanum River watershed comparing the three methods of estimating EIA based on 75% TIA. This percentage TIA was applied throughout the entire watershed, regardless of current conditions, and translated into an EIA via each method.

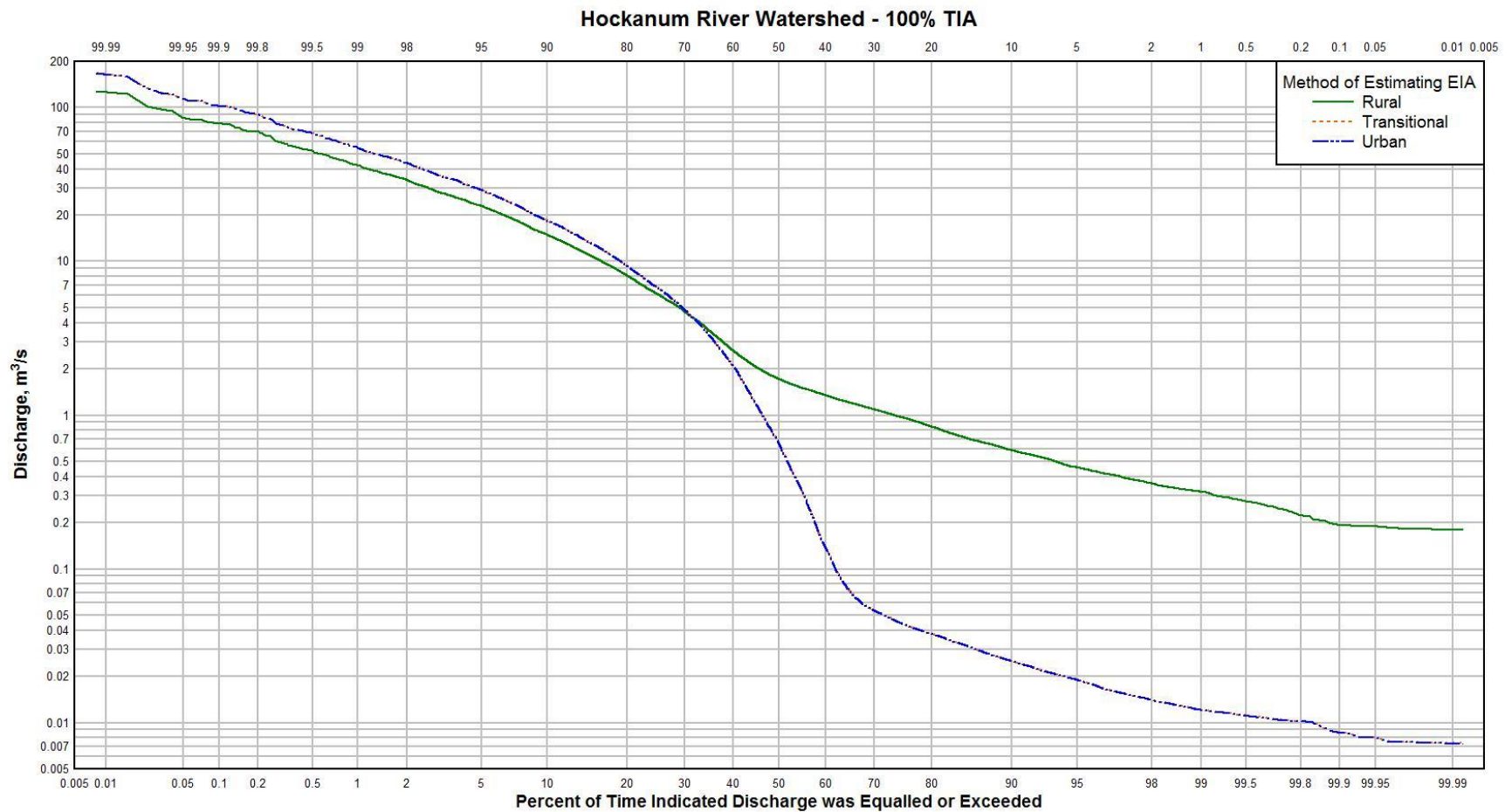


Figure 35. Flow duration curve for the Hockanum River watershed comparing the three methods of estimating EIA based on 100% TIA. This percentage TIA was applied throughout the entire watershed, regardless of current conditions, and translated into an EIA via each method.

OVERALL CONCLUSIONS

The Pomperaug River model was successfully updated and calibrated to the current PRMS software and new study time period data. This satisfies an objective set forth in the Bjerklie et al. study (2010) that the parameterization process be reproducible. Zoning based buildout produced statistically significant increases in surface runoff in both minimum and maximum stormwater collection scenarios, and maximum stormwater collection produced a significant decrease in groundwater flow. The current zoning regulations in the Pomperaug River watershed limited changes in the flow exceedances for both the low and high flows caused by full buildout.

A PRMS model was successfully parameterized and calibrated for the Hockanum River watershed. This validates another objective in the Bjerklie et al. study (2010), which created a parameterization scheme that could be applied to other watersheds in Connecticut. A working model for the Hockanum River watershed provides an example that PRMS is capable of simulating complex and developed watersheds.

A full buildout analysis was conducted for this watershed to determine the extent of impervious surface based on current zoning regulations. Full buildout of the Hockanum River watershed with increased stormwater collection produced statistically significant increases in streamflow and surface runoff and significant decreases in groundwater flow. Large increases in impervious surface in the Hockanum River watershed are limited because the watershed is either already developed or protected from it by zoning regulations.

Upstream and downstream effects of increased impervious area are additive in PRMS and translated throughout the stream network. Therefore, it is difficult to see if the effects upstream have impacts downstream. For example, increased surface runoff upstream might change stream

channel morphology, which could not be captured in the model. Additionally, higher resolution data would be required to determine more localized effects that development or the addition of a pumping well might have on streams.

The method chosen to estimate EIA must be carefully decided on based upon characteristics of the HRU or on the basin-wide scale because impervious surface is a highly sensitive parameter for predicting peak flows. For example, the Hockanum River PRMS model could potentially be improved if each HRU had a method of estimating EIA that was related to its TIA because downstream is highly developed while upstream remains relatively rural. These methods of estimating EIA are imperative for simulating streamflow response to precipitation events.

WATERSHED COMPARISON

By strict comparison of the Nash-Sutcliffe Efficiency statistics, the Hockanum River watershed model would appear to outperform the Pomperaug River watershed model. The Hockanum watershed contains more glacial coarse stratified drift than the Pomperaug, which could indicate that these conditions are easier to model than a watershed with more glacial till. However, the complexity of the Hockanum River's water usage is reflected in the lack of flow duration curve matching between observed and simulated streamflow, whereas the Pomperaug's observed and simulated flow durations matched much more closely. The flow duration curve for the simulated Hockanum River streamflow could indicate what would naturally occur in the water balance had there not been any controls in the watershed, which is generally the case in the Pomperaug. Therefore, the differences between the observed and simulated streamflows are the effects that anthropogenic manipulations, e.g. diversions, reservoir releases, and wastewater treatment discharges, have on the water balance.

MODEL SENSITIVITY, ASSUMPTIONS, AND LIMITATIONS

Sensitivity analyses were used to finely adjust calculated parameters to optimize daily fluxes within the models' streamflow simulations. Different percent increases or decreases from the calculated values were tested to broadly see the effect the change had on the NSE, streamflow composition, and actual evapotranspiration. For this study, parameters that were noted to be especially sensitive for the PRMS models are listed in Table 20.

Table 20. List of sensitive PRMS parameters specific to this study.

| Sensitive Parameters | |
|-----------------------|-----------------------|
| <i>gwflow_coef</i> | <i>soil_moist_max</i> |
| <i>jh_coef</i> | <i>soil_rechr_max</i> |
| <i>jh_coef_hru</i> | <i>soil2gw_max</i> |
| <i>slowcoef_lin</i> | <i>ssr2gw_exp</i> |
| <i>snow_infil_max</i> | <i>ssr2gw_rate</i> |

Documentation of the assumptions made specific to the study areas, in addition to those related to the modeling software, when modeling are necessary for proper interpretation of results and to understand limitations.

In both watersheds, lakes and ponds were not explicitly modeled as lake HRU's, which require a number of additional input parameters. This has a greater impact on the Hockanum River model because the Shenipsit Lake is the largest water body between the two watersheds but is split between three HRU's. Surface or open water bodies are accounted for in the *smidx* parameters and were a simplification of parameterizing a lake HRU. Muskingum routing in PRMS accounts for a couple of localized issues. Within the Pomperaug River PRMS model, event flow storage in the O&G gravel ponds (Bjerklie et al., 2010) is accounted for with an increased **k_coef** (flood wave travel time). In the Hockanum River, the **x_coef** (flood wave attenuation) accounts for the attenuation of flood waves at the Shenipsit Lake reservoir. However, in both models Muskingum routing is the likely cause for underestimating high flow

events. These two routing parameters could be further calibrated for more accurate high flow simulation.

It was assumed that a high density buildout would occur for the Hockanum River watershed full buildout scenario. The potential buildout was based on current zoning restrictions to impervious surface coverage on new building developments. For simplification, there were only two categories of town growth, urban or rural. In order to have the highest density buildout, the maximum allowed lot coverages by each town were distributed to either urban or rural, which could over estimate potential total impervious coverage allotted by zoning in a given town. There were fewer implications for the water balance when protected open spaces were not developed, or those lands that are designated for preservation and conservation. Therefore, an assumption made was that protected open spaces were allowed to be developed to maximize impervious surfaces. Since this buildout was confined to data availability and assumptions applied to HRU-scale development, its uses outside of this should be considered.

The majority of the methodologies used to parameterize the Hockanum River model were documented in the PRMS-IV manual (Markstrom et al., 2015), the previous Pomperaug River study (Bjerklie et al., 2010), or the GIS Weasel User's manual (Viger & Leavesley, 2007) or PRMS metadata (Viger et al., 2014). However, in certain cases data were assumed when calculating parameters. For example, the transmissivity and storativity used to calculate the groundwater flow coefficients were averaged from a Connecticut water resources study (Ryder et al., 1981) and applied across the watershed.

The Hockanum River watershed PRMS model is limited in that the complexities of diversions, reservoir or wastewater treatment releases, or inter-basin transfers were not accounted for outside of the model. This is partly an issue of data availability. For example, in

addition to the total daily quantity of water supplied to consumers from Shenipsit Lake, the percentages of water distributed within and outside the watershed would be required for more precise modeling. Another complexity is the required reservoir releases. In theory, based on legislation the daily reservoir releases could be calculated. However, there is an extra ten day spring freshet to account for and in low flow months if the lake levels drop low enough, releases do not necessarily need to occur in order to protect public water supply. There are similar issues for the two wastewater treatment plants because it is unknown exactly where the water is coming from to the plant or how much is released from the treatment plant to the Hockanum River on a daily time-scale. Unlike in the Bjerklie et al. study (2010), water diversions were not accounted for in this study for simplification.

The Pomperaug River watershed model had to be updated to the new PRMS software because of a lack of compatibility between the old model and the new software. This prevented exact replication of the results from the previous study (Bjerklie et al., 2010). Although sustainability analyses helped recalibrate the new model, it is not entirely known what differences occurred between the two model results.

CONSIDERATIONS FOR FUTURE STUDIES

A number of changes occurred in the Hockanum River watershed after the study period of 1985 to 2015. The University of Connecticut required additional water supply to support developmental expansion. The approval to divert water from Shenipsit Lake as a backup supply for the University was permitted in 2015 and went into effect in 2017. Although complicated, this diversion transfers water out of the Hockanum River basin and should be considered in future studies. Reservoir release requirements were changed in Connecticut's legislation in 2017 so the Shenipsit Lake will have different seasonal discharges going forward. Lastly, the

Manchester wastewater treatment plant was upgraded in 2015, which could be reflected in a future discharge permit.

Water supply plans for municipalities and water companies are increasingly necessary with pressures caused by population growth, climate change, and environmental contamination. The results from hydrologic modeling studies can quantitatively supplement this type of water resources management. The accuracy of these studies and water supply plans would greatly benefit from increased data availability such as additional rain gages, streamgages, and open access to certain water distribution and usage information. For both watersheds in this study, having daily water diversion data would be helpful for understanding the hydrographs, changes in storage in the watershed, and flow duration curves. Without these data, varying amounts of uncertainty are introduced into the interpretation of model results, which limits the practical application of hydrologic models.

LITERATURE CITED

- Ahearn, E. A. (2008). Flow durations, low-flow frequencies, and monthly median flows for selected streams in Connecticut through 2005. *U.S. Geological Survey Scientific Investigations Report 2007-5270*.
- Ahearn, E. A. (2010). Regional regression equations to estimate flow-duration statistics at ungaged stream sites in Connecticut. *U.S. Geological Survey Scientific Investigations Report 2010-5052*.
- Aitken, J. M. (1955). The bedrock of the geology of the Rockville quadrangle. *State Geological and Natural History Survey of Connecticut*, 6.
- Alley, W. M., & Veenhuis, J. E. (1983). Effective impervious area in urban runoff modeling. *Journal of Hydraulic Engineering*, 109(2), 313–319. [https://doi.org/10.1061/\(ASCE\)0733-9429\(1983\)109:2\(313\)](https://doi.org/10.1061/(ASCE)0733-9429(1983)109:2(313))
- Anderson, E. A. (1973). National Weather Service river forecast system - Snow accumulation and ablation model. *NOAA Technical Memorandum NWS HYDRO-17*.
- Arnold Jr., C. L., & Gibbons, C. J. (1996). Impervious surface coverage: The emergence of a key environmental indicator. *American Planning Association Journal*.
- Arnold Jr., C. L., & Gibbons, C. J. (1999). Impacts of Development on Waterways, (February), 1–8. <https://doi.org/Yes>
- Barlow, P. M., Cunningham, W. L., Zhai, T., & Gray, M. (2015). USGS Groundwater Toolbox, a graphical and mapping interface for analysis of hydrologic data (Version 1.0) *U.S. Geological Survey Techniques and Methods*, (Book 3, Chapter B10). <https://doi.org/http://dx.doi.org/10.3133/tm3B10>

- Battaglin, W., Hay, L. E., & Markstrom, S. L. (2011). Simulating the potential effects of climate change in two Colorado basins and at two Colorado ski areas. *Earth Interactions*, 15(22), 1–23. <https://doi.org/10.1175/2011EI373.1>
- Beaulieu, K. M., Bell, A. H., & Coles, J. F. (2012). Variability in stream chemistry in relation to urban development and biological condition in seven metropolitan areas of the United States, 1999-2004. *U.S. Geological Survey Scientific Investigations Report 2012-5170*.
- Bellucci, C. (2007). Stormwater and aquatic Life: Making the connection between impervious cover and aquatic life impairments for TMDL development in Connecticut streams. *Proceedings of the Water Environment Federation*, 2007, 1003–1018. <https://doi.org/10.2175/193864707786619819>
- Bjerklie, D. M., Starn, J. J., & Tamayo, C. (2010). Estimation of the Effects of Land Use and Groundwater Withdrawals on Streamflow for the Pomperaug River , Connecticut. *Scientific Investigations Report 2010 – 5114*, 81. <https://doi.org/10.1002/hyp.6130>
- Brun, R., Reichert, P., & Ku, H. R. (2001). Practical identifiability analysis of large environmental simulation models. *Water Resources Research*, 37(4), 1015–1030. <https://doi.org/10.1029/2000WR900350>
- Bugden, T. (2018). Capturing spatial variation in the Precipitation-Runoff Modeling System. (Master's Thesis - Concurrent). University of Connecticut, College of Agriculture, Health and Natural Resources.
- Coles, J. F., Cuffney, T. F., McMahon, G., & Beaulieu, K. M. (2004). The effects of urbanization on the biological, physical, and chemical characteristics of coastal New England streams. *U.S. Geological Survey Professional Paper 1695*, 47 p.

- Connecticut Department of Environmental Protection. Vernon Municipal NPDES Permit (2004). Retrieved from <https://www3.epa.gov/region1/npdes/permits/2004/ct0100609permit.pdf>
- Connecticut Department of Environmental Protection. Manchester Municipal NPDES Permit (2006). Retrieved from <https://www3.epa.gov/region1/npdes/permits/2006/finalct0100293permit.pdf>
- Connecticut Department of Environmental Protection. Minimum Stream Flow Standards, Pub. L. No. 26–141a, 1 (2015). United States.
- Connecticut Department of Environmental Protection. Stream Flow Standards and Regulations, Pub. L. No. 26–141b, 1 (2015). United States.
- Devi, G. K., Ganasri, B. P., & Dwarakish, G. S. (2015). A review on hydrological models. *Aquatic Procedia*, 4, 1001–1007. <https://doi.org/10.1016/j.aqpro.2015.02.126>
- Dingman, S. L. (2015). *Physical Hydrology* (3rd ed.). Long Grove, IL: Waveland Press, Inc.
- Dockter, D., & Palmer, P. L. (2008). Computation of the Jensen-Haise Evapotranspiration Equations as Applied in the U . S . Bureau of Reclamation s Pacific Northwest AgriMet Program. *Reclamation: Managing Water in the West*, 28.
- Dudley, R. W. (2008). Simulation of the quantity, variability, and timing of streamflow in the Dennys River basin, Maine, by use of a precipitation-runoff watershed model. *U.S. Geological Survey Scientific Investigations Report 2008-5100*.
- Elbashir, S. (2011). *Flood routing in natural channels using Muskingum methods*. Dublin Institute of Technology.

- Flynn, R. H. (2003). A Stream-Gaging Network Analysis for the 7-Day , 10-Year Annual Low Flow in New Hampshire Streams. *U.S. Geological Survey Water-Resources Investigations Report 03-4023*.
- Ford, A. (2010). *Modeling the environment* (2nd ed.). Washington, D. C.: Island Press.
- Freeze, R. A., & Harlan, R. L. (1969). Blueprint for a Physically-Based, Digitally-Simulated Hydrologic Response Model. *Journal of Hydrology*, 9, 237–258.
[https://doi.org/10.1016/0022-1694\(69\)90020-1](https://doi.org/10.1016/0022-1694(69)90020-1)
- Furtsch, E. B. (2015). *The effects of urbanization on baseflow over time: An analysis of changing watersheds and stream flow response in Georgia*. Georgia State University.
- Fuss & O'Neill. (2005). *The Hockanum River state of the watershed report*.
- Giannotti, L., & Prisloe, S. (1998). Do it yourself! Impervious surface buildout analysis. *Nonpoint Education for Municipal Officials: Technical Paper Number 4*.
- Giddings, E. M. P., Bell, A. H., Beaulieu, K. M., Cuffney, T. F., Coles, J. F., Brown, L. R., ... McMahon, G. (2009). Selected physical, chemical, and biological data used to study urbanizing streams in nine metropolitan areas of the united states, 1999-2004. *U.S. Geological Survey Data Series 423*.
- Goode, D. J., Koerkle, E. H., Hoffman, S. A., Regan, R. S., Hay, L. E., & Markstrom, S. L. (2010). Simulation of runoff and reservoir inflow for use in a flood-analysis model for the Delaware River, Pennsylvania, New Jersey, and New York, 2004-2006. *U.S. Geological Survey Open-File Report 2010-1014*.
- Hay, L. E., & Umemoto, M. (2006). Multiple-objective stepwise calibration using LUCA. *U. S. Geological Survey Open-File Report 2006-2323*, 25.

- LaFontaine, J. H., Hay, L. E., Viger, R. J., Markstrom, S. L., Regan, R. S., Elliott, C. M., & Jones, J. W. (2013). Application of the Precipitation-Runoff Modeling System (PRMS) in the Apalachicola-Chattahoochee-Flint River Basin in the southeastern United States, 118.
- Leavesley, G. H., Lichty, R. W., Troutman, B. M., & Saindon, L. G. (1983). Precipitation-runoff modeling system: User's manual. *U.S. Geological Survey Water-Resources Investigations Report 83-4238*, 207.
- Lee, J. G., & Heaney, J. P. (2003). Estimation of urban imperviousness and its impacts on storm water systems. *Journal of Water Resources Planning and Management*, 129(5), 419–426.
[https://doi.org/10.1061/\(ASCE\)0733-9496\(2003\)129:5\(419\)](https://doi.org/10.1061/(ASCE)0733-9496(2003)129:5(419))
- Markstrom, S. L., Hay, L. E., & Clark, M. P. (2016). Towards simplification of hydrologic modeling: Identification of dominant processes. *Hydrology and Earth System Sciences*, 20(11), 4655–4671. <https://doi.org/10.5194/hess-20-4655-2016>
- Markstrom, S. L., Hay, L. E., Ward-Garrison, C. D., Risley, J. C., Battaglin, W. A., Bjerklie, D. M., ... Walker, J. F. (2012). Integrated watershed-scale response to climate change for selected basins across the United States. *U.S. Geological Survey Scientific Investigations Report 2011–5077*. Retrieved from <http://pubs.usgs.gov/sir/2011/5077/>
- Markstrom, S. L., Regan, R. S., Hay, L. E., Viger, R. J., Webb, R. M. T., Payn, R. A., & LaFontaine, J. H. (2015). PRMS-IV , the Precipitation-Runoff Modeling System, Version 4. *U.S. Geological Survey Techniques and Methods, Book 6: Modeling Techniques*, 158.
<https://doi.org/http://dx.doi.org/10.3133/tm6B7>

- Meinzer, O. E., & Stearns, N. D. (1929). A study of groundwater in the Pomperaug River watershed, Connecticut, with special reference to intake and discharge. *U.S. Geological Survey Water-Supply Paper 597-B*, 73–146.
- Moriasi, D. N., Arnold, J. G., Van Liew, M. W., Binger, R. L., Harmel, R. D., & Veith, T. L. (2007). Model evaluation guidelines for systematic quantification of accuracy in watershed simulations. *Transactions of the ASABE*, 50(3), 885–900.
<https://doi.org/10.13031/2013.23153>
- Mullaney, J. R., & Grady, S. J. (1997). Hydrogeology and water quality of a surficial aquifer underlying an urban area, Manchester, Connecticut. *U.S. Geological Survey Water-Resources Investigations Report 97-4195*, 40.
- Natural Resources Conservation Service, U. S. Department of Agriculture. Soil Survey Geographic (SSURGO) Database. Retrieved from <https://websoilsurvey.nrcs.usda.gov/> (accessed March 2016).
- Pierce, M. A. (2017). "Documentary history of American water-works: Rockville, Connecticut". Retrieved from <http://www.waterworkshistory.us/CT/Rockville/>
- Robinove, C. J. (1962). Ground-water studies and analog models. *Geological Survey Circular* 468.
- Rose, S., & Peters, N. E. (2001). Effects of urbanization on streamflow in the Atlanta area (Georgia, USA): A comparative hydrological approach. *Hydrological Processes*, 15(8), 1441–1457. <https://doi.org/10.1002/hyp.218>
- Rozum, J. S., Arnold, C. L., & Wilson, E. H. (2008). About buildouts: A brief guide to buildout analysis, and why and how to do them. CT Nemo.

- Ryder, R. B., Thomas, M. P., & Weiss, L. A. (1981). Water resource inventory of Connecticut part 7: Upper Connecticut River basin. *Connecticut Water Resources Bulletin No. 24*, 76.
- Sauer, V. B., Thomas Jr., W. O., Stricker, V. A., & Wilson, K. V. (1983). Flood characteristics of urban watersheds in the United States. *U.S. Geological Survey Water-Supply Paper 2207*, 69. Retrieved from <http://pubs.er.usgs.gov/publication/wsp2207>
- Searcy, J. K. (1959). Flow duration curves. *Geological Survey Water-Supply Paper 1542-A*. <https://doi.org/10.1002/047147844X.sw321>
- Sleavin, W. J., Civco, D. L., Prisloe, S., & Giannotti, L. (2000). Measuring impervious surfaces for non-point source pollution modeling. In *Proceedings of the ASPRS 2000 Annual Conference* (pp. 22–26). <https://doi.org/Yes>
- Smucygz, B., Clayton, J. A., & Comarova, Z. (2010). Comparison of changes in runoff and channel cross-sectional area as a consequence of urbanization for three Chattahoochee River subbasins, Georgia, USA. *Southeastern Geographer*, 50(4), 468–483.
- Steuer, J. J., & Hunt, R. J. (2001). Use of a watershed-modeling approach to assess hydrologic effects of urbanization, North Fork Pheasant Branch Basin near Middleton, Wisconsin. *U.S. Geological Survey Water-Resources Investigations Report 01-4113*, 56.
- Sun, G. E., & Caldwell, P. (2015). Impacts of urbanization on stream water quantity and quality in the United States. *Water Resources Impact*, 17(1), 17–20.
- Suro, T. P., & Gazoorian, C. L. (2011). Changes in Low-Flow Frequency from 1976 – 2006 at Selected Sites in New York , Excluding Long Island. *U.S. Geological Survey Scientific Investigations Report 2011-5112*.

- Taniguchi, K. T., & Biggs, T. W. (2015). Regional impacts of urbanization on stream channel geometry: A case study in semiarid southern California. *Geomorphology*, 248, 228–236. <https://doi.org/10.1016/j.geomorph.2015.07.038>
- Thornton, P. E., Thornton, M. M., Mayer, B. W., Wei, Y., Devarakonda, R., Vose, R. S., & Cook, R. B. (2017). Daymet: Daily surface weather data on a 1-km grid for North America, Version 3. ORNL DAAC, Oak Ridge, Tennessee, USA. <https://doi.org/https://doi.org/10.3334/ORNLDAAC/1328>
- U.S. Environmental Protection Agency. (1998). *Guidance manual for implementing municipal storm water management programs*. Washington, D. C.
- Viger, R. J., Hay, L. E., Markstrom, S. L., Jones, J. W., & Buell, G. R. (2011). Hydrologic effects of urbanization and climate change on the Flint River basin, Georgia. *Earth Interactions*, 15(20), 1–25. <https://doi.org/10.1175/2010EI369.1>
- Viger, R. J., & Leavesley, G. H. (2007). *The GIS Weasel user 's manual*. U.S. Geological Survey *Techniques and Methodes 6-B4*.
- Viger, R. J., Markstrom, S. L., & Hay, L. E. (2014). Preliminary spatial parameters for PRMS based on the Geospatial Fabric, NLCD, and SSURGO. U.S. Geological Survey. Retrieved from <http://dx.doi.org/doi:10.5066/F7WM1BF7>
- Wilson, W. E., Burke, E. L., & Thomas Jr., C. E. (1974). Water resources inventory of Connecticut part 5: Lower Housatonic River basin. *Connecticut Water Resources Bulletin No. 19*, 79.
- Zimmerman, C. L. (2011). *Determining directly connected impervious areas in residential land-use*. University of Connecticut.

APPENDIX A

Table A - 1. List of software and programs used in this study.

| Name | Version | Publisher | Year |
|--------------------------------------|-------------|-------------------------|------|
| Precipitation-Runoff Modeling System | 4.0.1 | USGS | 2015 |
| ArcGIS for Desktop | 10.4 & 10.5 | ESRI | 2016 |
| Groundwater Toolbox | 1.3 | USGS | 2017 |
| Dplot | 2.3.5.7 | Hydesoft Computing, LLC | 2017 |

Table A - 2. List of data sources and the watershed that the data were used with (if applicable). HRW denotes the Hockanum River watershed, and PRW denotes the Pomperaug River watershed.

| Observed Streamgage | | | |
|---|---|-----------|-----------|
| Description | Source | Watershed | Year(s) |
| Hockanum River - Number: 01192500 | U. S. Geological Survey | HRW | 1980-2015 |
| Pomperaug River - Number: 01204000 | U. S. Geological Survey | PRW | 1980-2015 |
| Nonnewaug River - Number: 01203600 | U. S. Geological Survey | PRW | 2003-2015 |
| Weekeepeemee River - Number: 01203805 | U. S. Geological Survey | PRW | 2003-2015 |
| Climate Inputs | | | |
| Description | Source | Watershed | Year (s) |
| Bradley Airport - Station Number: 063456 | NOAA COOP Station | PRW | 1980-2015 |
| Woodbury - Station Number: 069775 | NOAA COOP Station | PRW | 1980-2015 |
| Danbury - Station Number: 061762 | NOAA COOP Station | PRW | 1980-2015 |
| Middletown - Station Number: 064767 | NOAA COOP Station | PRW | 1980-2015 |
| Daylength | Daymet: Daily Surface Weather Data - ORNL | HRW | 1980-2015 |
| Solar Radiation | Daymet: Daily Surface Weather Data - ORNL | HRW | 1980-2015 |
| Maximum Daily Temperature | Daymet: Daily Surface Weather Data - ORNL | HRW | 1980-2015 |
| Minimum Daily Temperature | Daymet: Daily Surface Weather Data - ORNL | HRW | 1980-2015 |
| Daily Precipitation | Daymet: Daily Surface Weather Data - ORNL | HRW | 1980-2015 |

Table A - 2 continued. List of data sources.

| GIS Data | | |
|--|--|-------------|
| Description | Source | Year |
| Digital Elevation Model (DEM) - 1/3 arc second | National Elevation Dataset (NED) - USGS National Map | 2017 |
| Hydrography | Connecticut DEEP | 2005 |
| Inland Wetlands Soils | Soil Survey Geographic Database (SSURGO) - NRCS | 2007 |
| Percentage Sand, Clay, Silt | USGS Data Series: Issue #866 | 2014 |
| Land Use-Land Cover | National Land Cover Database - USGS | 2011 |
| Tree Canopy Analytical | National Land Cover Database - USGS | 2011 |
| Percent Developed Imperviousness | National Land Cover Database - USGS | 2011 |
| Zoning Regulations | Capitol Region Council of Governments | 2014 |
| Coarse Stratified Drift | USGS | 1992 |
| Protected Open Space | Connecticut DEEP | 2011 |
| Available Water Capacity | Soil Survey Geographic Database (SSURGO) - NRCS | 2014 |
| Saturated Hydraulic Conductivity | Soil Survey Geographic Database (SSURGO) - NRCS | 2014 |

APPENDIX B

Table B - 1. List of PRMS modules used for each of the two watershed models.

| Required by PRMS, only one option | | |
|--|----------------------|--|
| Module Category | Module Used | Simulated Processes |
| Basin | <i>basin</i> | Physical parameters and variables of watershed and HRU's |
| Solar Table | <i>soltab</i> | Solar radiation and sunlight hours for each day of the year |
| Snow Distribution | <i>snowcomp</i> | Snow area and snowmelt |
| Interception | <i>intcp</i> | Interception and ET |
| Groundwater Runoff | <i>gwflow</i> | Groundwater runoff |
| Pomperaug | | |
| Module Category | Module Used | Simulated Processes |
| Combined Climate-Distribution | <i>xyz_dist</i> | Precipitation and air temperature |
| Solar-Radiation Distribution | <i>ddsolrad</i> | Degree-day solar radiation |
| Transpiration | <i>transp_tindex</i> | Temperature index/active transpiration |
| Potential Evapotranspiration | <i>potet_jh</i> | Jensen-Haise PET |
| Surface Runoff | <i>srunoff_smidx</i> | Surface runoff/soil-moisture index |
| Soil Zone | <i>soilzone</i> | Capillary/gravity soil zone processes |
| Streamflow | <i>muskingum</i> | Routes water between stream segments |
| Hockanum | | |
| Module Category | Module Used | Simulated Processes |
| Climate-by-HRU Distribution | <i>climate_hru</i> | Precipitation, air temperature, solar radiation, and transpiration |
| Transpiration | <i>transp_tindex</i> | Temperature index/active transpiration |
| Potential Evapotranspiration | <i>potet_jh</i> | Jensen-Haise PET |
| Surface Runoff | <i>srunoff_smidx</i> | Surface runoff/soil-moisture index |
| Soil Zone | <i>soilzone</i> | Capillary/gravity soil zone processes |
| Streamflow | <i>muskingum</i> | Routes water between stream segments |

APPENDIX C

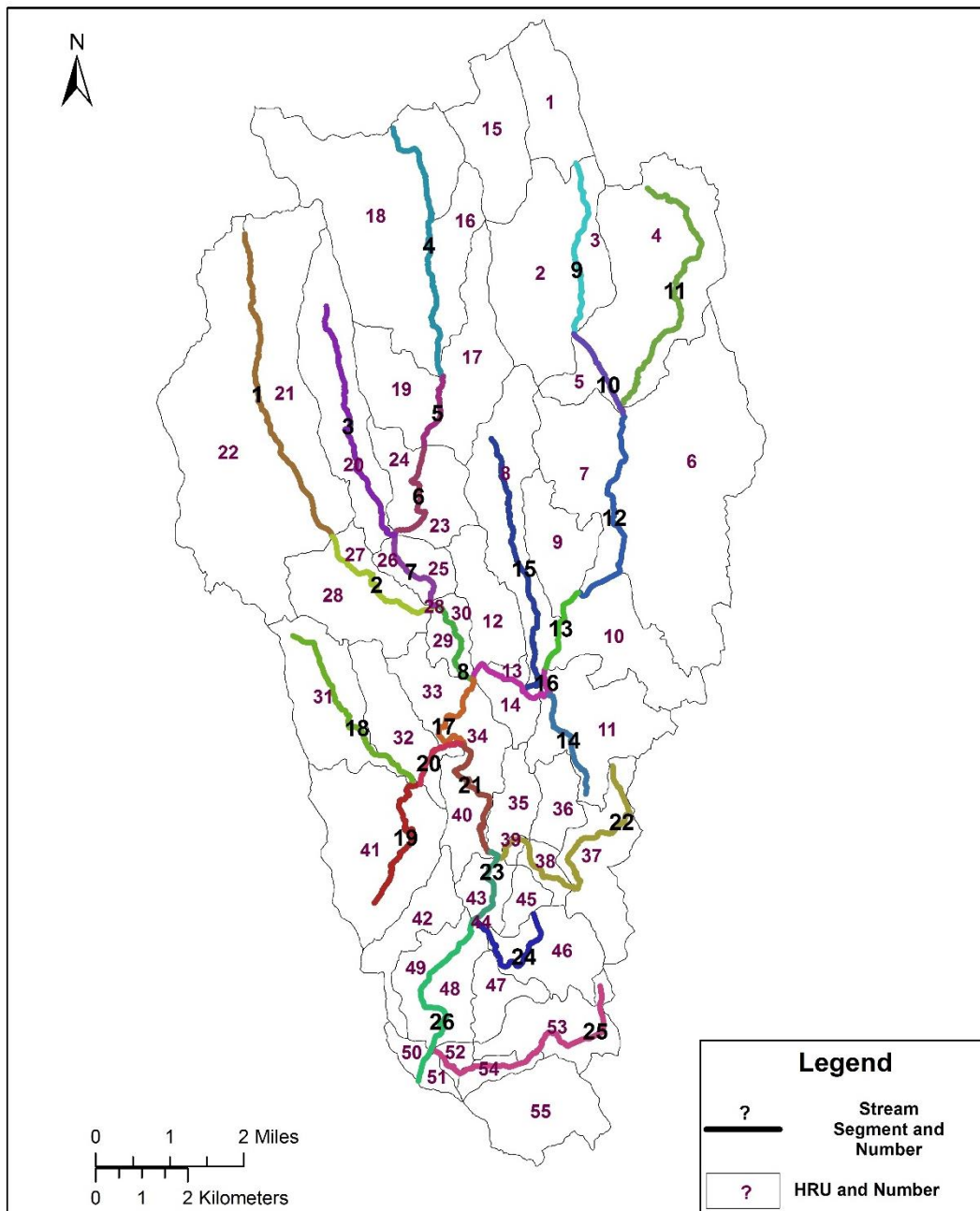


Figure C – 1. Stream segments delineated for Muskingum Routing in the Pomperaug River watershed PRMS model.

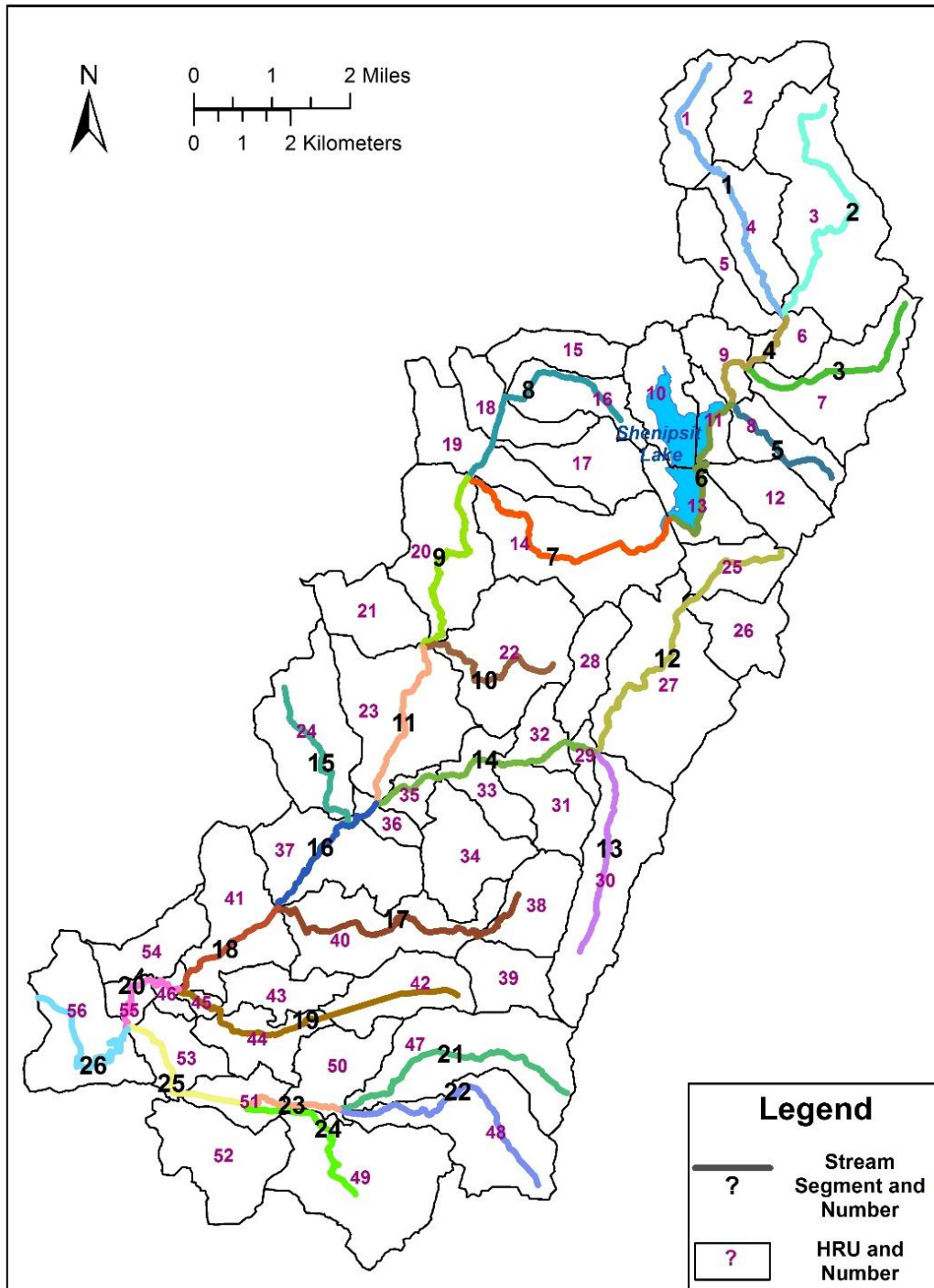


Figure C – 2. Stream segments delineated for Muskingum Routing in the Hockanum River watershed PRMS model.

APPENDIX D

Table D-1. Registered and permitted water diversions in the Hockanum River watershed, Connecticut.

| Name | Type | Quantity | | Source | Use | Town | Active Dates |
|---|--------------|----------|--------------------|---------------|--------------|------------------|------------------------|
| | | Mgal/d | ft ³ /s | | | | |
| Cellu Tissue, LLC | Permit | 0.850 | 1.32 | Groundwater | Industrial | East Hartford | 1/18/2012 - 12/31/2036 |
| Cellu Tissue, LLC | Permit | 1.800 | 2.79 | Groundwater | Industrial | East Hartford | 11/1/2001 - 10/29/2011 |
| Cellu Tissue, LLC | Permit | 1.800 | 2.79 | Groundwater | Industrial | East Hartford | 9/10/1987 - 12/31/1991 |
| Manchester Water Department Risley Reservoir and Lydall St. Reservoirs 1 & 2 | Permit | 1.600 | 2.48 | Surface water | Public water | Manchester | 1/17/1985 - 1/17/2035 |
| Union Pond Skating Rink | Permit | 0.180 | 0.28 | Surface water | Industrial | Manchester | 2/4/2002 - 12/31/2021 |
| Connecticut Water Company Vernon Well #6 | Permit | 0.135 | 0.21 | Groundwater | Public water | Vernon | 7/24/1987 - 12/31/1992 |
| Connecticut Water Company Regional Pipeline and the University of Connecticut | Permit | 1.850 | 2.86 | Surface water | Public water | Ellington/Vernon | 6/2/2015 - 5/29/2040 |
| Connecticut Water Company | Permit | 0.430 | 0.67 | Surface water | Public water | Ellington/Vernon | 8/26/2014 - 7/18/2039 |
| Ansaldo Company Folly Pond | Registration | 0.86 | 1.33 | Surface water | Industrial | Manchester | Prior to 1983 |
| Lydall Incorporated Lydall Pond | Registration | 1.00 | 1.55 | Surface water | Industrial | Manchester | Prior to 1983 |
| Lydall Incorporated Well #1 | Registration | 0.58 | 0.90 | Groundwater | Industrial | Manchester | Prior to 1983 |
| Lydall Incorporated Well #2 | Registration | 0.72 | 1.11 | Groundwater | Industrial | Manchester | Prior to 1983 |
| Manchester Country Club #1 Pond | Registration | 0.22 | 0.34 | Surface water | Irrigation | Manchester | Prior to 1983 |
| Manchester Country Club #11 Pond | Registration | 0.86 | 1.33 | Surface water | Irrigation | Manchester | Prior to 1983 |
| Manchester Country Club #14 Lower Pond | Registration | 0.86 | 1.33 | Surface water | Irrigation | Manchester | Prior to 1983 |
| Manchester Country Club #14 Upper Pond | Registration | 0.86 | 1.33 | Surface water | Irrigation | Manchester | Prior to 1983 |
| Manchester Sand and Gravel #1 | Registration | 0.86 | 1.33 | Groundwater | Industrial | Manchester | Prior to 1983 |
| Manchester Sand and Gravel #2 | Registration | 2.02 | 3.13 | Groundwater | Industrial | Manchester | Prior to 1983 |
| Manchester Sand and Gravel Parcel Pond | Registration | 2.02 | 3.13 | Surface water | Industrial | Manchester | Prior to 1983 |
| Manchester Sand and Gravel Lagoons | Registration | 2.02 | 3.13 | Surface water | Industrial | Manchester | Prior to 1983 |

Table D-1 continued. Registered and permitted water diversions in the Hockanum River watershed, Connecticut.

| Name | Type | Quantity | | Source | Use | Town | Active Dates |
|---|--------------|----------|--------------------|---------------|--------------|------------|---------------|
| | | Mgal/d | ft ³ /s | | | | |
| Manchester Water Department Globe Hollow Reservoir | Registration | 2.50 | 3.87 | Surface water | Public water | Manchester | Prior to 1983 |
| Manchester Water Department Howard Reservoir | Registration | 3.75 | 5.80 | Surface water | Public water | Manchester | Prior to 1983 |
| Manchester Water Department New Bolton Well Field #1 | Registration | 0.23 | 0.36 | Groundwater | Public water | Manchester | Prior to 1983 |
| Manchester Water Department New Bolton Well Field #2 | Registration | 0.20 | 0.31 | Groundwater | Public water | Manchester | Prior to 1983 |
| Manchester Water Department New Bolton Well Field #3R | Registration | 0.43 | 0.67 | Groundwater | Public water | Manchester | Prior to 1983 |
| Manchester Water Department Porter Reservoir | Registration | 3.80 | 5.88 | Surface water | Public water | Manchester | Prior to 1983 |
| Manchester Water Department Fern Street #1 | Registration | 0.82 | 1.27 | Groundwater | Public water | Manchester | Prior to 1983 |
| Manchester Water Department Charter Oak Street #2A | Registration | 1.01 | 1.56 | Groundwater | Public water | Manchester | Prior to 1983 |
| Manchester Water Department Charter Oak Street #3 | Registration | 0.40 | 0.62 | Groundwater | Public water | Manchester | Prior to 1983 |
| Manchester Water Department Charter Oak Street #4 | Registration | 0.72 | 1.11 | Groundwater | Public water | Manchester | Prior to 1983 |
| Manchester Water Department Love Lane #5 | Registration | 0.58 | 0.90 | Groundwater | Public water | Manchester | Prior to 1983 |
| Manchester Water Department New State Road #6 | Registration | 0.86 | 1.33 | Groundwater | Public water | Manchester | Prior to 1983 |
| Manchester Water Department New State Road #7 | Registration | 0.86 | 1.33 | Groundwater | Public water | Manchester | Prior to 1983 |
| Manchester Water Department New State Road #8 | Registration | 0.57 | 0.88 | Groundwater | Public water | Manchester | Prior to 1983 |
| Manchester Water Department Bretton Road #9 | Registration | 0.19 | 0.29 | Groundwater | Public water | Manchester | Prior to 1983 |
| Manchester Water Department Parker Street #10 | Registration | 0.43 | 0.67 | Groundwater | Public water | Manchester | Prior to 1983 |
| Manchester Water Department Progress Drive #11 | Registration | 0.50 | 0.77 | Groundwater | Public water | Manchester | Prior to 1983 |
| Multi Circuits Incorporated Well #1 | Registration | 0.18 | 0.28 | Groundwater | Industrial | Manchester | Prior to 1983 |

Table D-1 continued. Registered and permitted water diversions in the Hockanum River watershed, Connecticut.

| Name | Type | Quantity | | Source | Use | Town | Active Dates |
|---|--------------|----------|--------------------|---------------|--------------|------------------|---------------|
| | | Mgal/d | ft ³ /s | | | | |
| Multi Circuits Incorporated Well #2 | Registration | 0.16 | 0.25 | Groundwater | Industrial | Manchester | Prior to 1983 |
| Multi Circuits Incorporated Well #3 | Registration | 0.30 | 0.46 | Groundwater | Industrial | Manchester | Prior to 1983 |
| Sumitomo Bakelite Incorporated Well #1 | Registration | 0.45 | 0.70 | Groundwater | Industrial | Manchester | Prior to 1983 |
| Connecticut Water Company Shenipsit Lake | Registration | 15.00 | 23.21 | Surface water | Public water | Ellington/Vernon | Prior to 1983 |
| Culbro Tobacco Farm #11 Well #1 | Registration | 0.72 | 1.11 | Groundwater | Irrigation | Ellington | Prior to 1983 |
| Culbro Tobacco Farm #11 Well #2 | Registration | 0.58 | 0.90 | Groundwater | Irrigation | Ellington | Prior to 1983 |
| Culbro Tobacco Farm #11 Well #3 | Registration | 0.43 | 0.67 | Groundwater | Irrigation | Ellington | Prior to 1983 |
| Moser Farms Well #1 | Registration | 0.22 | 0.34 | Groundwater | Industrial | Ellington | Prior to 1983 |
| Connecticut Water Company Vernon Well #1 | Registration | 0.17 | 0.26 | Groundwater | Public water | Vernon | Prior to 1983 |
| Connecticut Water Company Vernon Well #2 | Registration | 0.17 | 0.26 | Groundwater | Public water | Vernon | Prior to 1983 |
| Connecticut Water Company Vernon Well #3 | Registration | 0.14 | 0.22 | Groundwater | Public water | Vernon | Prior to 1983 |
| Connecticut Water Company Vernon Well #4 | Registration | 0.17 | 0.26 | Groundwater | Public water | Vernon | Prior to 1983 |
| Connecticut Water Company Vernon Well #5 | Registration | 0.43 | 0.67 | Groundwater | Public water | Vernon | Prior to 1983 |
| Amerbelle Textiles Hockanum River | Registration | 2.94 | 4.55 | Surface water | Industrial | Vernon | Prior to 1983 |
| Schutz from Charter Brook | Registration | 0.0864 | 0.13 | Surface water | Irrigation | Tolland | Prior to 1983 |
| Schutz from Unnamed Brook | Registration | 0.0864 | 0.13 | Surface water | Irrigation | Tolland | Prior to 1983 |
| Connecticut Water Company Pine Knob Well | Registration | 0.648 | 1.00 | Groundwater | Public water | South Windsor | Prior to 1983 |
| Connecticut Water Company Woodland Park Well | Registration | 0.252 | 0.39 | Groundwater | Public water | South Windsor | Prior to 1983 |
| Manchester Water Department Buckingham Reservoir* | Registration | 3.00 | 4.64 | Surface water | Public water | Glastonbury | Prior to 1983 |

APPENDIX E

This appendix details parameterization of the Hockanum River watershed PRMS model.

Input parameters are denoted by a boldface font. Parameters that are calculated by PRMS are denoted by an italicized font, or denominate module names.

MODEL DIMENSIONS

Table E-1 contains the dimensions used in the Hockanum River watershed PRMS parameter file and are detailed in the PRMS-IV manual (Markstrom et al., 2015). “nmonths” and “ndays” are the number of months and days used by the model, respectively. The dimension “one” refers to the dimension that contains scalar parameters and variables. The number of streamflow observation stations is “nobs”. The “ntemp” and “nrain” are set to 0 because climate stations are not used in the Climate by HRU module. The “nsegment” value is the number of stream segments that were delineated for Muskingum routing. “ndepl” refers to the number of snow depletion curves the model can choose from. “ndeplval” refers to the total number of values in all of the snow depletion curves used. Since there 11 values in each curve, “ndeplval” is equal to “ndepl” multiplied by 11. Only one snow depletion curve is necessary, but multiple curves are useful in mountainous ranges above timberlines (Viger & Leavesley, 2007). The number of HRU’s, groundwater reservoirs, and subsurface reservoirs the model will use are described by “nhru”, “ngw”, “nssr”, and “nsub” respectively.

Table E-1. Model dimension sizes used in the Hockanum River watershed PRMS model.

| Dimension | Size | Dimension | Size |
|------------------|-------------|------------------|-------------|
| nmonths | 12 | nsegment | 26 |
| ndays | 366 | ndepl | 1 |
| one | 1 | ndeplval | 11 |
| nobs | 1 | nhru | 56 |
| ntemp | 0 | nssr | 56 |
| nrain | 0 | ngw | 56 |

INPUT PARAMETERS

The procedures used to calculate parameters were either from the manuals for the PRMS, the GIS Weasel, GSFLOW, the PRMS metadata, or published articles. The majority of input parameters into PRMS for the Hockanum River watershed were determined by available ArcGIS data and ArcMap tools. Sensitivity analyses helped optimize certain parameters. Therefore, parameters may vary slightly from calculated or observed GIS data.

GEOGRAPHIC PARAMETERS

Table E-2 lists parameters that can be determined from GIS and are geographically related to the watershed. Each of these parameters is determined for each HRU to better represent the spatial variability that occurs in nature.

Table E-2. Geographic parameters and the source from which they are determined.

| Parameter | Parameter Name | Data Source |
|------------------------|-------------------|-------------------------|
| HRU Area | hru_area | HRU Shapefile |
| HRU Latitude (NAD1983) | hru_lat | HRU Shapefile |
| HRU Elevation | hru_elev | Digital Elevation Model |
| HRU Slope | hru_slope | Digital Elevation Model |
| HRU Aspect | hru_aspect | Digital Elevation Model |

INPUT CLIMATIC AND OBSERVED DATA – GDP & USGS STREAMGAGE

The Climate by HRU module was used in PRMS for the Hockanum River watershed, which meant that mean daily solar radiation, precipitation, maximum temperature (tmax), and minimum temperature (tmin) data were required for each HRU. A shapefile of the 56 HRU's was uploaded to the USGS Geo Data Portal (GDP) – Daymet Daily Surface Data on a 1-km Grid for North America, Version 3 to retrieve daily climate data for each HRU. The aforementioned climate data, along with daylength, were outputted from 1980 to 2015, which was the extent of available Daymet data. The algorithm selected for processing was Area Grid Statistics

(weighted). This algorithm applied area-weighted values to each HRU's calculated mean daily climate data.

The outputted climate data from the GDP required unit conversions in Microsoft Excel for correct input into PRMS. Daylength was required in hours/day for the solar radiation conversion. Solar radiation outputted in W/m², but the PRMS uses Langleys/day. The conversion required was:

$$\frac{\text{Langleys}}{\text{day}} = \text{solar radiation} \left(\frac{\text{W}}{\text{m}^2} \right) \times 0.085985 \left(\frac{\text{Langleys}}{\text{hour}} \right) \times \text{daylength} \left(\frac{\text{hours}}{\text{day}} \right)$$

T_{max} and T_{min} were outputted in degrees Celsius and were converted into degrees Fahrenheit. Lastly, the precipitation data were in units of mm/day and were converted to in/day. Individual PRMS input text files were created for solar radiation, tmax, tmin, and precipitation data. These text files can be created by opening a comma-separated values (CSV) file in Microsoft Word, replacing the commas with spaces, and then copying the data over into a Microsoft Notepad text file.

The fifth input text file created included the observed daily streamflow from USGS streamgage #01192500 for the Hockanum River near East Hartford, Connecticut. Daily values for streamflow were retrieved from the USGS National Water Information System website. This file is useful for PRMS output of observed streamflow so that it and simulated streamflow can be readily compared. However, it should be stressed that this file is ONLY used for comparison and not by the model itself during its simulation. Other PRMS climate modules, such as the *xyz_dist* used in the Pomperaug, would use this file to import tmin, tmax, precipitation, and other weather data from multiple weather stations into the modeling software.

CLIMATIC AND EVAPOTRANSPIRATION PARAMETERS

The 11 snow depletion curve (**snarea_curve**) values used for the Hockanum River were originally described by Anderson (1973) and modified in the PRMS-IV manual (Markstrom et al., 2015).

Five monthly parameters were required with only the dimension “nmonths”. Of the five monthly parameters, only **jh_coef** was calculated and used equations from the Dockter & Palmer study (2008).

$$\mathbf{jh_{coef}} = \frac{1}{(C_1 + C_2 \times C_H)}$$

where

$$C_1 = 68 - 3.6 \times \frac{\text{ELEV}}{1000}$$

ELEV is the mean weather station elevation (feet) for the stations used to calculate average monthly T_{\min} and T_{\max} . ELEV for Storrs, Bradley, and Brainard COOP stations was 295 feet.

$$C_2 = 13^\circ\text{F}$$

$$C_H = \frac{50 \text{ milibars}}{e_2 - e_1}$$

e_2 and e_1 are vapor pressures calculated for monthly T_{\max} and T_{\min} , respectively, as:

$$e_2 = 6.105 \times e^{\left(\frac{(25.22 \times \frac{5}{9} \times (T_{\max} - 32) + 273) - 273}{\frac{5}{9} \times (T_{\max} - 32) + 273} - 5.31 \times \ln \left(\frac{\frac{5}{9} \times (T_{\max} - 32) + 273}{273} \right) \right)}$$
$$e_1 = 6.105 \times e^{\left(\frac{(25.22 \times \frac{5}{9} \times (T_{\min} - 32) + 273) - 273}{\frac{5}{9} \times (T_{\min} - 32) + 273} - 5.31 \times \ln \left(\frac{\frac{5}{9} \times (T_{\min} - 32) + 273}{273} \right) \right)}$$

T_{\max} is the average monthly maximum temperature ($^\circ\text{C}$).

The **jh_coef** is used to determine potential evapotranspiration, from which actual evapotranspiration is then determined. The **jh_coef** varies by month due to differences in

average minimum and maximum monthly temperatures, which correlates to seasonal variations in solar radiation. The **jh_coef** values were adjusted manually to determine how the parameter affected the seasonal evapotranspiration and subsequent streamflow; the **jh_coef** was a highly sensitive parameter.

The **jh_coef_hru** is also used to calculate potential evapotranspiration, but it relative to each HRU's elevation. For this study, it was decreased after calculation to better match the expected evapotranspiration reported by literature. It was originally calculated for each HRU as follows (Markstrom et al., 2015):

$$\text{jhcoefhru} = 22 - \frac{\text{hru_elev}}{1000}$$

The parameter **adjmix_rain** adjusted the proportion of rain for mixed rain and snow events. The default value of 1.0 does not alter the original calculated precipitation proportions by PRMS. Only February was decreased to 0.7 because the proportion of rain was over predicted on average for the full period of record. The **cecn_coef** parameter set the coefficient of convection condensation energy; the values applied were determined in the Bjerklie et al. study (2010). **Tmax_allrain** determined the maximum air temperature for mixed precipitation events. If the air temperature was greater than **tmax_allrain**, then precipitation was rain. **Tstorm_mo** was a PRMS flag for the prevalent storm type for a given month, i.e. either frontal or convective (thunderstorm) events. Both **tmax_allrain** and **tstorm_mo** were set to best match climatic conditions for Connecticut. Two other precipitation adjustment parameters were required for the Climate by HRU module, **rain_cbh_adj** and **snow_cbh_adj**, but were required for each HRU as well, i.e. 56 HRUs multiplied by 12 months equaled 672 values for each parameter. **Rain_cbh_adj** was reduced to match observed average annual precipitation because the Daymet input data overestimated precipitation when interpolated across the watershed by PRMS.

COVER TYPE, COVER DENSITY, AND INTERCEPTION

Raster data from the National Land Cover Database (NLCD) was processed in ArcMap to determine the vegetative cover type of each HRU. First, the land cover data were reclassified using the scheme in Table 1 of The GIS Weasel User's Manual (Viger & Leavesley, 2007). This set the data to values of bare = 0, grass = 1, shrub = 2, deciduous forest = 3, and coniferous forest = 4. The "Tabulate Area" tool in ArcMap's Spatial Analyst extension determined the number of pixels representing each of the five cover types by a given HRU. The percentage of each vegetative cover type was determined by:

$$\% \text{ Cover Type} = (C_{\text{pix}} \div S_{\text{pix}}) \times 100$$

in which C_{pix} is the number of pixels for a given cover type in an HRU, and S_{pix} is the sum of all cover type pixels for an HRU.

Figure E-1 was created to mimic the GIS Weasel user manual's procedure for categorizing the parameter **cov_type** for each HRU in PRMS (Viger & Leavesley, 2007). One change in procedure was that the bare type threshold had to be ignored due to large amounts of impervious area, which prevented PRMS from estimating interception and evapotranspiration from those HRU's. The flowchart differs slightly from the PRMS – IV input, which separates out

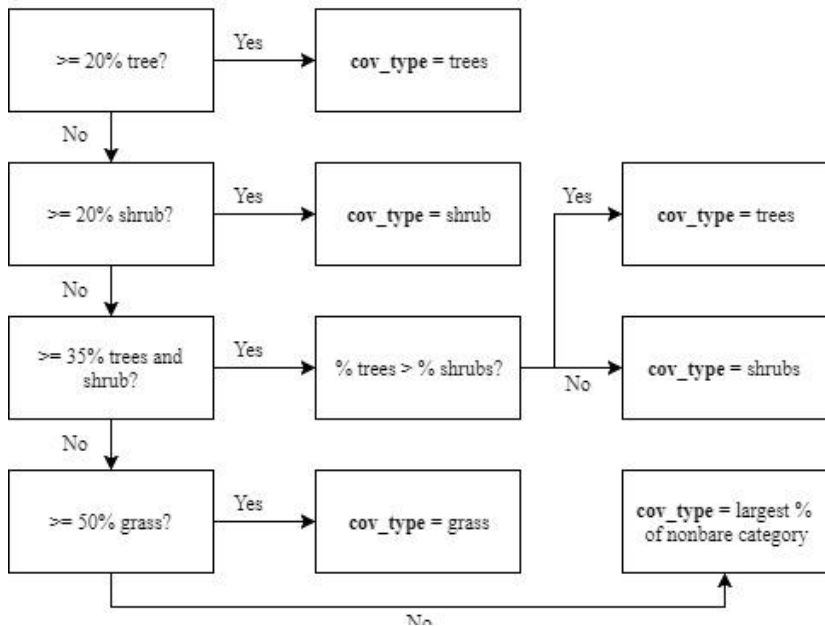


Figure E-1. Flow chart depicting categorization of the **cov_type** parameter based on the GIS Weasel user manual (Viger & Leavesley, 2007).

deciduous and coniferous forests. However, the percentage of coniferous trees in the Hockanum River watershed was not large enough to be considered coniferous forest. Therefore, trees and deciduous forest were used interchangeably.

The module *intcp* simulates interception of precipitation by the plant-cover density. The plant-cover density for each HRU can be estimated from the Analytical Tree Canopy data using the “Zonal Statistics by Table” tool in ArcMap. These values are set to the parameter **covden_sum**. However, this is only representative of summer months when leaves remain on trees. In order to simulate leaf-loss and estimate a winter cover density, **covden_win**, a leaf keep value was assigned to each cover type as described in the GIS Weasel User’s Manual (Viger & Leavesley, 2007). For example, deciduous trees were assigned a leaf keep value of 0.6 (60%). This leaf keep value, respective to each HRU’s **cov_type**, was multiplied by the **covden_sum** to approximate **covden_win**.

Three interception storage parameters are required for the *intcp* module to simulate a maximum precipitation-interception storage capacity in the summer (**srain_intcp**), winter (**wrain_intcp**), and one specifically for snow (**snow_intcp**). To calculate the interception parameters, each category of NLCD land cover was weighted and multiplied by an interception storage value defined the GIS Weasel User’s Manual (Viger & Leavesley, 2007). There were different interception storage values for each category of land cover for the three aforementioned parameters. For example, the following calculation would occur for each interception parameter:

$$\mathbf{srain_intcp} = \left(\frac{C1_{pix}}{S_{pix}} \times I_{C1} \right) + \dots + \left(\frac{Cx_{pix}}{S_{pix}} \times I_{Cx} \right)$$

where Cx_{pix} is the number of pixels for a given cover type in an HRU, S_{pix} is the sum of all cover type pixels for an HRU, and I_{Cx} is the interception value for summer or winter rain, or snow, for a given cover type such as grassland or forest.

When computing the water balance with seasonal values, PRMS assumes that if transpiration has been flagged to occur, it should use a summer value in its calculation and vice-versa. PRMS also assumes that all intercepted precipitation evaporates (Markstrom et al., 2015).

SOIL-MOISTURE AND EVAPOTRANSPIRATION

Three soil types, sand, loam, and clay, are accounted for in PRMS under one **soil_type** parameter. Soil data from the Natural Resources Conservation Service's (NRCS) Soil Survey Geographic Database (SSURGO) were used to determine the soil type in each HRU (Natural Resources Conservation Service, 2016). SSURGO provides percentages of sand, silt, and clay for various partitioned areas in ArcMap. These values were averaged into a given HRU, and assigned a soil based on the flow chart (Figure E-2) outlining the procedure (Viger et al., 2014).

An important component and limiting factor of the rate of evapotranspiration is the amount of available soil moisture. The maximum amount of water available for evapotranspiration is set by the parameter **soil_moist_max**. AET is also regulated by PET, precipitation, soil type, and surficial geology. In certain summer months such as July or August, the rate of AET may be reduced at times

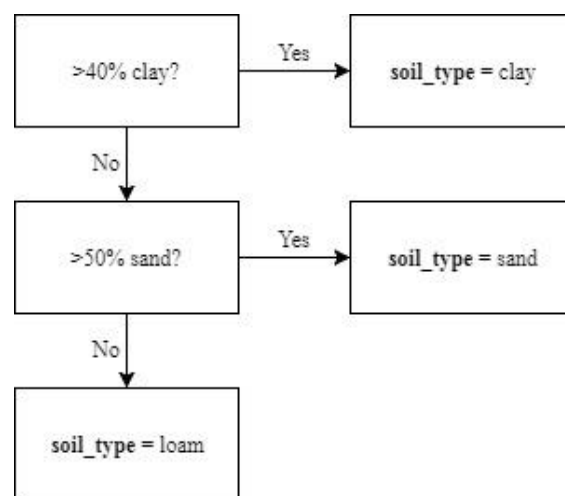


Figure E-2. Flow chart depicting categorization of the **soil_type** parameter based on the PRMS parameter metadata (Viger et al., 2014).

because of a lack available water. Areas that contain more stratified drift would have a greater rate of percolation and thus AET would be reduced. Since soil moisture contributes to the subsurface and groundwater storage, AET largely affects recharge of these two reservoirs. In Connecticut, net recharge of subsurface and groundwater typically occurs during October

through April (Mullaney & Grady, 1997), which is when AET is lower and it is the non-growing season. In PRMS, the vegetative cover type, **cov_type**, along with the **soil_type** parameter are used in the evapotranspiration calculations (Markstrom et al., 2015).

RUNOFF PARAMETERS

The following subsections are of the three runoff modules and their parameterization.

SURFACE RUNOFF MODULES – SRUNOFF_SMIDX

Surface runoff is generated by numerous contributing areas in a watershed. In PRMS, surface runoff is determined from open water, wetlands, variable-source contributing areas, and impervious surface. Variable-source contributing areas act as impervious surface when precipitation events fully saturate them (Bjerklie et al., 2010). Surface runoff was simulated by the *srunoff_smidx* module. The rate of growth of variable-source contributing area is calculated as:

$$ca_fraction = \mathbf{smidx_coef} \times 10^{(\mathbf{smidx_exp} \times smidx)}$$

in which the *ca_fraction* is the fraction of an HRU that are variable-source contributing areas, **smidx_coef** is the fraction of surface water area in each HRU, **smidx_exp** is a function of drainage density and was calibrated via LUCA (Hay & Umemoto, 2006), and *smidx* is a soil-moisture index calculated in PRMS (Bjerklie et al., 2010, Markstrom et al., 2015). The growth of contributing area is limited by the contributing area maximum parameter, **carea_max**. Initially, **carea_max** was set to the fraction of class D soils in each HRU.

SOILZONE MODULE

In this study, the two soil-zone reservoirs used were the capillary and gravity reservoirs, and the optional preferential-flow reservoir was disregarded for simplification. Conceptually, the reservoirs are not physical, but rather they represent soil-water water content for various

degrees of saturation (Markstrom et al., 2015). Each reservoir accounts for different soil-zone water processes and has a maximum storage capacity based on physical properties of the HRU.

The water content between the wilting point and field capacity for each HRU is represented by the capillary reservoir. This reservoir only exists where the HRU is not impervious and is therefore governed by the **hru_percent_imperv** parameter. Movement of water in this reservoir is restricted by capillary forces, therefore it is only available for evapotranspiration and not for discharge (Markstrom et al., 2015). The maximum amount of water available in the capillary reservoir (available for evapotranspiration) is set by the parameter **soil_moist_max**, which is calculated from rooting depth and available water capacity data using methodology from the PRMS parameter metadata (Viger et al., 2014). Rooting depth (in inches) was weighted by HRU using the same method discussed in the preceding interception section with each cover type assigned a different rooting depth (Viger & Leavesley, 2007), while available water capacity data were taken from the SSURGO database and determined in GIS.

$$\mathbf{soil_moist_max} = \text{rooting depth} \times \text{available water capacity}$$

The capillary reservoir is divided into a recharge and lower zone. The recharge zone has a maximum water content set by **soil_rechr_max**. Water in the recharge zone can evaporate and transpire at the land surface. If the recharge zone is saturated beyond **soil_rechr_max**, it transfers and adds water to the lower zone. Water can only transpire from the lower zone; it cannot evaporate. Water cannot discharge to the stream network from the capillary reservoir (Markstrom et al., 2015). Initially, **soil_rechr_max** was set by the PRMS parameter metadata methodology (Viger et al., 2014).

Gravity and hydraulic conductivity control water content in the gravity reservoir along with a maximum storage capacity. Unlike with the capillary reservoir, water in the gravity

reservoir is able to discharge to the stream network as interflow. Recharge from the gravity reservoir to the groundwater reservoir represents the process of percolation; this is the portion of water that flows through soil pore space vertically because of gravity. Gravity-driven lateral subsurface flow that discharges from the gravity reservoir is considered the slow interflow component of streamflow. Fast interflow from the preferential-flow reservoir would be lateral subsurface flow through large pathways such as animal borrows or leaf litter, but was not considered in this study.

PRMS is programmed to follow a series of sequential computation order of 14 steps (not including preferential flow in this study) for different saturation levels within the soil zone. This procedure is documented in the PRMS Manual (Markstrom et al., 2015). These steps compute inflow and outflow of water to and from the soil zone.

Subsurface-runoff, also known as interflow, is the most difficult component of the water budget to accurately estimate because it is highly variable. Unlike groundwater flow and surface runoff, which have baseflow recession curves and streamgage responses, there are no exact measures of subsurface-runoff. Therefore, the basic strategy was to calibrate groundwater flow and surface runoff parameters first and then optimize subsurface flow. Daily subsurface-runoff can be estimated by subtracting daily groundwater and surface runoff from the overall daily streamflow.

Subsurface-runoff is simulated by the soil-zone module in PRMS and represents non-groundwater aquifers such as shallow unsaturated layers of soil. First, excess water from the capillary reservoir (i.e. when **soil_moist_max** is reached) is allocated to the groundwater reservoir. This water is regulated by the **soil2gw_max** parameter; if increased, more water will percolate to the groundwater reservoir, and if decreased, more water will transmit to the gravity

(subsurface) reservoir. It was initially calculated with the saturated hydraulic conductivity (K_{sat}), which is related to surficial geology, and then was linearly scaled (Viger et al., 2014) to fit the PRMS Manual's range of acceptable values before the parameter was optimized through sensitivity analyses. In this study only, linear scaling was a division by 1.5.

$$\text{soil2gw_max} = \frac{(K_{\text{sat}})^3}{1.5}$$

Next, horizontal flow from the gravity reservoir to the stream network is determined by the **slowcoef_lin** and **slowcoef_exp** parameters. This is related to an HRU's slope and fraction of coarse stratified drift (Bjerklie et al., 2010).

$$\text{slowcoeflin} = (1 - X_{\text{CSD}}) \times (S \div \bar{S}) \times F$$

where X_{CSD} is the fraction of coarse stratified drift for a given HRU, S is the slope for a given HRU, \bar{S} is the average slope over the entire watershed, and F is a **slowcoef_lin** factor used from the Bjerklie et al. study (2010) that was equal to 0.57. However, both **slowcoef_lin** and **slowcoef_exp** were subjected to further calibration through LUCA (Hay & Umemoto, 2006) due to degree of difficulty in estimating these parameters.

Vertical flow of water from the gravity reservoir to the groundwater reservoir is then determined by the **ssr2gw_rate** parameter. The amount of vertical to horizontal flow is based on the surficial geology, which would make vertical flow greater in areas of higher amounts of coarse stratified deposits (Bjerklie et al., 2010). It was calculated before adjustment as follows:

$$\text{ssr2gwrate} = X_{\text{CSD}} + \text{NR} - X_{\text{CSD}} \times \text{NR}$$

where X_{CSD} is the fraction of coarse stratified drift for a given HRU and NR is a nominal recharge value used from the Bjerklie et al. study (2010) that was equal to 0.25.

GROUNDWATER MODULE

The **gwflow_coef** is the linear routing coefficient to calculate groundwater flow from the groundwater reservoir to the stream network. In order to most accurately allocate groundwater spatially and temporally in the basin the **gwflow_coef** is based on physical characteristics of the surficial geology. The larger the coefficient value, the more hydrologically conductive the soil materials are and vice-versa. **Gwflow_coef** was calculated using the method discussed in the Bjerklie et al study (2010).

$$\mathbf{gwflow}_{coef} = 1 - e^{-1 \times \left(\frac{T_{HRU} \times \pi^2}{4 \times GFL^2 \times S_{HRU}} \right)}$$

The groundwater flow length (GFL) in feet was calculated by:

$$GFL = \frac{1}{\left(\frac{2 \times SL_{HRU}}{A_{HRU}} \right)}$$

in which SL_{HRU} is the total stream length in each HRU (feet) and A_{HRU} is the total HRU area (ft^2). In Connecticut, the two most common types of aquifers are till and bedrock (denoted by subscript till) and coarse glacial stratified drift (denoted by subscript CSD). The following transmissivity (T) and storativity (S) properties for aquifers are (estimated over Hockanum River watershed from values in the Connecticut Water Resources Inventory, Part 7 (Ryder et al., 1981)

$$T_{CSD} = 5,500 \text{ ft}^2/\text{day} \quad S_{CSD} = 0.20$$

$$T_{till} = 150 \text{ ft}^2/\text{day} \quad S_{till} = 0.005$$

Transmissivity (ft^2/day) and storativity for each HRU were then calculated as:

$$T_{HRU} = \frac{T_{CSD} \times T_{till}}{(1 - X_{CSD}) \times T_{CSD} + X_{CSD} \times T_{till}}$$

$$\text{and } S_{HRU} = X_{CSD} \times S_{CSD} + (1 - X_{CSD}) \times S_{till}$$

where X_{CSD} is the fraction of glacial coarse stratified drift deposit.

Groundwater flow to the stream network is calculated by the following linear equation:

$$gwres_flow = \mathbf{gwflow_coef} \times gwres_stor$$

gwres_stor represents storage in the groundwater reservoir and *gwres_flow* is the amount of discharge from the reservoir. *Gwres_stor* is calculated from antecedent storage in a given HRU's groundwater reservoir along with inflows from the soil zones and outflows to the stream network and to the groundwater sink.

APPENDIX F

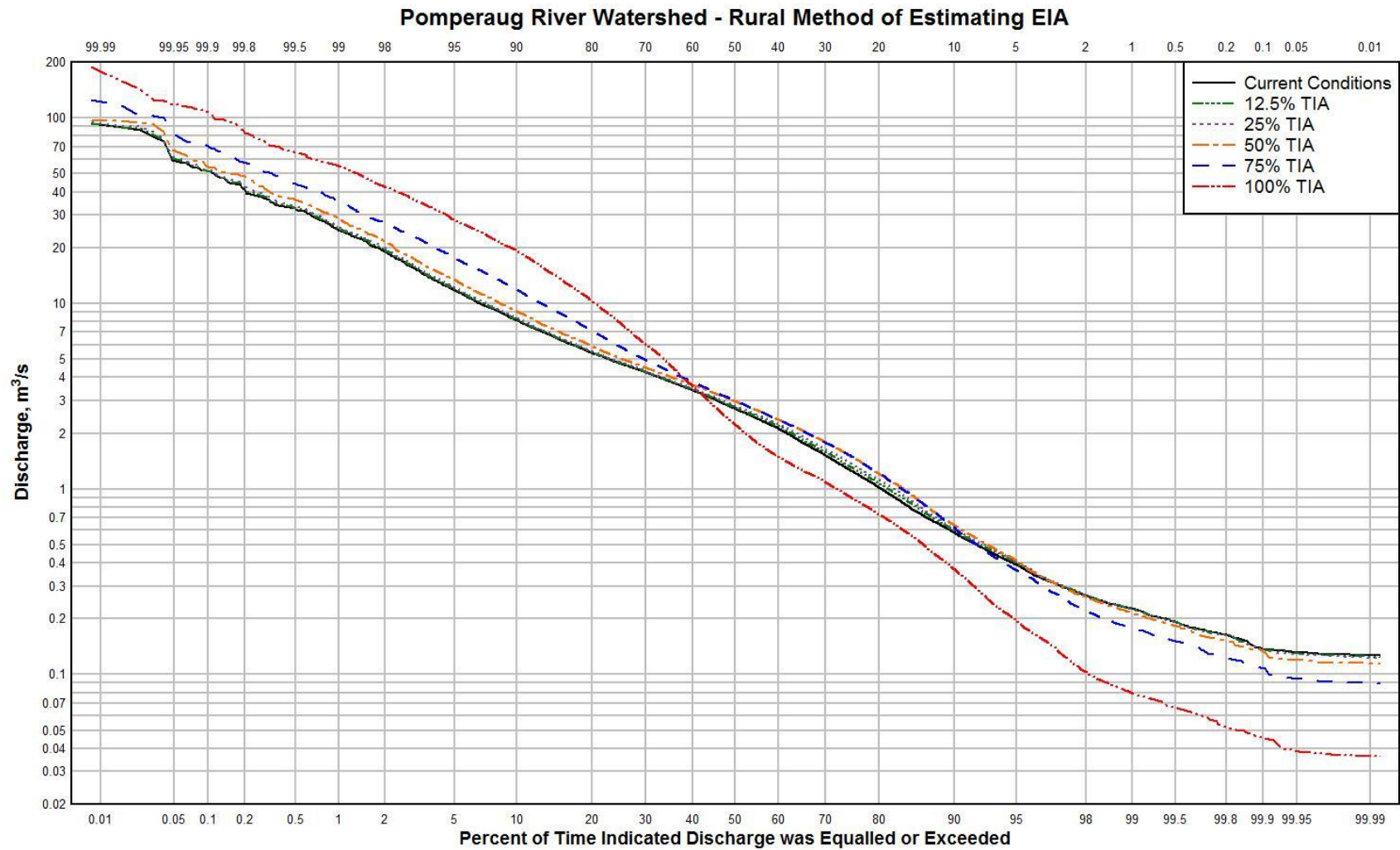


Figure F-1. Results of the Rural Method of estimating EIA that compares each TIA for the Pomperaug River watershed.

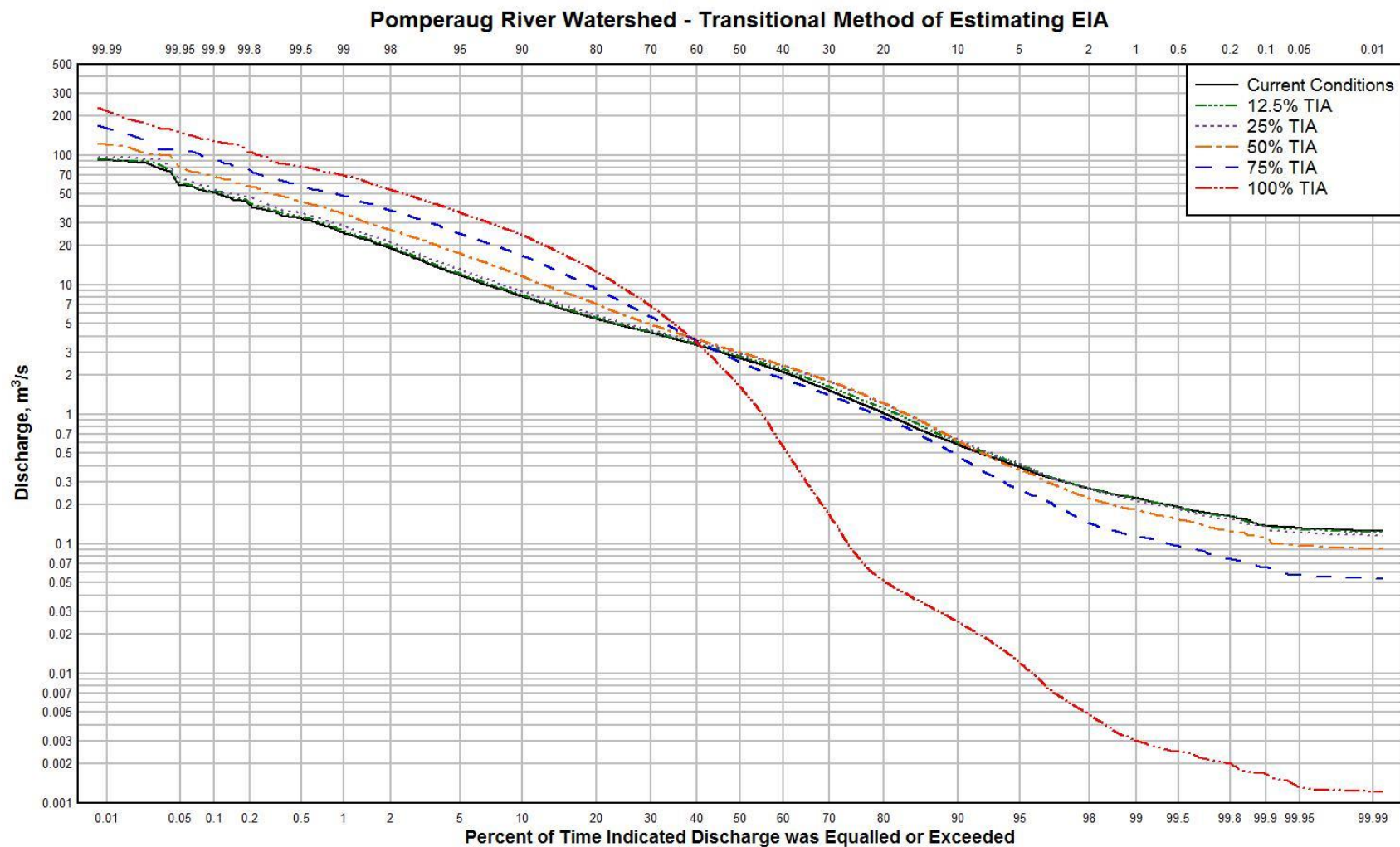


Figure F-2. Results of the Transitional Method of estimating EIA that compares each TIA for the Pomperaug River watershed.

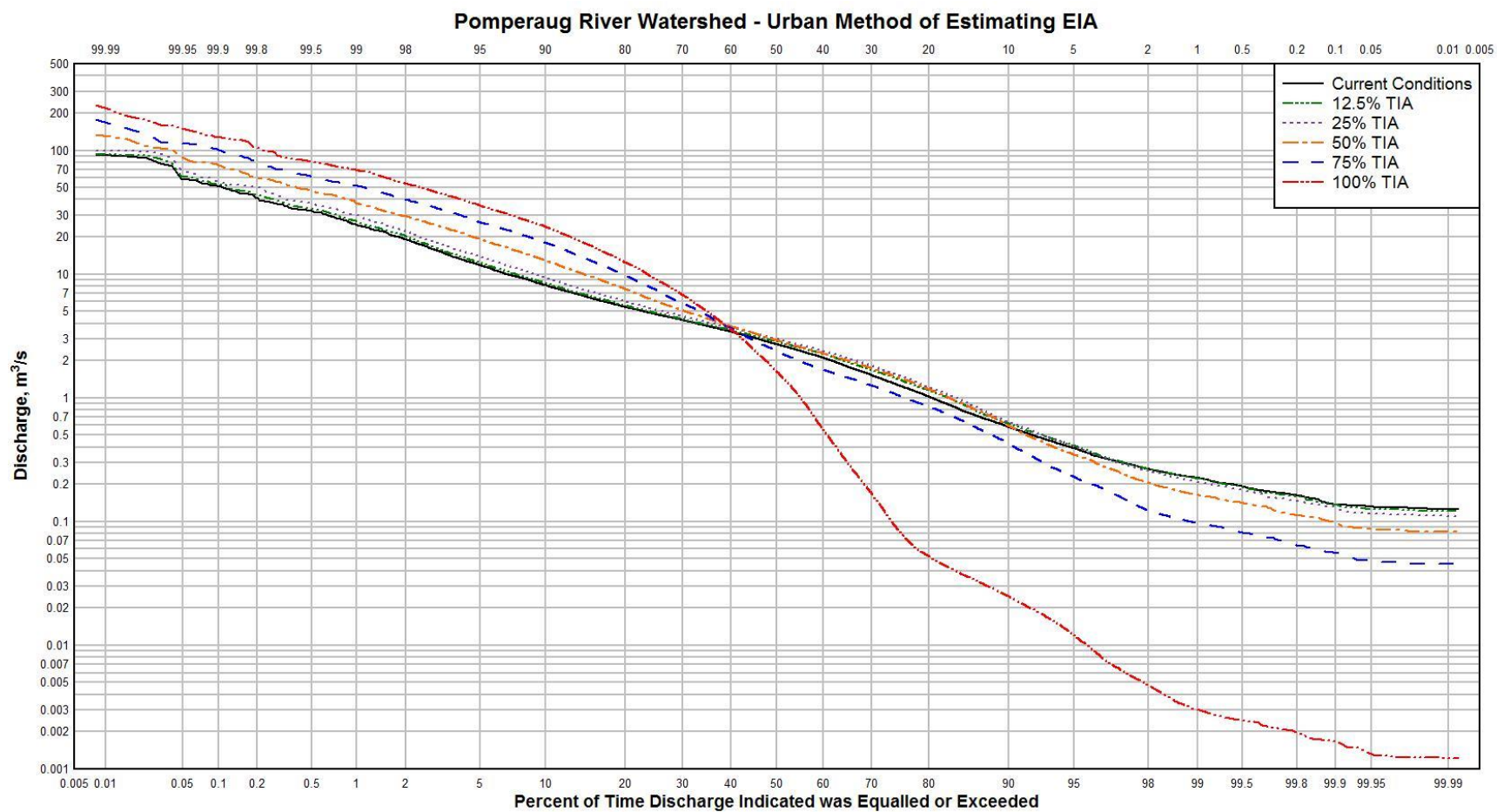


Figure F-3. Results of the Urban Method of estimating EIA that compares each TIA for the Pomperaug River watershed.

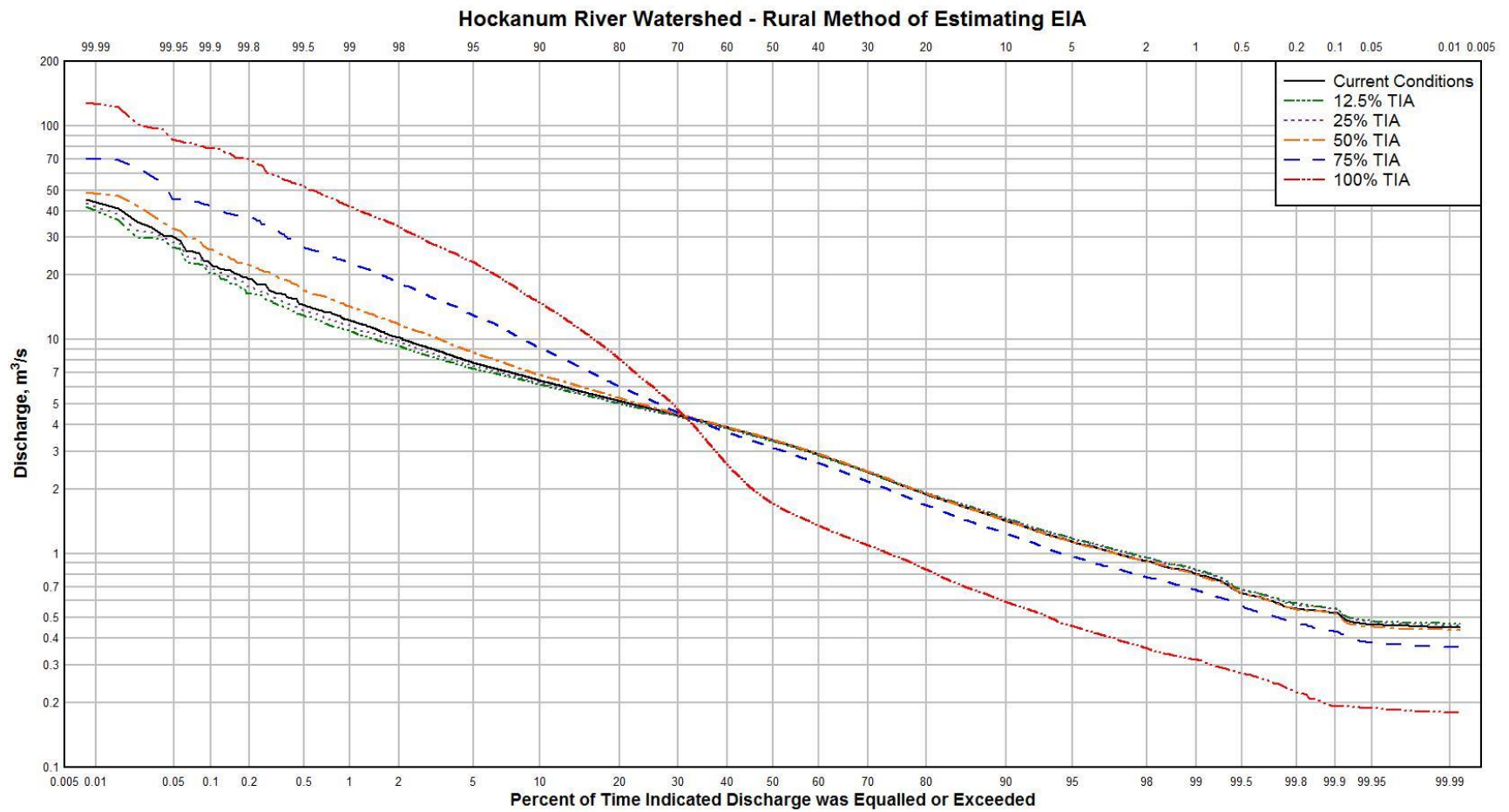


Figure F-4. Results of the Rural Method of estimating EIA that compares each TIA for the Hockanum River watershed.

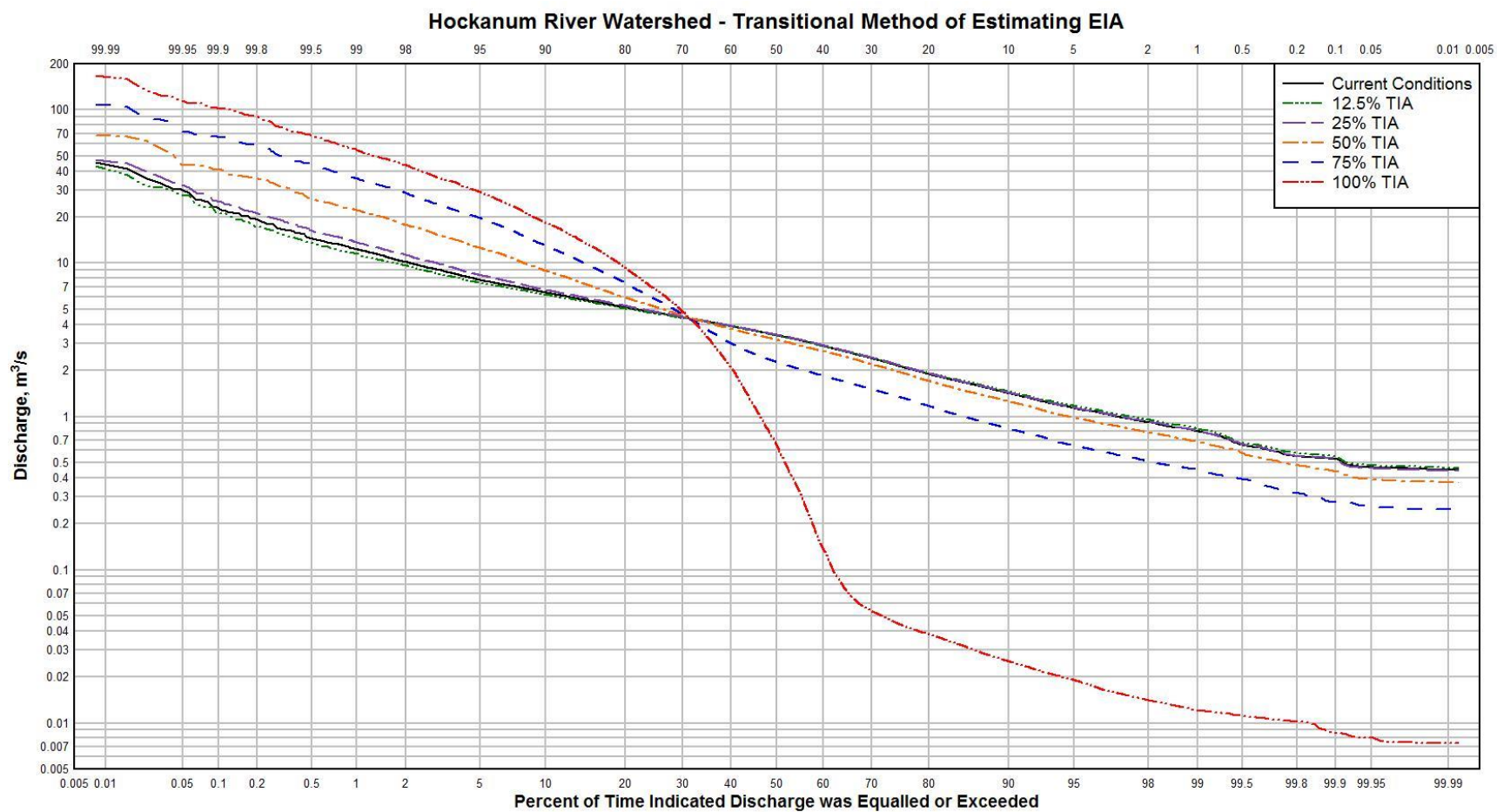


Figure F-5. Results of the Transitional Method of estimating EIA that compares each TIA for the Hockanum River watershed.

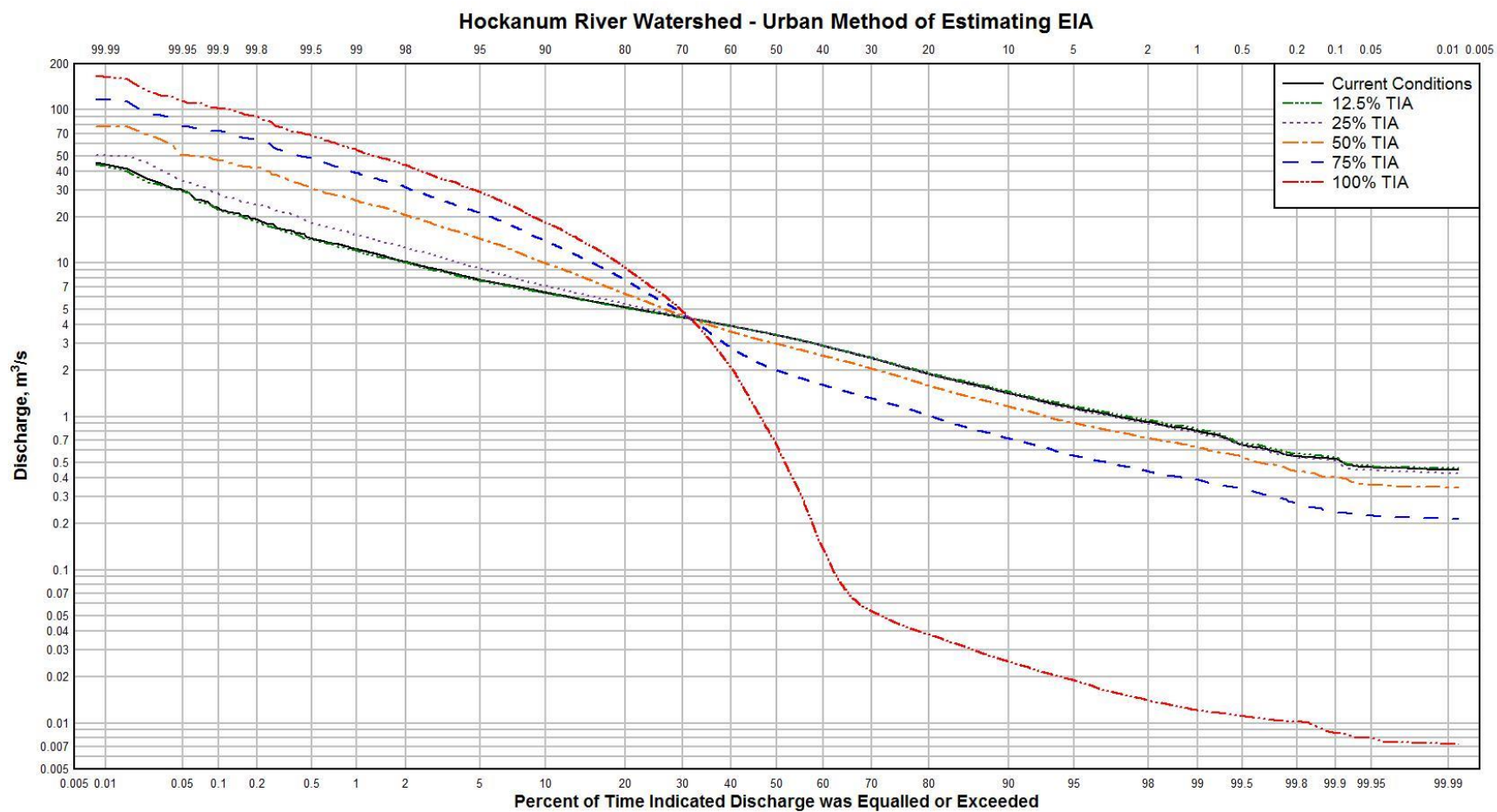


Figure F-6. Results of the Urban Method of estimating EIA that compares each TIA for the Hockanum River watershed.

APPENDIX G

Parameters used for the two current condition models, as well as parameters used in each development scenario, are available electronically from the University of Connecticut's Digital Commons Network, "OpenCommons@UConn". For further information regarding this study, please contact the author via his permanent email address:

sdtardif@gmail.com